Math-for-industry
Education & Research Hub

ISSN2188-1200

IMI-La Trobe Joint Conference

Geometric Numerical Integration and its Applications

Editors: QUISPEL, G. Reinout W. (La Trobe University) BADER, Philipp (La Trobe University)
MCLAREN, David I. (La Trobe University) TAGAMI, Daisuke (Kyushu University)

九州大学マス・フォア・インダストリ研究所

MI Lecture Note Vol.74 : Kyushu University

IMI-La Trobe Joint Conference

Geometric Numerical Integration and its Applications

Editors: QUISPEL, G. Reinout W. (La Trobe University)

BADER, Philipp (La Trobe University)

MCLAREN, David I. (La Trobe University)

TAGAMI, Daisuke (Kyushu University)

About MI Lecture Note Series

The Math-for-Industry (MI) Lecture Note Series is the successor to the COE Lecture Notes, which were published for the 21st COE Program "Development of Dynamic Mathematics with High Functionality," sponsored by Japan's Ministry of Education, Culture, Sports, Science and Technology (MEXT) from 2003 to 2007. The MI Lecture Note Series has published the notes of lectures organized under the following two programs: "Training Program for Ph.D. and New Master's Degree in Mathematics as Required by Industry," adopted as a Support Program for Improving Graduate School Education by MEXT from 2007 to 2009; and "Education-and-Research Hub for Mathematics-for-Industry," adopted as a Global COE Program by MEXT from 2008 to 2012.

In accordance with the establishment of the Institute of Mathematics for Industry (IMI) in April 2011 and the authorization of IMI's Joint Research Center for Advanced and Fundamental Mathematics-for-Industry as a MEXT Joint Usage / Research Center in April 2013, hereafter the MI Lecture Notes Series will publish lecture notes and proceedings by worldwide researchers of MI to contribute to the development of MI.

October 2014
Yasuhide Fukumoto
Director
Institute of Mathematics for Industry

IMI-La Trobe Joint Conference
Geometric Numerical Integration and its Applications

MI Lecture Note Vol.74, Institute of Mathematics for Industry, Kyushu University
ISSN 2188-1200
Date of issue: March 31, 2017
Editors: QUISPEL, G. Reinout W. / BADER, Philipp / MCLAREN, David I. /
TAGAMI, Daisuke
Publisher:
Institute of Mathematics for Industry, Kyushu University
Graduate School of Mathematics, Kyushu University
Motooka 744, Nishi-ku, Fukuoka, 819-0395, JAPAN
Tel +81-(0)92-802-4402, Fax +81-(0)92-802-4405
URL http://www.imi.kyushu-u.ac.jp/

Printed by
Kijima Printing, Inc.
Shirogane 2-9-6, Chuo-ku, Fukuoka, 810-0012, Japan
TEL +81-(0)92-531-7102 FAX +81-(0)92-524-4411

Preface

Welcome to the "Geometric Numerical Integration and its Applications" (GNI&A) international conference held at La Trobe University, Melbourne, Australia, December 5-7, 2016.

The aim of this international conference, jointly organised by the Institute of Mathematics for Industry (IMI), Kyushu University, and La Trobe University, was to foster interaction between new and established numerical analysts from across the globe interested in Geometric Integration and showcasing the latest developments in theory and applications.

Since its conception in the early nineties, geometric integration has caused a shift of paradigms in the numerical solution of differential equations. The previous efforts of finding all-purpose integrators were redirected to in-depth analysis of the problems at hand and their classification such that specifically tailored schemes could take advantage of the underlying structural properties and outperform all-purpose integrators. Over the last decades, the field has evolved and influenced neighbouring areas and applications. This conference aims to provide insight into cutting-edge research and exhibit applications of the developed methods.

The present volume is the proceedings of GNI&A. Several invited talks attract and inspire the attendees working with numerical techniques to solve mathematical and industrial problems.
The list of invited speakers collects a large proportion of the experts in the field and includes John C. Butcher (U Auckland), Elena Celledoni (NTNU), Jason E. Frank (Utrecht U), Volker Grimm (KIT), Arieh Iserles (U Cambridge), Robert I. McLachlan (Massey U), Taketomo Mitsui (Nagoya U), Yuto Miyatake (Nagoya U), Hans Z. Munthe-Kaas (U Bergen) and Brynjulf Owren (NTNU).
The topics include symplectic integrators, methods on Lie groups, structure preservation for PDEs, discrete gradients in image processing and related results.

We are very grateful to the Institute of Mathematics for Industry (IMI), Kyushu University, for sponsoring this conference. We appreciate the hard work of all people involved in the realisation of this conference and wish to thank all contributing authors and participants for their involvement. We hope that all the participants enjoyed this exciting event in Melbourne.

The organisers

G. R. W. Quispel
P. Bader
D. I. McLaren
D. Tagami

IMI-La Trobe Joint Conference

GEOMETRIC NUMERICAL INTEGRATION AND ITS APPLICATIONS

Dates: Dec.5(Mon.)–Dec.7(Wed.), 2016

Invited speakers:

BUTCHER, John C.
(University of Auckland)

CELLEDONI, Elena
(Norwegian University of Science and Technology)

FRANK, Jason E.
(Utrecht University)

GRIMM, Volker
(Karlsruhe Institute of Technology)

ISERLES, Arieh
(University of Cambridge)

MCLACHLAN, Robert I.
(Massey University)

MITSUI, Taketomo
(Nagoya University)

MIYATAKE, Yuto
(Nagoya University)

MUNTHE-KAAS, Hans Z.
(University of Bergen)

OWREN, Brynjulf
(Norwegian University of Science and Technology)

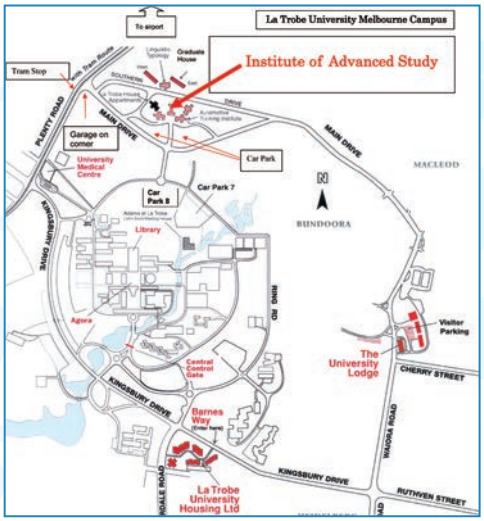

Venue:

The Institute of Advanced Study, La Trobe University, Bundoora, VIC, Australia

Organizing Committee:

QUISPEL, G. Reinout W.
(La Trobe University)

BADER, Philipp
(La Trobe University)

MCLAREN, David I.
(La Trobe University)

TAGAMI, Daisuke
(Kyushu University)

Contact: Quispel, G.R.W. (La Trobe University)
e-mail: prof.quispel@latrobe.edu.au

	MONDAY 5th	TUESDAY 6th	WEDNESDAY 7th
9:30 - 10:00	***REGISTRATION***	*arrive*	*arrive*
10:00 -10:30	Iserles	Frank	Owren
10:30 - 11:00	Matsuo	Yaguchi	Mitsui
11:00 - 11:30	*morning tea/coffee*	*morning tea/coffee*	*morning tea/coffee*
11:30 - 12:00	McLachlan	Minesaki	Munthe-Kaas
12:00 - 12:30	Itoh	Benning	Sasaki
12:30 - 13:30	*lunch*	12:45 DEPART by bus	*lunch*
12:30 - 13:30		*(BYO packed lunch)*	
13:30 - 14:00	Butcher	13:45 (approx) ARRIVE	Celledoni
14:00 - 14:30	Miyatake	walk	Ishikawa
14:30 - 15:00	*afternoon tea/coffee*		*afternoon tea/coffee*
15:00 - 15:30	Furihata		Grimm
15:30 - 16:00	Tagami	wine tasting	Bader
16:00 - 16:30	*day end*		*day end*
16:30 - 17:00			
17:00 - 17:30			
17:30 - 18:00		dinner	
18:00 - 18:30			
18:30 - 19:00			
19:00 - 19:30			
19:30 - 20:00			
20:00 - 20:30		20:00 DEPART by bus	
20:30 - 21:00			
21:00 - 21:30		21:00 (approx) ARRIVE	

Table of Contents

Discretization of the Schwarzian derivative and its application

Toshiaki Itoh

Doshisha University, 3-1, Miyakodani, Tatara, Kyotanabe, Kyoto, 610-0394, JAPAN
toito@mail.doshisha.ac.jp

1 INTRODUCTION

We consider numerical treatment of Schwarzian derivatives. It is well known that Schwarzian derivative plays important role in many application, for example, 2nd order ODE, conformal mapping and geometry [1, 2]. By the way, it is known that Cross ratio is counter part of Schwarzian derivative in the difference representation [3, 4, 5]. Therefore we can consider the application of Cross-ratio instead of the Schwarzian derivative. Main result is possibility of construction of fundamental region of Fuchsian (special) function that are defined by triangles with arcs in complex plane. Then simultaneous equation by two Mëbius transformation give conformal mapping of that region with singularity. From geometrical point of view, we can construct mapping for curve with constant curvature with singular point in complex plane. By this approach, we can find discrete integrable system respect to special functions also.

2 Schwarzian derivative in 2nd order ODE and Cross-ratio as the counter part

We shortly review Schwarzian derivative [1, 3] relate to this study. Let's consider following 2nd order ODE,

$$y''(x) + p(x)y'(x) + q(x)y(x) = 0, \tag{1}$$

here y' and y" are the first and second derivatives of $y(x)$ by x. By variable transformation,

$$y = \exp\left(-\frac{1}{2}\int p(x)dx\right)u(x),$$

we get another form of (1),

$$u''(x) = \frac{1}{2}\left[p'(x) + \frac{1}{2}p^2(x) - 2q(x)\right]u(x) = -\frac{1}{2}\{\zeta, x\}u(x), \tag{2}$$

$$\{\zeta, x\} = 2q(x) - p'(x) - \frac{1}{2}p^2(x). \tag{3}$$

here $\{\zeta, x\}$ is called Schwarzian derivative of (1). It is also defined with two fundamental solutions $y_1(x)$ and $y_2(x)$ of (2) and $\zeta = y_1/y_2$.

$$\{\zeta, x\} = \frac{2\zeta'\zeta''' - 3\left(\zeta''\right)^2}{2\left(\zeta'\right)^2} \tag{4}$$

The remarkable property of Schwarzian derivative is invariant of the Mëbius (Γ) transformation, $\xi = \Gamma(\zeta) = (a\zeta + b)/(c\zeta + d), ad - bc \neq 0$. That is $\{\zeta, x\} = \{\xi, x\}$. Therefore, if $u(x)$ in (2) is automorphic function (Fuchsian), then (2) becomes invariant of Mëbius transformation.

Next, we consider linear 2nd order finite difference equation which corresponds to (1),

$$P(k)y^{(k+1)} + Q(k)y^{(k)} + R(k)y^{(k-1)} = 0, \tag{5}$$

here integer k is abbreviation for $x^{(k)} = x_0 + k\Delta$ and upper suffix (k) of $x^{(k)}$ and $y^{(k)} = y(x^{(k)})$ means step number of variable x and y like usual numerical treatment. We take x_0 is an initial point of x and Δ is finite difference of x. For simplicity, we treat Δ as constant. Using variable $\zeta^{(k)} = y_2^{(k)}/y_1^{(k)}$ in discrete case we get Cross-ratio from the Mëbius transformation [4],

$$\frac{\left(\xi^{(k+1)} - \xi^{(k-1)}\right)\left(\xi^{(k+2)} - \xi^{(k)}\right)}{(\xi^{(k)} - \xi^{(k-1)})(\xi^{(k+2)} - \xi^{(k+1)})} = \frac{Q(k+1)Q(k)}{R(k+1)P(k)}. \tag{6}$$

The left hand side of (6) is Cross ratio and its right hands is function by coefficient function of (5). Equation (6) resembles to (3) remarkably. Therefore, we can regard Cross-ratio is the counterpart of Schwarzian derivative. There were many previous works relate to this topics, for recent example, see [4, 5] . We use this correspondence to conformal mapping as an example of application in the next section.

3 Conformal mapping of arc polygon with singular vertices

It is well known that Schwarzian derivative is useful for conformal mapping of rectangles whose each edge is arc [1, 2]. Then (6) give the conformal mapping instead of Schwarzian derivative. Here we assume that any order of the derivative of Schwarzian derivative of (1) which we need are given. Using abbreviation that the left hand side of (6) equals to $Cr^{(k+1/2)}$, (6) becomes

$$\xi^{(k+2)} = \frac{\left\{(1 - Cr^{(k+1/2)})\xi^{(k)} + Cr^{(k+1/2)}\xi^{(k-1)}\right\}\xi^{(k+1)} - \xi^{(k)}\xi^{(k-1)}}{\xi^{(k+1)} - Cr^{(k+1/2)}\xi^{(k)} - (1 - Cr^{(k+1/2)})\xi^{(k-1)}}. \tag{7}$$

We regard (7) as the evolutional equation and mapping for $\xi^{(k)}$. Then $\xi^{(k+2)}$ is obtained from (7) with $\xi^{(k+1)}, \xi^{(k)}, \xi^{(k-1)}$ and $Cr^{(k+1/2)}$ sequentially. Note that (7) is Mëbius transformation from $\xi^{(k+1)}$ to $\xi^{(k+2)}$. Using (7) we can construct mapping at vertex of intersection of two arcs by different circles.

Because there are many cases of the intersection or crossing of arbitrary two arcs of circles, we have to treat them on a case-by-case practically. For simplicity, we use symbols

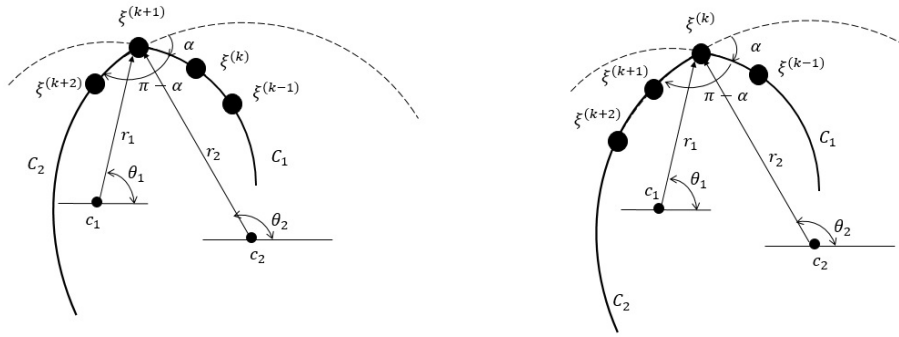

Figure 1: Configurations of VO type nodes at the vertex. VO1 (left) and VO2 (right).

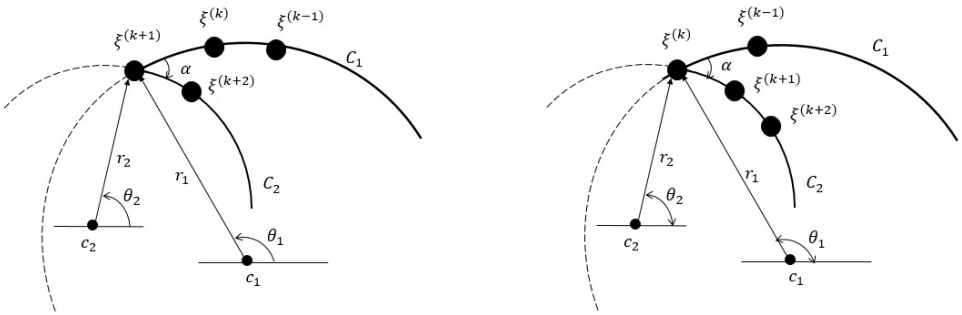

Figure 2: Configurations of VR type nodes at the vertex. VR1 (left) and VR2 (right).

for the each case of the configuration of vertex and nodes as VO1, VO2, VR1 and VR2 defined in Fig. 1 and 2. In figures, we define the angle of intersection also. Each vertex can be regarded as the singular point of conformal mapping.

VO1: Two arcs intersect at a vertex with same direction of each circles. In other words, points on two arcs are defined same directions which are defined by angles of each circle. Then four points on two arcs, $\xi^{(k-1)}, \xi^{(k)}, \xi^{(k+1)}$ and $\xi^{(k+2)}$ are located as $\xi^{(k-1)}, \xi^{(k)}, \xi^{(k+1)}$ are on arc of C_1, and $\xi^{(k+1)}, \xi^{(k+2)}$ are on arc of C_2. $\xi^{(k+1)}$ is a common point of the two arcs. VO2: Like VO1, two arcs intersect at a vertex with same direction of each circle. Though $\xi^{(k-1)}, \xi^{(k)}$ are on C_1, and $\xi^{(k)}, \xi^{(k+1)}, \xi^{(k+2)}$ are on C_2. VR1: Two arcs intersect at a vertex with reverse direction of each circle. In other words, points on two arcs are defined opposite directions which are defined by angles of each circle. Then four points are located as $\xi^{(k-1)}, \xi^{(k)}, \xi^{(k+1)}$ are on C_1, and $\xi^{(k+1)}, \xi^{(k+2)}$ are on C_2. $\xi^{(k+1)}$ is a common point of the two arcs. VR2: Like VR1, two arcs intersect at a vertex with reverse direction of each arc. $\xi^{(k-1)}, \xi^{(k)}$ are on C_1, and $\xi^{(k)}, \xi^{(k+1)}, \xi^{(k+2)}$ are on C_2. $\xi^{(k)}$ is a common point of the two arcs.

For simplicity, summary of the four cases to evaluate Cr are listed in the following. Here we use notation for the Cross ratio as $Cr_{O1}, Cr_{O2}, Cr_{R1}$ and Cr_{R2}. Lower suffix of the notation corresponds to each case of vertices.
Case VO1,

$$Cr_{O1} = (1 + \exp(-i\Delta)) \left(\frac{r_1}{r_2} \exp(i\alpha) + \exp(i\Delta) \right). \tag{8}$$

here, we use $\xi^{(k+1)} = r_1 \exp(i\theta_1) + c_1 = r_2 \exp(i\theta_2) + c_2$ by the definition and $\alpha = \theta_1 - \theta_2$.
Case VO2,

$$Cr_{O2} = (1 + \exp(i\Delta)) \left(\frac{r_2}{r_1} \exp(-i\alpha) + \exp(-i\Delta) \right). \tag{9}$$

here, $\xi^{(k)} = r_1 \exp(i\theta_1) + c_1 = r_2 \exp(i\theta_2) + c_2$.
Case VR1,

$$\begin{aligned} Cr_{R1} &= (1 + \exp(i\Delta)) \left(1 - \frac{c_1 - \xi^{(k+1)}}{c_2 - \xi^{(k+1)}} \right) \\ &= (1 + \exp(i\Delta)) \left(1 - \frac{r_1}{r_2} \exp(i\alpha) \right). \end{aligned} \tag{10}$$

Case VR2,

$$\begin{aligned} Cr_{R2} &= (1 + \exp(i\Delta)) \left(1 - \frac{c_2 - \xi^{(k)}}{c_1 - \xi^{(k)}} \right) \\ &= (1 + \exp(i\Delta)) \left(1 - \frac{r_2}{r_1} \exp(-i\alpha) \right). \end{aligned} \tag{11}$$

In the case of all $\xi^{(j)}, j = k-1, k, k+1, k+2$ are on the same arc (it corresponds to constant curvature),

$$Cr = 4 \cos^2 \left(\frac{\Delta}{2} \right). \tag{12}$$

Using above relations, Cross-ratio can be obtained at the near point of vertex with singularity. From the application of mapping, angles of intersection α which are picked up

from the plan of the conformal mapping we desired. For the mapping, we use (8)-(11) to evaluate Cr in (7) with given angles α_j, circles C_j and locations of vertices. Then using initial vale of $\xi(0), \xi(1), \xi(2)$ on C_1 and Cr of each two arcs, we can calculate $\xi(3)$ and the sequence of $\xi(k)$ by (7).

4 Summary and discussion

Though one of the discrete representation of Schwarzian derivative is following maybe,

$$\{\zeta, x\}_{approx}^{(k+1/2)} = \frac{2\tilde{\zeta}'^{(k+1)}\tilde{\zeta}'''^{(k+2)} - 3\tilde{\zeta}''^{(k+2)}\tilde{\zeta}''^{(k+1)}}{2\tilde{\zeta}'^{(k+2)}\tilde{\zeta}'^{(k)}}. \tag{13}$$

here,

$$\tilde{\zeta}'^{(k)} = \frac{\zeta^{(k)} - \zeta^{(k-1)}}{\Delta}, \tilde{\zeta}''^{(k)} = \frac{\zeta'^{(k)} - \zeta'^{(k-1)}}{\Delta}, \tilde{\zeta}'''^{(k)} = \frac{\zeta''^{(k)} - \zeta''^{(k-1)}}{\Delta}, \tag{14}$$

we can get more clear understanding of it from (6) or (7), because (13) can be obtained from (6) easily. In this meaning, discrete counterpart of Schwarzian derivative of 2nd order ODE (1) is (6) that is given by Cross-ratio and coefficient functions. As mentioned in the introduction, the Schwarzian derivative appears many area. Here we have treated a simple topic about conformal mapping relate to the Schwarzian derivative. One of the left and next problem continues to this work is that calculating accessory parameters in arc polygon with many vertices using cross ratio. As for this problem, we can obtain linear equation of accessory parameters using formula in the previous section. Then taking account of invariance of Cross-ratio and Schwarzian derivative under Mëbius transformation, we can calculate accessory parameters with order of accuracy $O(\Delta^2)$. It should be studied next. Is is well known that Hypergeometric ODE that has the same form to ODE (1) is characterized by three parameters α, β, γ in the coefficient function $p(x)$ and $q(x)$. These three parameters correspond to three inner angles of fundamental region which are given by triangle with arc polygon. Now we can relate these angles to three pair of Cross-ratio at the three vertices with (8), (9), (10) and (11) .

Relate to this work, we found the possibility of constructing truncated exact difference equations which have same Γ invariant symmetry to the original ODE also. It is unmentioned in this article, because of compactness. These truncated exact difference equation are candidates of discrete representations of ODEs whose solution functions are some parts of special functions. On more related topics is discrete integrable system or discrete representation of the special functions. It has given by many previous works [6] etc. However, these works seem still apart little from actual purpose. From this approach, we can rediscover the start-point of discretization of ODE which have special function as the solution function. For example, we can obtain a difference equation by elimination of $r_1/r_2 \exp(i\alpha)$ with (8) and (9). Then we get evolutional equation for Cr,

$$Cr^{(k+1)} = \frac{Cr^{(k)}(1 + \exp(i\Delta))}{Cr^{(k)} - (1 + \exp(-i\Delta))}. \tag{15}$$

Here we put Cr of VO1 as $Cr^{(k+1)}$ and Cr of VO2 as $Cr^{(k)}$. This equation is again Mëbius transformation for Cr. We can regard this equation and (7) to the simultaneous equation that gives integrable difference equation, because it is really the same type to

the discrete integrable system in [6]. Therefore we have found again the same type of difference equation from orthodox approach. In addition we can regard (7) as Mëbius integrator [7]. Then Mëbius integrator from (7) with variable change $y_2^{(k)}/y_1^{(k)} = \zeta^{(k)}$ is given by separation numerator and denominator as two difference equations for $y_2^{(j)}$ and $y_1^{(j)}$ respectively,

$$y_2^{(k+2)} = \phi\left[\{(1 - Cr^{(k+1/2)})y_2^{(k)}y_1^{(k-1)} + Cr^{(k+1/2)})y_2^{(k-1)}y_1^{(k)}\}y_2^{(k+1)} - y_2^{(k)}y_2^{(k-1)}y_1^{(k+1)}\right],$$
$$y_1^{(k+2)} = \phi\left[y_1^{(k)}y_1^{(k-1)}y_2^{(k+1)} + \{(1 - Cr^{(k+1/2)})y_2^{(k-1)}y_1^{(k)} + Cr^{(k+1/2)})y_2^{(k)}y_1^{(k-1)}\}y_1^{(k+1)}\right]. \quad (16)$$

here ϕ is arbitrary function introduced to separate numerator and denominator.

Acknowledgment

Special thanks to Numerical Analysis group of Mathematisches Institut, Universitat Tübingen in Germany for this work.

References

[1] Nehari Z., *Conformal mapping*, McGraw-Hill, 1952.

[2] Louis H., *Numerical conformal mapping of circular arc polygons*, Journal of Computational and Applied Mathematics, 46 (1993), pp. 7–28.

[3] Ahlfors L. V., *Cross-ratios and Schwarzian Derivatives in R^n, Complex Analysis, Hersch J. and Huber A., eds.* , Birkhäuser Verlag, Basel, 1988.

[4] Itoh T., *Correspondence between Schwarzian derivative of ODE and cross-ratio of ordinary difference equation* , AIP Conference Proceedings, Vol. 1558, 2167 (2013).

[5] Itoh T., *Discretization of the Schwarzian derivative* , AIP Conference Proceedings, Vol.1776, 090025 (2016).

[6] Tamizhmani K. M., Ramani A., Tamizhmani T. and Grammaticos B., *Special functions as solutions to discrete Painlevé equations*, Journal of Computational and Applied Mathematics, 160 (2003), pp. 307–313.

[7] Schiff J. and Shnider S., *A natural approach to the numerical integration of Riccati differential equations*, SIAM J. Numer. Anal, 36(5): (1999), pp. 1392–1413.

The construction of high order G-symplectic methods

BUTCHER, J. C.
University of Auckland, Auckland, New Zealand
j.butcher@auckland.ac.nz

1 INTRODUCTION

G-symplectic methods are a special type of general linear method which are, at the same time, a generalization of symplectic Runge–Kutta methods. Although they cannot conserve quadratic invariants they can, under certain conditions, achieve a good approximation to this conservation property for a large number of time steps.

Many methods are known up to order 4 and the aim in this paper is to show how methods with higher order can be constructed. In particular we will summarise the derivation of a sixth order method [4].

The structure of the paper is as follows. In Section 2 the properties of the multivalue methods known as general linear methods will be reviewed, with special reference to methods with the G-symplectic property. This is followed by Section 3, which reviews the use of B-series to represent numerical processes. Finally, the derivation of G-symplectic methods, including the new sixth order method, is discussed in Section 4.

2 G-SYMPLECTIC GLMS

2.1 General linear methods

We will consider an initial-value problem in the form $y'(x) = f(y(x))$, $f : \mathbb{R}^N \to \mathbb{R}^N$, $y(x_0) = y_0 \in \mathbb{R}^N$. A general linear method is both multivalue, as in a linear multistep method, and multistage, as in a Runge-Kutta method. Assume there are r inputs $y_i^{[n-1]}$, $i = 1,2,\ldots,r$, to step number n, r outputs $y_i^{[n]}$, $i = 1,2,\ldots,r$, from step number n, s stages Y_i, $i = 1,2,\ldots,s$, computed in step n and s derivatives $F_i = f(Y_i)$, $i = 1,2,\ldots,s$, evaluated in step n.

Write

$$y^{[n]} = \begin{bmatrix} y_1^{[n]} \\ y_2^{[n]} \\ \vdots \\ y_r^{[n]} \end{bmatrix}, \quad Y = \begin{bmatrix} Y_1 \\ Y_2 \\ \vdots \\ Y_s \end{bmatrix}, \quad F = \begin{bmatrix} f(Y_1) \\ f(Y_2) \\ \vdots \\ f(Y_s) \end{bmatrix}$$

and the equations relating these become

$$\begin{aligned} Y &= h(A \otimes \mathbb{R}^N)F + (U \otimes \mathbb{R}^N)y^{[n-1]}, \\ y^{[n]} &= h(B \otimes \mathbb{R}^N)F + (V \otimes \mathbb{R}^N)y^{[n-1]}, \end{aligned} \tag{1}$$

where A, U, B, V characterize a specific method.

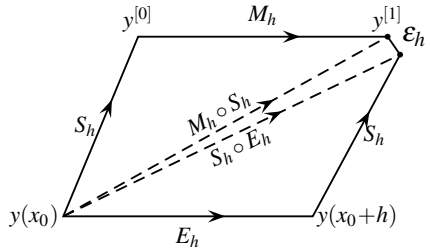

Figure 1: Representation of order of M_h, relative to S_h

2.2 The order of methods

For Runge–Kutta methods, and many traditional multistep methods, such as Adams and BDF, the meaning of the various components is obvious and clear-cut. However, the meaning of the r components input to a step of a GLM can be quite complicated.

Like all multivalue methods, a starting method is always needed and this has to be consistent with the meaning of the input components. In Figure 1, S_h is the starting method and E_h is the exact flow of the problem. Also M_h will denote the action of computing $y^{[1]}$ for given $y^{[0]}$ and ε_h can be thought of as the local truncation error.

Definition 1 *A method has order p relative to S_h, if $\varepsilon_h = O(h^{p+1})$.*

2.3 G-symplectic methods

We will be concerned with the special class of "G-symplectic" general linear methods.

Definition 2 *A method is G-symplectic if*

$$\begin{bmatrix} DA + A^{\mathsf{T}}D - B^{\mathsf{T}}GB & DU - B^{\mathsf{T}}GV \\ U^{\mathsf{T}}D - V^{\mathsf{T}}GB & G - V^{\mathsf{T}}GV \end{bmatrix} = 0,$$

where G is a non-singular symmetric matrix and D is a diagonal matrix.

Methods with this property conserve a generalization of symplectic behaviour and preserve quadratic invariants in a generalized sense.

If parasitic growth factors are zero, G-symplectic methods closely adhere to conservative behaviour for extended time intervals and a large number of time steps. They have the advantage of a lower computational cost than genuine symplectic methods. There is an emerging theory to explain their good behaviour.

We will discuss methods of order 4 and higher. As an example of the conservation properties of these methods consider a problem $y' = f(y)$ satisfying $\langle f(\eta), Q\eta \rangle = 0$, where Q is symmetric. For this problem $\langle y(x), Qy(x) \rangle$ is invariant because

$$\tfrac{d}{dx}\langle y(x), Qy(x)\rangle = \langle y'(x), Qy(x)\rangle + \langle y(x), Qy'(x)\rangle = \langle f(y(x)), Qy(x)\rangle + \langle y(x), Qf(y(x))\rangle = 0.$$

We will write

$$[\eta, \eta] := \langle \eta, Q\eta \rangle = \langle Q\eta, \eta \rangle.$$

Following the lead of Germund Dahlquist, in his work on G-stability, we will introduce a "G-norm". This is based on

$$[y^{[n]}, y^{[n]}]_G = \sum_{i,j=1}^{r} g_{ij} [y_i^{[n]}, y_j^{[n]}].$$

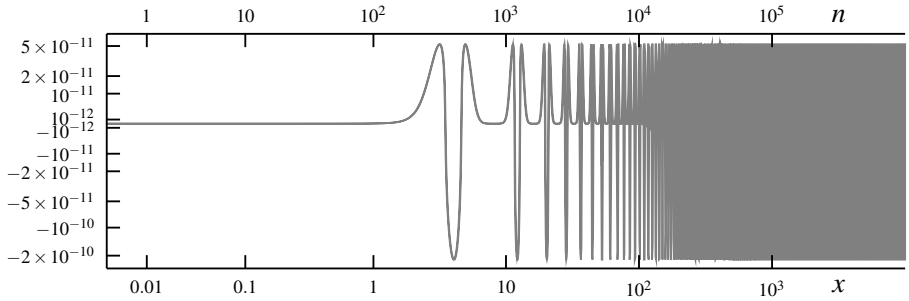

Figure 2: Deviation of the Hamiltonian H from its initial value for the simple pendulum using method (2)

In the study of stability questions, G is a positive-definite matrix and the actual G-norm is defined as

$$\sqrt{[y^{[n]}, y^{[n]}]_G}$$

but for *conservation* questions, there is no need for G to be positive-definite.

It is still worthwhile to look at the conservation of $[y^{[n]}, y^{[n]}]_G$ with the hope of approximately preserving

$$[y_1^{[n]}, y_1^{[n]}],$$

where $y_1^{[n]}$ is the "principal component" of $y^{[n]}$. The matrix G will be the same as in the definition of the G-symplectic property.

It could be asked why this is a credible hope? It could be because the non-principal components are equal to quantities like hy' or h^2y'' and they are likely to make a less significant contribution to the value of $[y^{[n]}, y^{[n]}]_G$. The preservation of $[y^{[n]}, y^{[n]}]_G$ can occur in many problems which possess quadratic invariants.

Theorem 3 *A G-symplectic method conserves the value of* $[y^{[n]}, y^{[n]}]_G$ *for a problem satisfying* $[f(\eta), \eta] = 0$.

2.4 An example of a G-symplectic method

An example method is

$$\left[\begin{array}{cc} A & U \\ B & V \end{array}\right] = \left[\begin{array}{cccc|cc} \frac{1}{12} & 0 & 0 & 0 & 1 & \frac{1}{2} \\ -\frac{1}{3} & \frac{1}{6} & 0 & 0 & 1 & 1 \\ \frac{5}{3} & -\frac{2}{3} & \frac{1}{6} & 0 & 1 & -1 \\ \frac{7}{6} & -\frac{5}{12} & \frac{1}{12} & \frac{1}{12} & 1 & -\frac{1}{2} \\ \hline \frac{2}{3} & -\frac{1}{6} & -\frac{1}{6} & \frac{2}{3} & 1 & 0 \\ 1 & -\frac{1}{2} & \frac{1}{2} & -1 & 0 & -1 \end{array}\right]. \tag{2}$$

This method is known to have order 4 and to have zero parasitic growth parameters. To show that (2) is capable of mimiccing symplectic behaviour, the simple pendulum problem $y_1' = y_2$, $y_2' = -\sin(y_2)$, with initial values $y_1(0) = 3.0 \approx 172^\circ$, $y_2(0) = 0$ was solved with $h = 1/100$ for $n = 10^6$ time steps. A symplectic method would be able to approximately conserve $H = \frac{1}{2}y_2^2 - \cos(y_1)$ and the deviation of H for (2), shown in Figure 2, behaves in a similar way.

3 B-SERIES

3.1 Trees and forests

Recall earlier discussions of "order" based on Figure 1. The aim of this section is to represent the various mappings in Figure 1 in a convenient form so that we can compare the Taylor series for $M_h \circ S_h$ and $S_h \circ E_h$ and find criteria for these agreeing up to a specified order.

In the B-series approach, these Taylor series, are based on trees and forests. Let T denote the set of graphs such as the following

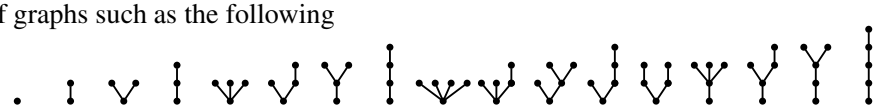

Members of T are "rooted trees" or simply "trees". A forest is a juxtaposition of trees, such as $t_1 t_2 \cdots t_n$ or the empty forest 1.

If the members of a forest $t_1 t_2 \cdots t_n$ are attached to a new root, we obtain a tree written as $[t_1 t_2 \cdots t_n]$ or, in Hopf Algebra language, $B^+(t_1 t_2 \cdots t_n)$. Thus $[t_1 t_2 \cdots t_n]$ is the tree

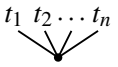

The order of t, written $|t|$, is the number of vertices and the symmetry, $\sigma(t)$, is the order of the automorphism group of t. These, together with $t!$, the factorial of t, can be defined and evaluated recursively:

$$
\begin{aligned}
|\tau| &= 1, & |t| &= \sum_{i=1}^{n} |t_i|, & t &= [t_1 t_2 \cdots t_n], \\
\sigma(\tau) &= 1, & \sigma(t) &= \prod_{i=1}^{n} m_i! \sigma(t_i)^{m_i}, & t &= [t_1^{m_1} t_2^{m_2} \cdots t_n^{m_n}], \\
\tau! &= 1, & t! &= |t| \prod_{i=1}^{n} t_i!, & t &= [t_1 t_2 \cdots t_n].
\end{aligned}
$$

For the empty tree $\varnothing$, $|\varnothing| = 0$, $\sigma(\varnothing) = 1$, $\varnothing! = 1$.

3.2 Elementary differentials and B-series

Throughout this paper, $\mathbf{f}$ will denote $f(y_0)$. Similarly the linear operator equal to the matrix of partial derivatives evaluated at y_0 will be written as $\mathbf{f}'$. The higher derivatives are multilinear operators and we also evaluate these at y_0: $\mathbf{f}^{(n)} = f^{(n)}(y_0)$.

Definition 4 *The elementary differential* $\mathbf{F}(t)$ *evaluated at* y_0 *is equal to*

$$
\mathbf{F}(t) = \begin{cases} \mathbf{f}, & t = \tau, \\ \mathbf{f}^{(n)} \mathbf{F}(t_1) \mathbf{F}(t_2) \cdots \mathbf{F}(t_n), & t = [t_1 t_2 \cdots t_n]. \end{cases}
$$

Definition 5 *The B-series based on B-series coefficients* $a : \varnothing \cup T \to \mathbb{R}$ *is defined by*

$$
B(a, h, y_0) = a(\varnothing) y_0 + \sum_{t \in T} \frac{a(t) h^{|t|}}{\sigma(t)} \mathbf{F}(t).
$$

To construct series that will represent the terms in $M_h \circ S_h$ and $S_h \circ E_h$, we need to be able to find the B-series coefficients for E_h, the components of S_h and the output from the operation $M_h \circ S_h$. Compositions will be represented by substituting a B-series to replace y_0 in a second B-series. If the coefficients in these two series are a and b then the product ab will be defined by

$$B(ab,h,y_0) = B(b,h,B(a,h,y_0)). \tag{3}$$

To write the formulae for $(ab)(t)$ we need to use subtrees formed by removing some of the vertices in t to yield a connected tree u which shares the same root as t, together with a forest $t \setminus u$ representing the connected components of the vertices removed. The value of $a(t_1 t_2 \cdots t_n)$ is defined to be $\prod_{i=1}^{n} a(t_i)$. It is always assumed that ab has a meaning only if $a(\varnothing) = 1$. With these assumptions and notations we have

Theorem 6 *The product ab is given by*

$$\begin{aligned}(ab)(\varnothing) &= b(\varnothing),\\ (ab)(t) &= a(t)b(\varnothing) + \sum_{u \le t} a(t \setminus u)b(u).\end{aligned}$$

3.3 Some special B-series

We will start by introducing the B-series for E_h, denoted by E.

Theorem 7 *The value of* E *is given by*

$$\begin{aligned}\mathrm{E}(\varnothing) &= 1,\\ \mathrm{E}(t) &= \frac{1}{t!}, \quad t \in T.\end{aligned}$$

A basic operation used in every numerical method is the calculation of $hf(a)$ where $a(\varnothing) = 1$. This can be seen as the product aD, where D is the B-series

$$B(\mathrm{D},h,y_0) = hf(y_0),$$

so that we have

Theorem 8 *The value of* D *is given by*

$$\begin{aligned}\mathrm{D}(\varnothing) &= 0,\\ \mathrm{D}(\tau) &= 1,\\ \mathrm{D}(t) &= 0, \quad |t| > 1.\end{aligned}$$

We can now find a convenient formula for aD by applying Theorem 6, to Theorem 3.3.

Theorem 9 *Given that* $a(\varnothing) = 1$*, the value of* aD *is given by*

$$\begin{aligned}(a\mathrm{D})(\varnothing) &= 0,\\ (a\mathrm{D})(t) &= a(t_1)a(t_2)\ldots a(t_n), \quad t = [t_1 t_2 \ldots t_n].\end{aligned}$$

3.4 B-series representation of order conditions

Denote the B-series for the starting method S_h by ξ. This is a vector of dimension r of mappings from $\varnothing \cup T$ to $\mathbb{R}$. Also the stage vectors Y are represented by the s dimensional vector η. This will mean that the vector of scaled stage derivatives hF is given by the component-by-component product ηD. From these elements we can write the B-series representation of (1) as $B\eta\mathrm{D} + V\xi$, where $\eta = A\eta\mathrm{D} + U\xi$. Our aim of obtaining a representation of the order condition $S_h \circ E_h - M \circ S_h = \varepsilon_h = O(h^{p+1})$ can now be completed, where we will write the B-series coefficients for ε_h by the symbol ε.

Theorem 10 *The method (A,U,B,V) given by (1) is of order p relative to S_h if*

$$\eta = A\eta\mathrm{D} + U\xi,$$
$$\mathrm{E}\xi = B\eta\mathrm{D} + V\xi + \varepsilon,$$

where $\varepsilon(\varnothing) = \varepsilon(t) = 0$, for $|t| \le p$.

4 NEW SIXTH ORDER G-SYMPLECTIC METHOD

Runge–Kutta methods satisfying $\mathrm{diag}(b)A + A^{\mathsf{T}}\mathrm{diag}(b) = bb^{\mathsf{T}}$ and characterized by their ability to conserve quadratic invariants [7] and symplectic behaviour [8], have a simplified set of order conditions [9] because many families of conditions become equivalent. In [3] it was shown how to generalize this result to general linear methods.

Many fourth order G-symplectic methods have been derived with promising numerical performance. However, sixth order is a challenge and at present only a single method has been derived in detail [4, 6].

For the new method, the values $r = 4$ and $s = 5$ were chosen because they gave enough freedom to satisfy the requirements of order and efficiency. Since the eigenvalues of V must be on the unit circle, the simple choice ± 1 and $\pm \mathrm{i}$ was made.

Considerable simplifications were possible by requiring the method to be symmetric [2] and to be built on B-series consistent with the $C(2)$ condition first introduced in [1].

Amongst many experiments performed with the new method, a single one is presented here, based on the Hénon–Heiles problem given by

$$H(p,q) = \tfrac{1}{2}\left(p_1^2 + p_2^2\right) + \tfrac{1}{2}\left(q_1^2 + q_2^2\right) + q_1^2 q_2 - \tfrac{1}{3}q_2^3, \qquad q_0 = \left[0, \tfrac{3}{10}\right]^{\mathsf{T}}, \quad p_0 = \left[\sqrt{\tfrac{69}{500}}, \tfrac{1}{5}\right].$$

In Figure 3, with computations by H. Podhaisky, the variation in $H(p,q)$ is shown for $4 \cdot 10^8$ time steps with $h = 0.025$.

The result of this and other numerical tests have given very encouraging results for millions of time steps and it is tempting to assume that there is no real limit as to how far stable behaviour would continue.

However, this is an unrealistic expectation because, from the analysis in [5], parasitism will eventually take over and destroy the integrity of the numerical results.

I am grateful to Yousaf Habib, Adrian Hill, Gulshad Imran, Terry Norton and Helmut Podhaisky. for collaborations which contributed to this paper.

References

[1] Butcher, J. C., *Implicit Runge–Kutta processes*, Math. Comp. 18 (1964), pp. 50–64.

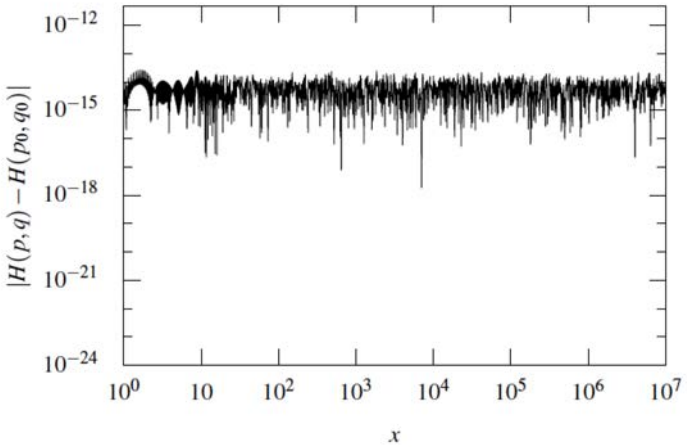

Figure 3: Variation in $H(p,q)$ for $4 \cdot 10^8$ time steps.

[2] Butcher, J. C., Hill, A.T. and Norton, T. J.T., *Symmetric general linear methods*, BIT Numer. Math., DOI :10.1007/s10543-016-0613-1.

[3] Butcher, and Imran, G, *Order conditions for G-symplectic methods*, BIT Numer. Math. 55 (2015), pp. 927–948.

[4] Butcher, Imran, G. and Podhaisky, H. *A G-symplectic method of order 6*, BIT (2016) doi:10.1007/s10543-016-0630-0).

[5] D'Ambrosio, R. and Hairer, E., *Long-term stability of multi-value methods for ordinary differential equations*, J. Sci. Comput. 60 (2014), pp. 627–640 .

[6] Imran, G., *Accurate and efficient methods for differential systems with special structures*, Ph.D. thesis, University of Auckland, 2014.

[7] Lasagni, F. M., *Canonical Runge–Kutta methods*, Z. Angew. Math. Phys. 39 (1988) pp. 952–953.

[8] Sanz-Serna, J, M., *Runge–Kutta schemes for Hamiltonian systems*, BIT 39 (1988), pp. 877–883.

[9] Sanz-Serna, J, M. and Abia, L., *Order conditions for canonical RK schemes*, SIAM J Numer. Anal. 28 (1991), pp. 1081–1096.

Structure-preserving Galerkin methods based on variational structure

Yuto Miyatake

Nagoya University, Furo-cho, Chikusa-ku, Nagoya, 464-8603, Japan
miyatake@na.nuap.nagoya-u.ac.jp

1 Introduction

For evolutionary partial differential equations (PDEs) that enjoy the energy preservation or dissipation property, numerical schemes inheriting the property are often advantageous in that they give qualitatively better numerical solutions than more general purpose methods. In the last two decades, much effort has been devoted in this topic to find out several frameworks to derive energy-preserving/dissipative schemes [2, 3, 4, 5]. These frameworks have been extended in various ways, applied to many PDEs, and correct long time behaviour is often observed. However, most of the frameworks, such as the discrete variational derivative method, are based on finite difference methods, and thus the application to spatial discretization has been restricted to uniform meshes. This is problematic especially in multidimensional problems, since such a restriction requires rectangular domains. Even in one-dimensional cases, nonuniform meshes are often useful when solutions exhibit locally complicated behaviour. For these reasons, several researchers have extended the energy-preserving/dissipative methods to nonuniform meshes [6, 11]. Among them, in this talk, we consider the Galerkin framework proposed by Matsuo [6], which we refer to as the discrete partial derivative method. In this talk, we point out a drawback of the original discrete partial derivative method, solve the defect to make the method completely systematic, and mention further extensions and recent applications, based on the papers [1, 7, 8, 9, 10].

2 Discrete partial derivative method and its limitation

We consider PDEs of the form

$$u_t = \mathcal{D}\frac{\delta \mathcal{H}}{\delta u}, \quad \mathcal{H}[u] = \int H(u, u_x, \dots)\,\mathrm{d}x, \tag{1}$$

where $\mathcal{D}$ is a differential operator. If $\mathcal{D}$ is skew-symmetric, (1) has a conservation property $\frac{\mathrm{d}}{\mathrm{d}t}\mathcal{H}[u] = 0$ under appropriate boundary conditions. On the other hand, if $\mathcal{D}$ is negative semidefinite, (1) has a dissipation property $\frac{\mathrm{d}}{\mathrm{d}t}\mathcal{H}[u] \leq 0$ again under appropriate boundary conditions. In what follows, we call $\mathcal{H}$ the energy and consider only conservative PDEs defined on the torus $\mathbb{T}$ just for simplicity.

Basic procedure of the discrete partial derivative method [6] is as follows.

- We first construct an H^1-weak form that explicitly expresses the desired preservation property. Here, H^1 denotes the first order Sobolev space.
- We then spatially discretize the weak form such that the resulting semi-discrete scheme is consistent in some finite-dimensional approximation spaces of H^1, and it retains the preservation property.
- Finally, we temporally discretize the semi-discrete scheme such that the desired property is retained. This step is essentially that of the discrete gradient method.

However, finding an appropriate H^1-weak form is not straightforward, which complicates the application of the discrete partial derivative method. To explain the difficulty, we start discussion with the simplest case $\mathcal{D} = \partial_x$ and $H = H(u, u_x)$. In this case, the following weak form is straightforward.

Weak form 2.1 Suppose that $u(0, \cdot)$ is given in $H^1(\mathbb{T})$. Find $u(t, \cdot), p \in H^1(\mathbb{T})$ such that for any $v_1, v_2 \in H^1(\mathbb{T})$,

$$\begin{aligned}(u_t, v_1) &= (p_x, v_1),\\ (p, v_2) &= \left(\frac{\partial H}{\partial u}, v_1\right) + \left(\frac{\partial H}{\partial u_x}, (v_2)_x\right).\end{aligned}$$

Here, $(f, g) := \int_{\mathbb{T}} fg \,\mathrm{d}x$ denotes the L^2 inner product.

The conservation property of this weak form can be explicitly obtained:

$$\frac{\mathrm{d}}{\mathrm{d}t}\int_{\mathbb{T}} H(u, u_x)\,\mathrm{d}x = \left(\frac{\partial H}{\partial u}, u_t\right) + \left(\frac{\partial H}{\partial u_x}, u_{xt}\right) = (p, u_t) = (p, p_x) = 0.$$

However, if $\mathcal{D}$ is more complicated, or H consists of higher order derivatives, finding an appropriate H^1-weak form becomes increasingly difficult.

One solution to overcome this difficulty is to adopt smoother function spaces, however, we prefer H^1 because of the following reasons.

- The H^1-formulation can be implemented by computationally inexpensive P1 elements. This advantage is mandatory in multidimensional problems.
- For high-order PDEs with H^1 solutions, such as peakons of the Camassa–Holm equation, H^1-formulations are preferable.

3 Overcoming the difficulty by using L^2-projection operators

The above difficulty can be overcome by using L^2-projection operators.

Let X be a finite dimensional approximation space of $H^1(\mathbb{T})$. The L^2-projection operator is defined as $\mathcal{P}_X : L^2(\mathbb{T}) \to X \subset H^1(\mathbb{T})$ satisfying

$$(u, v) = (\mathcal{P}_X u, v)$$

for any $v \in X$. Furthermore, we denote $\mathcal{P}_X u_x$ by $\mathcal{D}_X u$, namely $\mathcal{D}_X := \mathcal{P}_X \partial_x : H^1(\mathbb{T}) \to X$. We can regard $\mathcal{D}_X^p (:= (\mathcal{D}_X)^p)$ as the operator that approximates ∂_x^p. It follows that

$$(\mathcal{D}_X u, v) = -(u, \mathcal{D}_X v), \quad \left(\mathcal{D}_X^2 u, v\right) = \left(u, \mathcal{D}_X^2 v\right), \tag{2}$$

for any $u, v \in X$.

Below, we illustrate the use of L^2-projection operators, taking the Camassa–Holm (CH) equation

$$u_t - u_{xxt} = uu_{xxx} + 2u_x u_{xx} - 3uu_x$$

as our working example. The CH can be written as the variational form

$$(1-\partial_x^2)u_t = (m\partial_x + \partial_x m)(1-\partial_x^2)^{-1}\frac{\delta \mathcal{H}}{\delta u}, \quad \mathcal{H}[u] = \int_{\mathbb{T}} \frac{u^2+u_x^2}{2}\,\mathrm{d}x,$$

where $m = (1-\partial_x^2)u$. Introducing an intermediate variable p, we can further translate the variational form into the system

$$\begin{aligned}(1-\partial_x^2)u_t &= (m\partial_x + \partial_x m)p,\\ (1-\partial_x^2)p &= \frac{\delta \mathcal{H}}{\delta u}.\end{aligned}$$

We then consider the following *formal* weak form.

Formal weak form 3.1 *Find u, p such that, for any v_1, v_2,*

$$\begin{aligned}\big((1-\partial_x^2)u_t, v_1\big) &= ((m\partial_x + \partial_x m)p, v_1),\\ \big((1-\partial_x^2)p, v_2\big) &= \left(\frac{\partial H}{\partial u}, v_2\right) + \left(\frac{\partial H}{\partial u_x}, (v_2)_x\right).\end{aligned}$$

Obviously, this formulation is not formulated within H^1 space, and thus it makes sense only formally (this is the reason why we call it a *formal* weak form). However, if we ignore this defect, we see that $\frac{\mathrm{d}}{\mathrm{d}t}\mathcal{H}[u] = 0$ by formal calculations:

$$\begin{aligned}\frac{\mathrm{d}}{\mathrm{d}t}\mathcal{H}[u] &= \left(\frac{\partial H}{\partial u}, u_t\right) + \left(\frac{\partial H}{\partial u_x}, u_{xt}\right)\\ &= \big((1-\partial_x^2)p, u_t\big) = \big(p, (1-\partial_x^2)u_t\big) = ((m\partial_x + \partial_x m)p, p) = 0.\end{aligned}$$

Here, the symmetry of $(1-\partial_x^2)$ and the skew-symmetry of $(m\partial_x + \partial_x m)$ are used.

In [9], we showed that, by making use of the formal weak form and L^2-projection operators, an intended energy-preserving H^1 semi-discrete scheme can be readily obtained. The procedure is to just replace ∂_x in the formal weak form with $\mathcal{D}_X$. For the above formal weak form to the CH equation, we immediately get the following semi-discrete scheme.

Semi-discrete scheme 3.1 Suppose $u(0,\cdot) \in X$ is given. We find $u(t,\cdot), p \in X$ such that, for any $v_1, v_2 \in X$,

$$\begin{aligned}\big((1-(\mathcal{D}_X)^2)u_t, v_1\big) &= ((m\partial_x + \partial_x m)p, v_1),\\ \big((1-(\mathcal{D}_X)^2)p, v_2\big) &= \left(\frac{\partial H}{\partial u}, v_2\right) + \left(\frac{\partial H}{\partial u_x}, (v_2)_x\right),\end{aligned}$$

where $m = (1-(\mathcal{D}_X)^2)u$.

This scheme is now consistent in $X(\subset H^1)$, and the energy-preservation property is still retained, thanks to the properties (2).

Applying the discrete gradient method for the temporal discretization leads to a fully discrete energy-preserving Galerkin scheme. We would also like to note that after finding an intended semi-discrete scheme, an underlying H^1-weak form can also be easily obtained.

4 Comments and Future work

The proposed method is applicable to numerous conservative and dissipative PDEs, but mathematical analyses such as unique solvability and convergence have not been studied so far.

We have also succeeded in extending the proposed method to the (local) discontinuous Galerkin framework [1], and by this extension we can automatically derive spatially high-order schemes. However, since linear/nonlinear equations associated with discontinuous Galerkin schemes are often ill-conditioned, care must be taken for the choice of linear/nonlinear solvers.

Based on the proposed method, with a little ingenuity, we could derive several energy-preserving/dissipative H^1-Galerkin schemes, and substantial differences between the numerical solutions obtained by different schemes are sometimes observed (see, for example, [7] for the application to the Hunter–Saxton equation). Thus, comparing several weak forms (and the corresponding Galerkin schemes) theoretically would also be interesting.

References

[1] Aimoto, Y., Matsuo, T. and Miyatake, Y., A local discontinuous Galerkin method based on variational structure, Discrete Contin. Dyn. Syst. Ser. S, 8 (2015), pp. 817–832.

[2] Celledoni, E., Grimm, V., McLachlan, R. I., McLaren, D. I., O'Neale, D., Owren, B. and Quispel, G. R. W., Preserving energy resp. dissipation in numerical PDEs using the "average vector field" method, J. Comput. Phys., 231 (2012), pp. 6770–6789.

[3] Christiansen, S. H., Munthe-Kaas, H. and Owren, B., Topics in structure-preserving discretization, Acta Numer., 20 (2011), pp. 1–119.

[4] Furihata, D., Finite difference schemes for $\partial u/\partial t = (\partial/\partial x)^\alpha \delta G/\delta u$ that inherit energy conservation or dissipation property, J. Comput. Phys., 156 (1999). pp. 181–205.

[5] Furihata, D. and Matsuo, T., Discrete Variational Derivative Method, CRC Press, Boca Raton, FL, 2011.

[6] Matsuo, T., Dissipative/conservative Galerkin method using discrete partial derivatives for nonlinear evolution equations, J. Comput. Appl. Math., 218 (2008), pp. 506–521.

[7] Miyatake, Y., Eom, G., Sogabe, T. and Zhang, S.-L., Energy-preserving H^1-Galerkin schemes for the Hunter–Saxton equation arXiv:1610.09918, 2016.

[8] Miyatake, Y. and Matsuo, T., Energy-preserving H^1-Galerkin schemes for shallow water wave equations with peakon solutions, Phys. Lett. A, 376 (2012), pp. 2633–2639.

[9] Miyatake, Y. and Matsuo, T., A general framework for finding energy dissipative/conservative H^1-Galerkin schemes and their underlying H^1-weak forms for nonlinear evolution equations, BIT, 54 (2014), pp. 1119–1154.

[10] Miyatake, Y., Yaguchi, T. and Matsuo, T., Numerical integration of the Ostrovsky equation based on its geometric structures, J. Comput. Phys., 231 (2012), pp. 4542–4559.

[11] Yaguchi, T. Matsuo, T. and Sugihara, M., An extension of the discrete variational method to nonuniform grids, J. Comput. Phys., 229 (2010), pp. 4382–4423.

Fast and structure-preserving schemes for PDEs based on discrete variational derivative method

Daisuke Furihata

Osaka University, 1-32 Machikaneyama, Toyonaka, Osaka 560–0043 JAPAN
furihata@cmc.osaka-u.ac.jp

1 Introduction

For nonlinear partial differential equations, we would like to construct some "structure preserving," "stable" and "fast" numerical schemes. As you know, we have to struggle with "nonlinearity" of the problems/schemes to obtain "fast" schemes. To see the computation cost to solve numerical schemes for nonlinear PDE problems, consider the following two toy problems, as common target nonlinear PDEs.

Toy problem type 1: These PDEs are "high order polynomial" problems. Let us consider the following toy PDE for unknown function $u = u(x,t)$:

$$\frac{\partial u}{\partial t} = \frac{\partial^2}{\partial x^2}\left(u^7\right). \tag{1}$$

Toy problem type 2: These PDEs are nonlinear and "non-polynomial" problems.

$$\frac{\partial u}{\partial t} = \frac{\partial^2}{\partial x^2}\left(e^u\right). \tag{2}$$

1.1 Conventional Discrete Variational Derivative Method

Via the conventional DVDM [1] for equations like $\dfrac{\partial u}{\partial t} = \left(\dfrac{\partial^2}{\partial x^2}\right)^2 \dfrac{\delta G}{\delta u}$, we propose the following scheme

$$\frac{U_k^{(n+1)} - U_k^{(n)}}{\Delta t} = \delta_k^{\langle 2\rangle} \frac{\delta G_{\mathrm{d}}}{\delta(\boldsymbol{U}^{(n+1)}, \boldsymbol{U}^{(n)})_k} \tag{3}$$

where $U_k^{(n)}$ is approximation of $u(k\Delta x, n\Delta t)$, $\dfrac{\delta G}{\delta u}$ is the variational derivative and $\dfrac{\delta G_{\mathrm{d}}}{\delta(\boldsymbol{U},\boldsymbol{V})_k}$ is the discrete varitaional derivative. For the toy problem type 1 equation: $\dfrac{\partial u}{\partial t} = \dfrac{\partial^2}{\partial x^2}\left(u^7\right) = \dfrac{\partial^2}{\partial x^2}\left(\dfrac{\delta u^8/8}{\delta u}\right)$, via

$$\sum_{k=0}^{N}{}'' \left(\frac{U_k^8}{8} - \frac{V_k^8}{8}\right)\Delta x = \sum_{k=0}^{N}{}'' \frac{\delta G_{\mathrm{d}}}{\delta(\boldsymbol{U},\boldsymbol{V})_k}(U_k - V_k)\Delta x, \tag{4}$$

we obtain the discrete variational derivative

$$\frac{\delta G_{\rm d}}{\delta(\boldsymbol{U},\boldsymbol{V})_k} = \frac{u^7+u^6v+u^5v^2+u^4v^3+u^3v^4+u^2v^5+uv^6+v^7}{8}, \tag{5}$$

where $u = U_k$, $v = V_k$, and we obtain the following DVDM scheme.

$$\frac{u-v}{\Delta t} = \delta_k^{\langle 2\rangle}\left\{\frac{u^7+u^6v+u^5v^2+u^4v^3+u^3v^4+u^2v^5+uv^6+v^7}{8}\right\} \tag{6}$$

where $u \stackrel{\rm def}{=} U_k^{(n+1)}, v \stackrel{\rm def}{=} U_k^{(n)}$. This result means that we have to solve a system of high-order polynomial equations to obtain new time step solutions. For the toy problem type 2, the DVDM scheme should be

$$\frac{u-v}{\Delta t} = \delta_k^{\langle 2\rangle}\left(\frac{e^u-e^v}{u-v}\right), \tag{7}$$

and we have to solve a system of non-polynomial nonlinear equations via this scheme. We would like to avoid this strong nonlinearity of these schemes.

1.2 Linearized DVDM

The "linearization technique" means decompositions of polynomial terms by introducing extra time steps of numerical schemes, and we can design linear or lineraly-implicit for polynomial-nonlinear PDEs using this technique [2, 3]. Let us see what happens if we use this technique for the toy problems. For the toy problem type 1 equation, via the **"symmetric"** decomposition: $u^8 \longrightarrow u^2\,v^2w^2\zeta^2$, we obtain the following linearized scheme:

$$\frac{u-\xi}{4\Delta t} = \delta_k^{\langle 2\rangle}\left\{\frac{v^2w^2\zeta^2(u+\xi)}{2}\right\}, \tag{8}$$

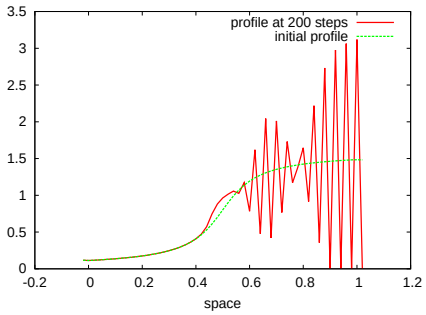

Figure 1. Unstable solution via the linearized scheme (8) where $\Delta x = 0.02$, $\Delta t = 5.0\times10^{-7}$.

where $u \stackrel{\rm def}{=} U_k^{(n+4)}, v \stackrel{\rm def}{=} U_k^{(n+3)}, w \stackrel{\rm def}{=} U_k^{(n+2)}, \zeta \stackrel{\rm def}{=} U_k^{(n+1)}, \xi \stackrel{\rm def}{=} U_k^{(n)}$. This is a "linear-implicit" system and easy-to-obtain new time step solutions, but this scheme is unstable, as we see in the Fig.1, because "extra 3" timesteps may be too many for this problem. For the toy problem 2, we cannot apply the linearization technique since the problem is not a polynomial equation. These results mean that we cannot expect the linearization technique to struggle with the strong nonlinearity.

2 Asymmetric Linearized DVDM

There are, of course, some simple ideas to weaken or overcome the nonlinear difficulties. The first one is a relaxation of the linearization technique. We must decompose the polynomial symmetrically by the original linearization technique; here we extend it so that we can decompose the term asymmetrically. For example, we can decompose the

polynomial term in the following manner for the toy problem 1: $u^8 \longrightarrow U_k^{(n+1)} (U_k^{(n)})^7$, and we obtain an "explicit" DVDM scheme. If we decompose as $u^8 \longrightarrow (U_k^{(n+1)})^2 (U_k^{(n)})^6$, we obtain a "quadratic" DVDM scheme. Both of obtained schemes are not strongly nonlinear and relatively easy to obtain numerical solutions. We can apply this idea to the toy problem 2, i.e., we can decompose the nonlinear-nonpolynomial terms as: $e^u \longrightarrow U_k^{(n+1)} \left(\dfrac{e^{U_k^{(n)}} - 1}{U_k^{(n)}} \right) + 1$, or, $e^u \longrightarrow (U_k^{(n+1)})^2 \left(\dfrac{e^{U_k^{(n)}} - 1 - U_k^{(n)}}{(U_k^{(n)})^2} \right) + 1 + U_k^{(n)}$. Base on this asymmetric decomposition, the definition of the discrete variational derivative shold be changed. We cannot describe the mathematical definition completely here due to space limitation and let us show one example when we decompose the energy function as $G(u, v) = u^2 f(v)$. In this case, we can show:

$$G(u, v) - G(v, w) = \frac{\delta G}{\delta(\boldsymbol{u})} \delta U(\boldsymbol{u}) \tag{9}$$

where

$$\frac{\delta G}{\delta(\boldsymbol{u})} \stackrel{\text{def}}{=} C(v, w)(u + v) \left(\frac{f(v) + f(w)}{2} \right), \tag{10}$$

$$\delta U(\boldsymbol{u}) \stackrel{\text{def}}{=} \frac{1}{C(v, w)} \left\{ (u - v) + \left(\frac{u^2 + v^2}{u + v} \right) \left(\frac{f(v) - f(w)}{f(v) + f(w)} \right) \right\}, \tag{11}$$

and $C(v, w)$ is a correction coefficient. This means that the relaxed DVDM schemes for toy problems should be

$$\frac{\delta U(\boldsymbol{u})}{\Delta t} = \delta_k^{\langle 2 \rangle} \frac{\delta G}{\delta(\boldsymbol{u})} \tag{12}$$

where $u \stackrel{\text{def}}{=} U_k^{(n+2)}, v \stackrel{\text{def}}{=} U_k^{(n+1)}, w \stackrel{\text{def}}{=} U_k^{(n)}$. These schemes nonlinearity are obviously weakened, i.e., they are explicit or quadratic, and we can expect that they are faster schemes than the conventional DVDM schemes. We introduced just one extra time step in this context, and we can expect that the obtained schemes' instability is not so strong. For example, we use this relaxed technique to the higher Cahn–Hilliard equation

$$\frac{\partial u}{\partial t} = \frac{\partial^2}{\partial x^2} \left(u^7 - u + q \frac{\partial^2 u}{\partial x^2} \right), \tag{13}$$

where $q < 0$, and it is stable with some appropriate parameters $(\Delta x, \Delta t)$. The obtained solutions are shown in the Fig. 2. The scheme is quadratic and about 30 times faster to obtain numerical solutions than the conventional DVDM scheme.

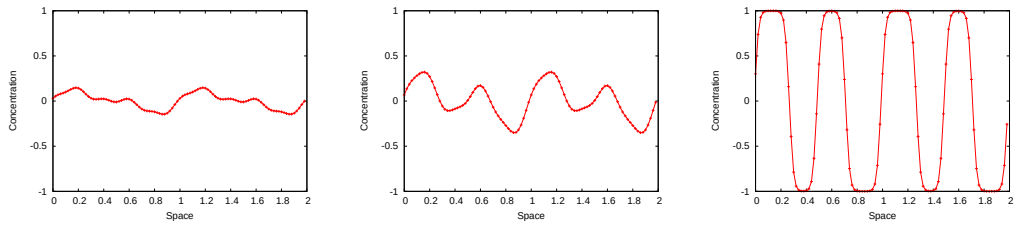

Initial profile Time step = 10000 100000

Figure 2. Solutions by the relaxed DVDM scheme for the higher Cahn–Hilliard equation.

3 Asymmetric Conventional DVDM

Another idea is a relaxation of the discrete variational derivative itself. In this context, we don't have to introduce any extra time step. On the conventional DVDM theory, we consider the following equality under summation: $G(u) - G(v) = (\delta G/\delta(u,v))\,(u-v)$, however, here we relax it as $G(u) - G(v) = (\delta G/\delta(\boldsymbol{u}))\,(\delta \boldsymbol{u})$, where $\delta G/\delta(\boldsymbol{u})$ should be an approximation of $\delta G/\delta u$ and $\delta \boldsymbol{u}$ should be an approximation of $\Delta t \partial u/\partial t$.

Let us show some examples. For the toy problem 1, we can show $u^8 - v^8 = (\delta G/\delta(\boldsymbol{u}))\,(\delta \boldsymbol{u})$ where $\delta G/\delta u = 8v^7$ and $\delta \boldsymbol{u} = \left(u^7 + u^6 v + u^5 v^2 + u^4 v^3 + u^3 v^4 + u^2 v^5 + u v^6 + v^7\right)(u - v)/8v^7$. For the toy problem 2, we can define $e^u - e^v = (\delta G/\delta(\boldsymbol{u}))\,(\delta \boldsymbol{u})$ where $\delta G/\delta u = e^v$ and $\delta \boldsymbol{u} = \left(e^{u-v} - 1\right)$. These definitions bring us **explicit DVDM schemes**, for example, the obtained scheme for the toy problem 2, i.e., an exponential heat equation problem, is

$$U_k^{(n+1)} = U_k^{(n)} + \log\left\{1 + \Delta t\, \delta_k^{\langle 2\rangle}\left(e^{U_k^{(n)}}\right)\right\}, \tag{14}$$

and the obtained numerical solutions are shown in Fig. 3. Comparing among some structure-preserving schemes for the exponential heat problem, this explicit DVDM scheme is the fastest to obtain numerical solutions.

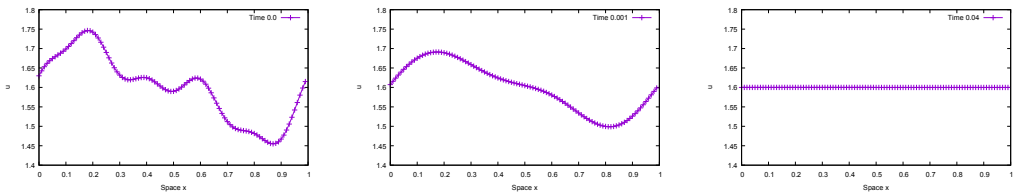

Initial profile Time step = 100 4000

Figure 3. Solutions by the explicit DVDM scheme for the toy problems 2.

We confirmed that the total energy of the solutions $\sum_{k=0}^{N} {}'' \exp(U_k^{(n)})\Delta x$ decreases monotonically and the total mass $\sum_{k=0}^{N} {}'' U_k^{(n)} \Delta x$ is conserved strictly through the computation. This idea is extremely flexible and we sometimes obtain superior DVDM schemes, however, we do not have sufficient theoretical knowledge of this idea so far and we should pay much effor to study it.

Acknowledgment

This work was supported by JSPS KAKENHI Grand number 25287030 and 26610038.

References

[1] D. Furihata and T. Matsuo, *Discrete Variational Derivative Method: A Structure-preserving Numerical Method for Partial Differential Equations*, CRC press, Florida, 2010.

[2] D. Furihata and T. Matsuo, *A Stable, Convergent, Conservative and Linear Finite Difference Scheme for the Cahn-Hilliard Equation*, Japan J. Indust. Appl. Math., Vol.20 (2003), pp.65–85.

[3] M. Dahlby and B. Owren, *A general framework for deriving integral preserving numerical methods for PDEs*, SIAM J. Sci. Comput., Vol.33 (2011), pp.2318–2340.

A generic thermostat for smooth vector fields and smooth target densities

FRANK, J. E.[1], LEIMKUHLER, B. J.[2], and MYERSCOUGH, K. W.[3]

1 Mathematical Institute, Utrecht University, P.O. Box 80010,
3508 TA Utrecht, THE NETHERLANDS
j.e.frank@uu.nl

2 School of Mathematics, University of Edinburgh, James Clerk Maxwell Building,
Kings Buildings Edinburgh EH9 3JZ, SCOTLAND
b.leimkuhler@ed.ac.uk

3 Department of Computer Science, KU Leuven, 3001 Leuven, BELGIUM
keith@myerscough.nl

Thermostat methods are routinely employed in molecular dynamics to simulate a system of particles at constant temperature. Molecular dynamics models are typically formulated as a classical mechanical n-body problem in high dimensions. The equations of motion constitute a Hamiltonian system

$$\frac{dy}{dt} = J\nabla H(y), \qquad H : \mathcal{R}^d \to \mathcal{R}, \quad J = -J^T, \tag{1}$$

with preserved total energy H. The motion is thus constrained to a surface of constant H (or the intersection of the level sets if more conserved quantities are present). If the motion is ergodic, then the flow samples the invariant measure

$$\mu(y) \propto \delta(H(y) - H_0), \qquad H(y(0)) = H_0.$$

On the other hand, a system that evolves in thermal equilibrium with respect to a large temperature reservoir of inverse temperature β does not evolve at constant energy. Instead, the states of the system are distributed according to the Gibbs canonical distribution

$$\mu(y) \propto \exp(-\beta H(y)).$$

To simulate a system at constant temperature, it is necessary to introduce some dynamic mechanism to perturb trajectories such that they ergodically sample the canonical distribution.

One well-known technique for canonical sampling is Langevin dynamics [3]. Here the Hamiltonian equations on $\mathcal{R}^d$ are equipped with a stochastic diffusion process. An alternative approach are the Nosé-Hoover type methods [10, 11, 6, 2, 12] where the phase space is augmented by one or more additional thermostat variables such that the projected motion on $\mathcal{R}^d$ again ergodically samples the canonical distribution. Construction of the

Nosé-Hoover dynamics makes explicit use of two properties: (1) the original dynamics is Hamiltonian (specifically, divergence free and Hamiltonian-conserving), and (2) the target distribution (Gibbs) is a smooth function of the conserved quantity H.

In a recent paper [9] we show how information theory can be used in combination with Nosé-Hoover type methods to correct dynamics for observations of the mean values of conserved quantities. Again, the approach of [9] is restricted to unperturbed systems with Hamiltonian structure, and observables that are functions of the conserved quantities. The methodology could be made significantly more generic if these restrictions on the dynamics and probability distributions could be removed. The purpose of this note is to describe a method that provides for this.

Specifically, we derive a thermostat that can be applied to an arbitrary, smooth differential equation to perturb its orbits such that they ergodically sample a generic, smooth target distribution. The target distribution can in principle be any distribution of the form $\rho(y) \sim \exp(-A(y))$, where $A : \mathcal{R}^d \to \mathcal{R}$ is bounded and differentiable. However, the thermostat is most effective when this distribution is 'close' in some sense to the invariant distribution of the unperturbed dynamics. In the §1 we review briefly an information theoretic approach to correcting a prior distribution for a set of observed expectations. In §2 we describe the new thermostat. In §2.1 we discuss ergodicity considerations. The new thermostat is ineffective in the classical setting of a Hamiltonian system and Gibbs distribution. Therefore, in Section §2.2 we describe necessary modifications for this case. Finally we demonstrate the new thermostats for some simple examples in Section §3.

1 BAYESIAN MODELLING

For the purpose of this section, suppose $y \in \mathcal{R}^d$ is a random variable with distribution (law) $y \sim \rho$, where $\rho : \mathcal{R}^d \to \mathcal{R}$ is unknown. Suppose further, that we are given a prior distribution $\pi : \mathcal{R}^d \to \mathcal{R}$, assumed to be close to ρ.

The Kullback-Leibler divergence, or relative entropy,

$$\mathcal{S}[\rho(y)] = \int \rho(y) \ln \frac{\rho(y)}{\pi(y)}\, dy$$

represents a (non-symmetric) distance between measures. In information theory it gives the information lost in approximating $\rho(y)$ by $\pi(y)$.

Next, suppose we are given a set of K observations of y in the form of expectations

$$\mathbb{E}_\rho C_k(y) = \int C_k(y)\rho(y)\, dy = c_k, \quad k = 1, \ldots, K. \tag{2}$$

Then the least biased distribution ρ consistent with the observations c_k and prior π is given by the solution of the constrained minimization problem

$$\rho = \arg\min_\rho \; \mathcal{S} - \lambda_0 \left(1 - \int \rho(y)\, dy\right) - \sum_{k=0}^{K} \lambda_k \left(c_k - \int C_k(y)\rho(y)\, dy\right),$$

where the λ_k are Lagrange multipliers associated with the observations (2). Solving the minimization problem is an exercise in variational calculus. One finds

$$\rho(y) = \lambda_0 \exp\left(-\lambda_1 C_1(y) - \cdots - \lambda_K C_K(y)\right) \pi(y), \tag{3}$$

where the λ_k are chosen such that the observations (2) are satisfied.

2 THERMOSTATS FOR THE POSTERIOR MEASURE

Now suppose that we are given a dynamical system, defined by the solution of a differential equation,

$$\frac{dy}{dt} = F(y),$$

which may be subject to model error. Further suppose we are given a prior distribution $\pi(y)$ that we believe to be close to the invariant distribution of the true dynamics, and a set of K observations of the system of the form (2). We construct a thermostat on the dynamics of y that samples the posterior distribution (3). To do this, let us write $\rho(y) = \exp(-A(y))$, and define the extended distribution $\hat{\rho}(y, \xi) = \rho(y)\exp(-\xi^2/2)$. Then we consider a thermostat of the form

$$dy = F(y)\,dt + \xi^2 G(y)\,dt \tag{4}$$

$$d\xi = \xi X(y)\,dt - \gamma\xi\,dt + \sqrt{2\gamma}\,dw, \tag{5}$$

where $\gamma > 0$ is a diffusion parameter.

The distribution $\hat{\rho}$ is stationary under the Fokker-Planck equation associated to this system if

$$\mathcal{L}^*\hat{\rho} = 0 = -\nabla\cdot\hat{\rho}F(y) - \xi^2\nabla\cdot\hat{\rho}G(y) - \partial_\xi\xi\hat{\rho}X(y), \tag{6}$$

since additional terms in the Fokker-Planck operator cancel automatically due to fluctuation-dissipation balance in the last two terms of (5) (an Ornstein-Uhlenbeck process). A possible solution of this equation is given by

$$X(y) = F\cdot\nabla A - \nabla\cdot F, \qquad \nabla\cdot(F+G) - (F+G)\cdot\nabla A = 0. \tag{7}$$

Hence, defining $X(y)$ by the first condition above and choosing a G to satisfy the second condition ensures stationarity of $\hat{\rho}$.

One possible choice (which we will not use) for G is $G = J\nabla A - F$, where J is any skew-symmetric matrix. Intuitively, since $\mathbb{E}_{\hat{\rho}}\xi^2 = 1$, this choice just replaces the dynamics F with the Hamiltonian dynamics $J\nabla A$ on average. This can obviously have dire consequences for the thermostated dynamics, unless the vector field $G(y)$ is small in some sense.

Having found a G that satisfies the above condition, any other vector field $\tilde{G} = G + B\nabla A$ for any skew-symmetric matrix B also satisfies the condition. This can be used to find an optimal skew-symmetric B, for instance, such that the norm of $\tilde{g}$ is minimized.

2.1 Ergodicity

In the previous section we have formally constructed a dynamics under which the target distribution is stationary. It is also necessary to prove that this distribution is unique and attracting. Because the distributions we consider have global support, we will see that it is sufficient to show a Hörmander condition on the vector fields F and G (see related proofs in [1, 8]). Establishing this condition is problem dependent.

By assumption the desired density $\hat{\rho}(y) > 0$ for all y. Since $\hat{\rho}$ is stationary under the Fokker-Planck operator, ergodicity of $\hat{\rho}$ can be established under the ergodic decomposition theorem if the Hörmander condition holds [7, 4, 5]. Consider the deterministic and

stochastic vector fields

$$U(y,\xi) = \begin{pmatrix} F(y) + \xi^2 G(y) \\ \xi X(y) - \gamma \xi \end{pmatrix}, \quad V(y,\xi) = \begin{pmatrix} 0 \\ \sqrt{2\gamma} \end{pmatrix}$$

The Hörmander condition requires that the Lie algebra generated by U and V span $\mathcal{R}^{n+1}$:

$$\mathcal{R}^{n+1} \subset \mathrm{Lie}\{U,V\} = \mathrm{span}\{U, V, [U,V], [U,[U,V]], [V,[U,V]], \dots\}.$$

Let us suppose that $G(y)$ is chosen such that the vector fields $F(y)$ and $G(y)$ satisfy the Hörmander condition on $\mathcal{R}^n$. Define vector fields $\hat{F} = (F(y), 0)$, $\hat{G} = (G(y), 0)$ in $\mathcal{R}^{n+1}$. We show that

$$\mathcal{R}^{n+1} \subset \mathrm{Lie}\{\hat{F}, \hat{G}, e_{n+1}\} \subset \mathrm{Lie}\{U,V\},$$

where $e_{n+1} = (0, \dots, 0, 1)$ is a canonical unit vector in the auxiliary variable direction. The first inclusion follows from the Hörmander condition on $\mathcal{R}^n$ and is immediate. Since $\gamma > 0$, it follows that V is proportional to e_{n+1}. We compute

$$U_1 = [U, e_{n+1}] = \begin{pmatrix} 2\xi\,[G(y) - F(y)] \\ X(y) - \gamma \end{pmatrix},$$

and

$$U_2 = \frac{1}{2}[U_1, e_{n+1}] = \begin{pmatrix} G(y) - F(y) \\ 0 \end{pmatrix} = \hat{G} - \hat{F}.$$

Next, define

$$V_1 = U - \frac{\xi^2}{2} U_1 - \frac{\xi}{2}(X(y) - \gamma) e_{n+1} = \begin{pmatrix} F(y) \\ 0 \end{pmatrix} = \hat{F}$$

Clearly, U_2 and V_1 are contained in $\mathrm{Lie}\{U,V\}$, as are their higher order commutators. But $V_1 = \hat{f}$ and $U_2 + V_1 = \hat{g}$, combined with e_{n+1}, form the basis for the intermediate Lie algebra, from which the inclusion follows.

2.2 A double thermostat for Hamiltonian systems

The approach of the previous section can fail in the standard canonical thermostating situation when the vector field $F = J\nabla H$ is divergence-free and the posterior measure is the Gibbs measure, i.e. $A(y) = \beta H(y)$. Here it can be checked that $X(y)$ in (7) is identically zero, and hence there is no feedback. We can extend the above approach with a Nosé-Hoover-Langevin thermostat to ensure that in the absence of observations, the system samples a prior $\pi \propto \exp(-\beta H(y))$. To do so, let us take $F(y) = J\nabla H(y)$, $A(y) = \beta H(y) + \lambda C(y)$, and introduce a second auxiliary variable η, with dynamics

$$dy = F(y)\,dt + \eta g(y)\,dt + \xi^2 G(y,\eta)\,dt, \tag{8}$$

$$d\eta = (\nabla \cdot g(y) - g(y) \cdot \nabla A(y))\,dt - \gamma_H \eta\,dt + \sqrt{2\gamma_H} dw_H, \tag{9}$$

$$d\xi = \xi X(y,\eta)\,dt - \gamma_A \xi\,dt + \sqrt{2\gamma_A}\,dw_2. \tag{10}$$

It can be checked that the composite measure $\rho \propto \exp(-\beta H(y) - \lambda C(y) - \eta^2/2 - \xi^2/2)$ is stationary under the associated Fokker-Planck equation if we define $X(y,\eta)$ by

$$X(y,\eta) = \nabla \cdot G(y,\eta) - G(y,\eta) \cdot \nabla A(y),$$

and ensure that $G(y,\eta)$ satisfies

$$\nabla \cdot G(y,\eta) - G(y,\eta) \cdot \nabla A - \lambda f(y) \cdot \nabla C.$$

We give an example below.

3 NUMERICAL EXPERIMENTS

In this section we present some specific examples.
Example 1 Consider a Harmonic oscillator, $y \in \mathcal{R}^2$,

$$y' = F(y) = J\nabla H(y), \qquad H(y) = \frac{1}{2}(y_1^2 + y_2^2), \quad J = \begin{bmatrix} 0 & 1 \\ -1 & 0 \end{bmatrix},$$

and suppose we wish to enforce the invariant measure $\rho(y) = \exp(-\frac{1}{2}(d_1 y_1^2 + y_2^2))$ following an observation of the variance of y_1. We use the method (4)–(5). Taking $A = (d_1 y_1^2 + y_2^2)/2$, we may choose G in the direction of the gradient of the observable $C(y) = y_1^2$ by taking

$$G(y) = (\alpha(y_2), 0)^T.$$

Recalling that $\nabla \cdot F \equiv 0$, the function α must satisfy

$$\nabla \cdot G - (F + G) \cdot \nabla A = 0 = (y_2 + \alpha(y_2), -y_1) \cdot (d_1 y_1, y_2) = d_1 y_1 y_2 + \alpha(y_2) d_1 y_1 - y_1 y_2 = 0$$

which we can solve to obtain

$$\alpha(y_2) = \frac{1 - d_1}{d_1} y_2.$$

We expect this to be a minimally intrusive perturbation. Figure 1 illustrates short trajectories for $d_1 = \{0.9, 0.75, 0.5, 0.25\}$. For the case $d_1 = 0.5$, Figure 2 illustrates the histograms of y_1 and y_2. We see that the variances of y_1, $\sigma_1^2 = 1.8$, and y_2, $\sigma_2^2 = 0.9$ are close to the target values of 2 and 1, respectively.

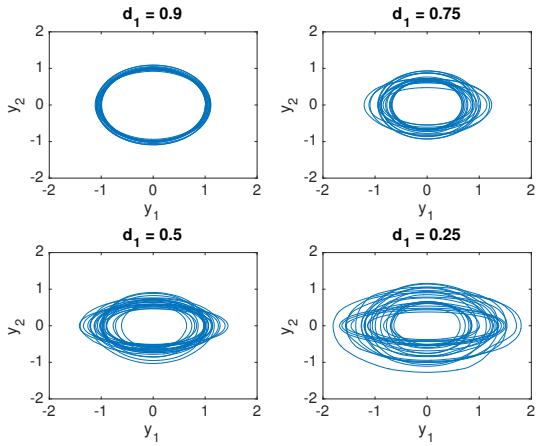

Figure 1: Simulation of harmonic oscillator with $A = (d_1 y_1^2 + y_2^2)/2$ and $\gamma = 0.1$.

Example 2 As a second example, we take a Hamiltonian system in $\mathcal{R}^2$ with double well potential, given by Hamiltonian:

$$H(q, p) = \frac{p^2}{2} + \frac{q^4}{4} - \frac{q^2}{2}. \tag{11}$$

We thermostat this system using (8)–(10). We choose the parameters as follows (note that these satisfy the necessary conditions)

$$g(q, p) = \begin{pmatrix} 0 \\ -p \end{pmatrix}, \quad G(q, p, \eta) = \begin{pmatrix} 0 \\ \frac{\lambda}{\beta}(q - 1) \end{pmatrix}, \quad X(q, p, \eta) = -\gamma p(q - 1).$$

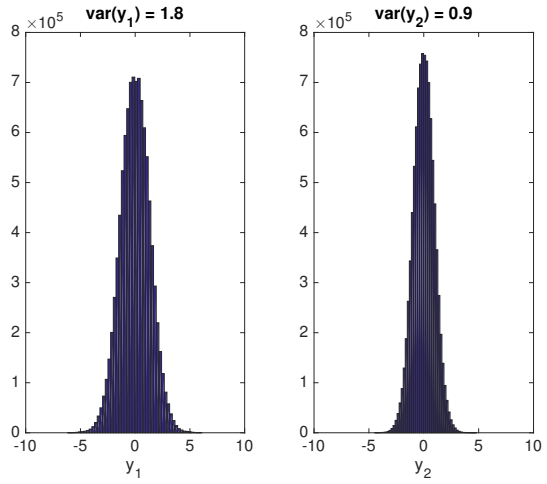

Figure 2: Thermostated harmonic oscillator with $A = (0.5y_1^2 + y_2^2)/2$ and $\gamma = 0.1$. Left: histogram of y_1; right: histogram of y_2.

To sample just the Gibbsian prior distribution we take $\beta = 10$, $\lambda = 0$. We obtain the dynamics and time series labeled *Prior* in Figure 3. The trajectory exhibits transition behavior, spending most of its time in the neighborhood of the fixed points $q = \pm 1$, and occasionally switching between these.

Suppose, now, we enforce the observation $\mathbb{E}(q-1)^2 = 0$. Constructing the posterior distribution as in §1, we take $A(y) = \beta H(y) + \lambda(q-1)^2/2$. In this case, the ratio λ/β can also be thought of as expressing our relative certainty between the prior and posterior distributions π and ρ, or put another way, a measure of the degree of confidence in our observation.

Figure 3 plots the phase trajectory of the dual thermostat (labelled *Posterior*) on top of the canonically thermostated trajectory for the case $\lambda = \beta = 10$. The trajectory now spends all of its time in the potential well around $q = 1$.

References

[1] Bajars, J., Frank, J., and Leimkuhler, B. Weakly coupled heat bath models for Gibbs-like invariant states in nonlinear wave equations. *Nonlinearity*, 26(7):1945, 2013.

[2] Bulgac, A. and Kusnezov, D. Canonical ensemble averages from pseudomicrocanonical dynamics. *Phys. Rev. A*, 42:5045–5048, Oct 1990.

[3] Frenkel, D. and Smit, B. *Understanding Molecular Simulation*. Academic Press, San Diego, second edition edition, 2002.

[4] Hairer, M. Convergence of Markov processes. Lecture notes, University of Warwick, 2010.

[5] Hairer, M. and Mattingly, J. Yet another look at Harris' ergodic theorem for Markov chains. In *Seminar on Stochastic Analysis, Random Fields and Applications VI*, volume 63 of *Progress in Probability*, pages 109–117, 2011.

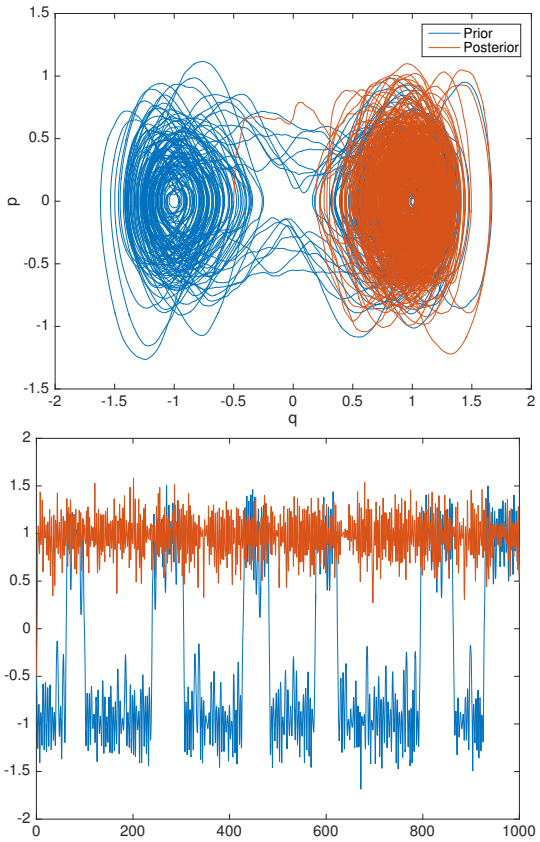

Figure 3: In red, a simulation of the double-well Hamiltonian (11) using the dual thermostat (8)–(9) with parameters $\beta = 10$ and $\lambda = 10$ and observation $\mathbb{E}(q-1)^2 = 0$. We observe that the transition behavior evident in the prior, Gibbs distribution (in blue) is suppressed. Upper plot: phase space orbits; lower plot: time series of $q(t)$.

[6] Hoover, W. Canonical dynamics: equilibrium phase-space distributions. *Physical Review A*, 31(3):1695, 1985.

[7] Kliemann, W. Recurrence and invariant measures for degenerate diffusions. *Annals of Probability*, 15(2):690–707, 1987.

[8] Leimkuhler, B., Noorizadeh, E., and Theil, F. A gentle thermostat for molecular dynamics. *J. Stat. Phys.*, 135(2):261–277, 2009.

[9] Myerscough, K. W., Frank, J., and Leimkuhler, B. Observation-based correction of dynamical models using thermostats. *Proc. R. Soc. A*, 2017.

[10] Nosé, S. A molecular dynamics method for simulations in the canonical ensemble. *Molecular physics*, 52(2):255–268, 1984.

[11] Nosé, S. A unified formulation of the constant temperature molecular dynamics methods. *The Journal of Chemical Physics*, 81(1):511–519, 1984.

[12] Samoletov, A., Dettmann, C., and Chaplain, M. Thermostats for "slow" configurational modes. *Journal of Statistical Physics*, 128(6):1321–1336, 2007.

Geometric-Mechanics-Inspired Model of Stochastic Dynamical Systems

YAGUCHI, T.[1]

1 Kobe University, 1-1 Rokkodai-cho, Nada-ku, Kobe, 657-8501 JAPAN
JST PRESTO, 4-1-8 Honcho, Kawaguchi, Saitama, 332-0012, JAPAN
yaguchi@pearl.kobe-u.ac.jp

1 INTRODUCTION

In this paper, we propose a geometric-mechanics-inspired model for stochastic time series. In the parametric approach for static stochastic systems, statistical models are used for analysis. A statistical model is a parametrised set of probabilistic distributions. As is known in information geometry [1], most of statistical models form a manifold with a suitable Riemannian structure and with a pair of affine connections. The model that is proposed in this paper is a model for stochastic time series, which is itself a time series on that manifold. In this model the point in the sequence corresponding to the time t represents a statistical model that generates the data at t. This time series is estimated in a similar way to the principle of least action with a Lagrangian that is a combination of the log-likelihood and a penalty term related to the smoothness of the series. As an application, the model is used for a statistical test of difference of the dynamics of two given time series.

2 OUTLINE OF THE MODEL

Suppose that a set of time series $x_n, n = 1, \ldots, N$ is given. We assume that for each time series and for each fixed n, x_n is a sample from a probabilistic distribution $P(X; \theta^{(n)})$ in a statistical model M of which parameters are $\theta^{(n)} = (\theta^{(n)}_1, \ldots, \theta^{(n)}_m)$, where m is the number of the parameters. The aim is estimating these $\theta^{(n)}$'s from the given data under the condition that the $\theta^{(n)}$'s are smooth in a certain sense.

To this end, we consider an application of discrete mechanics [2] to this estimation. Discrete mechanics is a framework for deriving numerical integrators for the equation of motion of analytical mechanics. This framework defines the discretised equation of motion on a given configuration manifold by applying the discretised principle of least action, if a discrete Lagrangian is given. As orbits of motions are typically smooth, we apply this approach to design a smooth trajectory on the manifold of the statistical model. Actually, as shown in information geometry, statistical models form manifolds, and hence this approach is available for dynamical series on statistical manifolds. In information geometry, quantities are defined so that they are invariant under the change of statistics between sufficient statistics [1]. In particular, the distance between two points on the

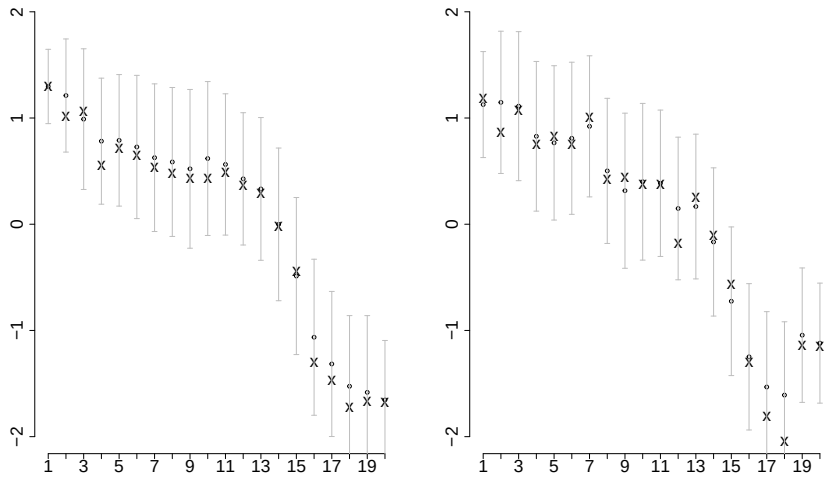

Figure 1: The normalised stock prices of Toyota (left) and Honda (right) and the estimated models are shown. The horizontal axis indicates the date and the vertical axis the normalised prices. The crosses represent the stock values and the circles the estimated mean values. The error bars represent the standard deviation.

manifold can be measured by the Kullback–Leibler divergence. The Lagrangian and the action sum should be defined by using these geometric quantities only. In this paper, we use the following action sum, which is a sum of the log-likelihood and the symmetrised Kullback–Leibler divergence:

$$\text{minimize} \quad \sum_{n=1}^{N-1} \frac{1}{2h} \left(D(\theta^{(n+1)} \,||\, \theta^{(n)}) + D(\theta^{(n)} \,||\, \theta^{(n+1)}) \right) - \sum_{n=1}^{N} \ln L(\theta^{(n)}),$$

where $D(\cdot \,||\, \cdot)$ is the Kullback–Leibler divergence and h is a parameter that determines the balance of the two terms. $L(\cdot)$ is the likelihood.

3 APPLICATION TO A TEST OF THE DIFFERENCE OF TWO TIME SERIES

As an application, we tried to fit this model to the stock prices of Toyota and Honda on July, 2016. All the calculations are performed by using R. We use the set of normal distributions as the statistical model M and the parameter $h = 1.0$. The data are normalised so that the mean values are 0 and the standard deviations 1. The data and the results are shown in Figure 1.

As shown in these figures, the dynamics of the normalised data of these stock prices are somewhat similar to each other. With that, we performed a statistical test of the difference of these two time series. The test is a Kolmogorov–Smirnov-type test. We used the Kullback–Leibler divergence as the test statistics. More precisely, the procedure of the test which we performed is as the following.

1. Let $\theta_{\mathrm{T}}^{(n)}$'s and $\theta_{\mathrm{H}}^{(n)}$'s be the estimated parameters for the Toyota and Honda data.

2. The null hypothesis H_0 is that the data of the Honda stock price are generated by the distribution with $\theta_{\mathrm{T}}^{(n)}$'s.

3. Set the level of significance α.

4. Compute the p-value by the Monte–Carlo method.

   (a) Generate samples from the model with $\theta_{\mathrm{T}}^{(n)}$'s.

   (b) For each sample, estimate the parameter $\tilde{\theta}^{(n)}$'s and compute the sum of the symmetrised KL divergence

$$T(\{\tilde{\theta}^{(n)}\}) = \sum_{n=1}^{N-1} \frac{1}{2} \left[D(\theta_{\mathrm{T}}^{(n)} \,||\, \tilde{\theta}^{(n)}) + D(\tilde{\theta}^{(n)} \,||\, \theta_{\mathrm{T}}^{(n)}) \right]$$

   (c) Compute the p-value by $p = \mathrm{Prob}(T(\{\tilde{\theta}^{(n)}\}) < T(\{\theta_{\mathrm{H}}^{(n)}\}))$

5. H_0 is rejected if $p \geq 1 - \alpha$.

Although the above test is of the null hypothesis H_0 that the data of the Honda stock price are generated by the distribution of Toyota, we also performed the alternative test where H_0 is that the data of Toyota are generated by the distribution of Honda. The number of samples in the Monte–Carlo method was 1000. If H_0 is the former one, the computed p-value was 0.626. In the case where H_0 is the latter, the computed p-value was 0.824. Although these p-values are relatively high, they are not enough for rejecting the hypothesis. That is, according to the tests above the difference is not significant.

Acknowledgment

This work was supported by JSPS KAKENHI Grant Number 26400200 and JST PRESTO.

References

[1] Amari, S. and Nagaoka H., *Methods of Information Geometry*, Translations of Mathematical Monographs, Vol. 191, American Mathematical Society, 2000.

[2] Marsden, J.E. and West M., *Discrete Mechanics and Variational Integrators*, Acta Numerica, 10 (2001), pp. 357–514.

Discrete-time N-body Problem and its Equilibrium Solutions

Yukitaka Minesaki

Tokushima Bunri University, Nishihama, Yamashiro-cho, Tokushima, 770-8514 JAPAN
minesaki@tks.bunri-u.ac.jp

1 INTRODUCTION

We proposed a discrete-time general N-body problem (abbreviated to d-GNBP here) [5], that retains all conserved quantities except the angular momentum of the original general N-body problem (abbreviated to GNBP here). d-GNBP is given by an extension of a d'Alembert-type scheme [1], which is an energy-preserving integration method for constrained autonomous Hamiltonian systems.

In this lecture note, we prove that d-GNBP has the same rotating polygon formed by its masses as GNBP for the common initial conditions. Therefore, d-GNBP can exactly trace the eccentric orbits of equilibrium solutions in the original GNBP, each of which corresponds to a vertex of the polygon. Contrastively, generic numerical integration methods cannot reproduce these orbits over a long time interval. Before this proof, no discrete-time system had been shown to retain the orbits of the equilibrium solutions in GNBP. Further, we obtain eighth-order d-GNBP through Yoshida's composition technique [9], which also trace the orbits of equilibrium solutions.

Although d-GNBP is merely second-order accurate, it can also precisely reproduce doubly-symmetric orbits of the general $(1+4)$-body problem, each of which passes near a square equilibrium solution. However, d-GNBP cannot trace a figure-eight orbit [2, 8] of the three-body problem since it does not preserve the angular momentum. Eighth-order d-GNBP overcomes this non-reproducibility, and moreover it as well as the original d-GNBP can exactly trace the orbits of equilibrium solutions.

2 DISCRETE-TIME N-BODY PROBLEM

Minesaki [5] proposed d-GNBP, which is based on an extension of a d'Alembert-type scheme [1]. Especially, the planar d-GNBP is expressed by

$$\begin{cases} \dfrac{\mathbf{Q}_{ij}^{(l+1)}-\mathbf{Q}_{ij}^{(l)}}{\Delta t^{(l,l+1)}} = \dfrac{M}{8m_im_j}\dfrac{|\mathbf{Q}_{ij}^{(l+1)}|^2+|\mathbf{Q}_{ij}^{(l)}|^2}{|\mathbf{Q}_{ij}^{(l+1)}|^2|\mathbf{Q}_{ij}^{(l)}|^2}\mathbf{P}_{ij}^{(l+1/2)} \quad 1\le i<j\le N, & \text{(1a)} \\ \displaystyle\sum_{i=1}^{j-1}\mathbf{G}_{ij}^{(l+1)}-\sum_{i=j+1}^{N}\mathbf{G}_{ji}^{(l+1)}=\mathbf{0},\ 1\le j\le N. & \text{(1b)} \\ \mathbf{\Phi}_{1ij}^{(l+1)}=\mathbf{0},\ 2\le i<j\le N. & \text{(1c)} \end{cases}$$

m_i $(i=1,\cdots,n)$ is the mass of the i-th particle, $M=\sum_{i=0} m_i$, $\Delta t^{(l,l+1)}$ $(l=0,1,\cdots)$ is a variable-width time step, $\mathbf{P}_{ij}^{(k)}$ and $\mathbf{Q}_{ij}^{(k)}$ mean the values of the Levi-Civita variables, $\mathbf{P}_{ij}$ and $\mathbf{Q}_{ij}$ [3] at (discrete) times $t^{(0)}=0$ and $t^{(k)}=\sum_{l=0}^{k-1}\Delta t^{(l,l+1)}$ $(k=1,2,\cdots)$, respectively, and

$$\begin{aligned}\mathbf{G}_{ij}^{(l+1)} \equiv & \frac{1}{2|\mathbf{Q}_{ij}^{(l+1/2)}|^2}\left(\frac{\mathbf{P}_{ij}^{(l+1)}-\mathbf{P}_{ij}^{(l)}}{\Delta t^{(l,l+1)}}-\frac{1}{|\mathbf{Q}_{ij}^{(l+1)}|^2|\mathbf{Q}_{ij}^{(l)}|^2}\right. \\ & \left.\cdot\left(\frac{M}{8m_im_j}\left(|\mathbf{P}_{ij}^{(l+1)}|^2+|\mathbf{P}_{ij}^{(l)}|^2\right)-2m_im_j\right)\mathbf{Q}_{ij}^{(l+1/2)}\right)\mathbf{L}\left(\mathbf{Q}_{ij}^{(l+1/2)}\right)^{\top},\ 1\le i<j\le N, \\ \mathbf{\Phi}_{1ij}^{(l+1)} \equiv & \mathbf{Q}_{1i}^{(l+1)}\mathbf{L}(\mathbf{Q}_{1i}^{(l+1)})^{\top}+\mathbf{Q}_{ij}^{(l+1)}\mathbf{L}(\mathbf{Q}_{ij}^{(l+1)})^{\top}-\mathbf{Q}_{1j}^{(l+1)}\mathbf{L}(\mathbf{Q}_{1j}^{(l+1)})^{\top},\ 2\le i<j\le N.\end{aligned}$$

Here, we define the midpoint value $(\bullet)^{(l+1/2)} \equiv \left((\bullet)^{(l+1)}+(\bullet)^{(l)}\right)/2$ of the function $(\bullet)(t)$, and the Levi–Civita matrix $\mathbf{L}(\mathbf{Q}_{ij}^{(k)})$ as

$$\mathbf{L}(\mathbf{Q}_{ij}^{(k)}) \equiv \begin{bmatrix} Q_{ij[1]}^{(k)} & -Q_{ij[2]}^{(k)} \\ Q_{ij[2]}^{(k)} & Q_{ij[1]}^{(k)} \end{bmatrix},\ k=l,l+\frac{1}{2},l+1.$$

Since we designed d-GNBP (1) based on a d'Alembert-type scheme [1] which is an energy-preserving integration method for constrained systems, d-GNBP is second-order accurate and conserves the total energy.

Setting Δt as 0 in d-GNBP (1), we can obtain GNBP in the Levi–Civita reference frame:

$$\begin{cases} \dfrac{d}{dt}\mathbf{Q}_{ij}=\dfrac{M}{4m_im_j}\dfrac{\mathbf{P}_{ij}}{|\mathbf{Q}_{ij}|^2}, & 1\le i<j\le N, \\ \displaystyle\sum_{i=1}^{j-1}\mathbf{G}_{ij}-\sum_{i=j+1}^{N}\mathbf{G}_{ji}=\mathbf{0}, & 1\le j\le N, \\ \mathbf{\Phi}_{1ij}(\mathbf{Q})=\mathbf{0}, & 2\le i<j\le N, \end{cases} \tag{2}$$

where

$$\mathbf{G}_{ij} \equiv \frac{1}{2|\mathbf{Q}_{ij}|^2}\left(\frac{d}{dt}\mathbf{P}_{ij}-\frac{1}{|\mathbf{Q}_{ij}|^4}\left(\frac{M}{4m_im_j}|\mathbf{P}_{ij}|^2-2m_im_j\right)\mathbf{Q}_{ij}\right)\mathbf{L}(\mathbf{Q}_{ij})^{\top},\ 1\le i<j\le N.$$

The form of GNBP (2) is very different from the well-known form of GNBP in the inertial barycentric frame, so (1) does not look like d-GNBP. However, through the canonical transformation from the Levi-Civita reference frame to the inertial relative frame [3]:

$$\mathbf{q}_{ij}=\mathbf{Q}_{ij}\mathbf{L}(\mathbf{Q}_{ij})^{\top},\ \mathbf{p}_{ij}=\frac{1}{2|\mathbf{Q}_{ij}|^2}\mathbf{P}_{ij}\mathbf{L}(\mathbf{Q}_{ij})^{\top},\ 1\le i<j\le N, \tag{3}$$

and the transformation from the inertial relative frame to the inertial barycentric frame:

$$\mathbf{q}_i'=\frac{1}{M}\left(\sum_{j=i+1}^{N}m_j\mathbf{q}_{ij}-\sum_{j=1}^{i-1}m_j\mathbf{q}_{ji}\right),\ \mathbf{p}_i'=\sum_{j=i+1}^{N}\mathbf{p}_{ij}-\sum_{j=0}^{i-1}\mathbf{p}_{ji},\ 1\le i\le N, \tag{4}$$

(2) leads to the well-known GNBP in the inertial barycentric frame:

$$\frac{d}{dt}\mathbf{q}_i'=\frac{\mathbf{p}_i'}{m_i},\ \frac{d}{dt}\mathbf{p}_i'=m_i\left(\sum_{k=1}^{i-1}\frac{m_k\left(\mathbf{q}_k'-\mathbf{q}_i'\right)}{|\mathbf{q}_k'-\mathbf{q}_i'|^3}-\sum_{k=i+1}^{N}\frac{m_k\left(\mathbf{q}_i'-\mathbf{q}_k'\right)}{|\mathbf{q}_i'-\mathbf{q}_k'|^3}\right),\ 1\le i\le N. \tag{5}$$

The transformations (3) and (4) ensure that the linear momentum and the point of center of mass are conserved.

3 EQUILIBRIUM SOLUTIONS IN D-GNBP

We give, analytically, the conditions under which d-GNBP (1) has some equilibrium solutions. In the solutions, all or $N-1$ of N masses form a rotating polygon whose shape is invariant and whose size does one of the following: increases or decreases monotonically; increases and decreases alternately; or is invariant. We obtain the following theorem regarding the equilibrium solutions.

Theorem 1 *(Equilibrium solutions for d-GNBP)*

Suppose that $(\mathbf{Q}_{ij}^{(l)}, \mathbf{P}_{ij}^{(l)})$ *for* $1 \le i < j \le N$ *in d-GNBP (1) satisfy the following conditions.*

1. $(\mathbf{Q}_{1N}^{(l)}, \mathbf{Q}_{1N}^{(l+1)}, \mathbf{P}_{1N}^{(l)}, \mathbf{P}_{1N}^{(l+1)})$ *is a solution of the discrete-time two-body problem (abbreviated to d-2BP here) [6]:*

$$\begin{cases} \dfrac{\mathbf{Q}_{1N}^{(l+1)} - \mathbf{Q}_{1N}^{(l)}}{\Delta t^{(l,l+1)}} = \dfrac{M}{8m_1 m_N} \dfrac{|\mathbf{Q}_{1N}^{(l+1)}|^2 + |\mathbf{Q}_{1N}^{(l)}|^2}{|\mathbf{Q}_{1N}^{(l+1)}|^2 |\mathbf{Q}_{1N}^{(l)}|^2} \mathbf{P}_{1N}^{(l+1/2)}, & \text{(6a)} \\ \dfrac{\mathbf{P}_{1N}^{(l+1)} - \mathbf{P}_{1N}^{(l)}}{\Delta t^{(l,l+1)}} = \dfrac{1}{|\mathbf{Q}_{1N}^{(l+1)}|^2 |\mathbf{Q}_{1N}^{(l)}|^2} \left(\dfrac{M}{8m_1 m_N} \left(|\mathbf{P}_{1N}^{(l+1)}|^2 + |\mathbf{P}_{1N}^{(l)}|^2 \right) - 2m_1 m_N \right) \mathbf{Q}_{1N}^{(l+1/2)}. & \text{(6b)} \end{cases}$$

2. $\mathbf{Q}_{ij}^{(l)} = c_{ij} \mathbf{Q}_{1N}^{(l)} R\left(\dfrac{\theta_{ij}}{2}\right)^\top$, $\mathbf{P}_{ij}^{(l)} = c_{ij}^3 \dfrac{m_i m_j}{m_1 m_N} \mathbf{P}_{1N}^{(l)} R\left(\dfrac{\theta_{ij}}{2}\right)^\top$ $(1 \le i \le j \le N)$ *is given, where* $c_{12}, \cdots, c_{1,N-1}, c_{1,N} \equiv 1$ *and* $\theta_{1N} = 0$ *are constants, and the rotation matrix by an angle* θ *is*

$$R(\theta) \equiv \begin{bmatrix} \cos\theta & -\sin\theta \\ \sin\theta & \cos\theta \end{bmatrix}.$$

Further, c_{ij}*, and* θ_{ij} $(1 \le i < j \le N)$ *are the solutions for the system composed of* $N(N-1)$ *equations:*

$$\begin{cases} \displaystyle\sum_{i=1}^{j-1} \frac{m_i}{c_{ij}^4}(c_{ij}^6 - 1)\cos\theta_{ij} - \sum_{i=j+1}^{N} \frac{m_i}{c_{ji}^4}(c_{ji}^6 - 1)\cos\theta_{ji} = 0,\ 2 \le j \le N, & \text{(7a)} \\ \displaystyle\sum_{i=1}^{j-1} \frac{m_i}{c_{ij}^4}(c_{ij}^6 - 1)\sin\theta_{ij} - \sum_{i=j+1}^{N} \frac{m_i}{c_{ji}^4}(c_{ji}^6 - 1)\sin\theta_{ji} = 0,\ 2 \le j \le N, & \text{(7b)} \\ c_{1i}^2 \sin\theta_{1i} + c_{ij}^2 \sin\theta_{ij} - c_{1j}^2 \sin\theta_{1j} = 0,\ 2 \le i < j \le N & \text{(7c)} \\ c_{1i}^2 \cos\theta_{1i} + c_{ij}^2 \cos\theta_{ij} - c_{1j}^2 \cos\theta_{1j} = 0,\ 2 \le i < j \le N. & \text{(7d)} \end{cases}$$

Then, $\mathbf{Q}_{ij}^{(l+1)}$*, and* $\mathbf{P}_{ij}^{(l+1)}$ *are obtained by*

$$\mathbf{Q}_{ij}^{(l+1)} = c_{ij} \mathbf{Q}_{1N}^{(l+1)} R\left(\frac{\theta_{ij}}{2}\right)^\top, \quad \mathbf{P}_{ij}^{(l+1)} = c_{ij}^3 \frac{m_i m_j}{m_1 m_N} \mathbf{P}_{1N}^{(l+1)} R\left(\frac{\theta_{ij}}{2}\right)^\top, \quad 1 \le i \le j \le N.$$

Further, Minesaki and Nakamura [6] proved that both of d-2BP (6) and the original continuous-time two-body problem have orbits uniquely determined by three common

functionally independent conserved quantities. This also describes a case in which d-2BP (6) has the same orbit as the original two-body problem to which d-2BP (6) reduces in the limit $\Delta t^{(l,l+1)} \to 0$ $(l = 0, 1, \cdots)$.

Theorem 1 shows that for an arbitrary discrete-time $t^{(l)}$ $(l = 0, 1, \cdots)$,

(a) the ratios between arbitrary two absolute values of the $N(N-1)/2$ vectors, $|\mathbf{Q}_{ij}^{(k)}|$ $(1 \le i < j \le N)$, and

(b) the angles between the same arbitrary pair of these $N(N-1)/2$ vectors, θ_{ij} $(1 \le i < j \le N)$

are invariant. Therefore, for the same initial conditions, the orbit of each of the N masses m_i $(i = 1, \cdots, N)$ in d-GNBP (1) is the same as its orbit in GNBP, and the shape of an $(N-1)$-gon around a large mass m_1 formed by $N-1$ small masses m_2, m_3, $\cdots$, m_N or N-gon composed of N masses m_1, m_2, $\cdots$, m_N is invariant.

4 Numerical Results

For some equilibrium solutions and some periodic solutions, we compare the orbits by the following methods.

1. *Non-regularized integration methods*

   1-(a). *RK8*: The eighth-order Runge–Kutta method with a *constant* time step, which is used to integrate GNBP in the heliocentric frame.

   1-(b). *McL8*: The eighth-order symplectic method with a *constant* time step, which is applied to GNBP in the heliocentric frame. A composition of the maps associated with the total kinetic energy and potential yields McL8. McL8 is one of some composition methods proposed by McLachlan [4].

2. *Regularized integration methods*

   2-(a). *LHA8*: The eighth-order symplectic method with a *variable* time step, which is used to integrate GNBP in the heliocentric frame. Mikkola and Tanikawa [7] gave a symmetric second-order method with a variable time step. LHA8 is derived from this symmetric method through Yoshida's composition technique [9].

   2-(b). *d-GNBP*: d-GNBP is obtained by (1) and is second-order accurate in $\Delta t^{(l,l+1)}$. However, d-GNBP cannot yield regular results for collisions because it is singular at each $\mathbf{Q}_{ij}^{(l)} = \mathbf{0}$ and $\mathbf{Q}_{ij}^{(l+1)} = \mathbf{0}$ $(1 \le i < j \le n)$. Through the new time transformation

$$\begin{aligned} \Delta s^{(l,l+1)} &\equiv s^{(l+1)} - s^{(l)} \\ &= \frac{2\Delta t^{(l,l+1)}}{\left(\sum_{i=1}^{N-1}\sum_{j=i}^{N} \frac{m_i m_j}{|\mathbf{Q}_{ij}^{(l)}|^2}\right)^{-1} + \left(\sum_{i=1}^{N-1}\sum_{j=i}^{N} \frac{m_i m_j}{|\mathbf{Q}_{ij}^{(l+1)}|^2}\right)^{-1}}, \end{aligned}$$

   d-GNBP can be rewritten as a regularized discrete-time system.

   2-(c). *8th-order d-GNBP*: The eighth-order d-GNBP in $\Delta t^{(l,l+1)}$, which is based on Yoshida's composition technique [9] of d-GNBP.

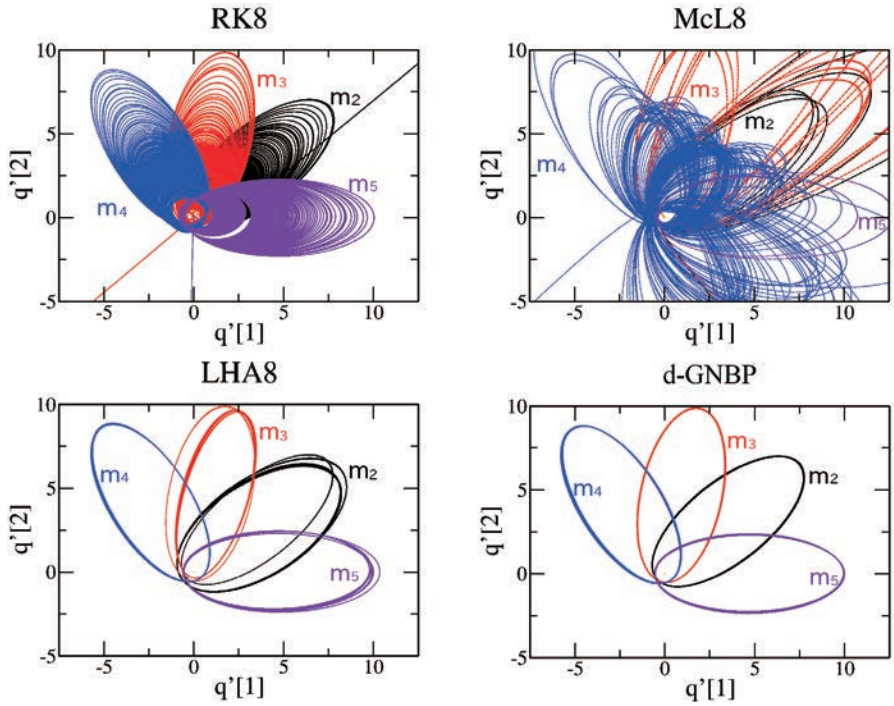

Figure 1: Elliptic relative equilibrium orbits in the G5BP with eccentricity 0.9 of m_i $(2 \leq i \leq 5)$ in the barycentric inertial reference frame. Each panel's title describes the numerical method used to produce it.

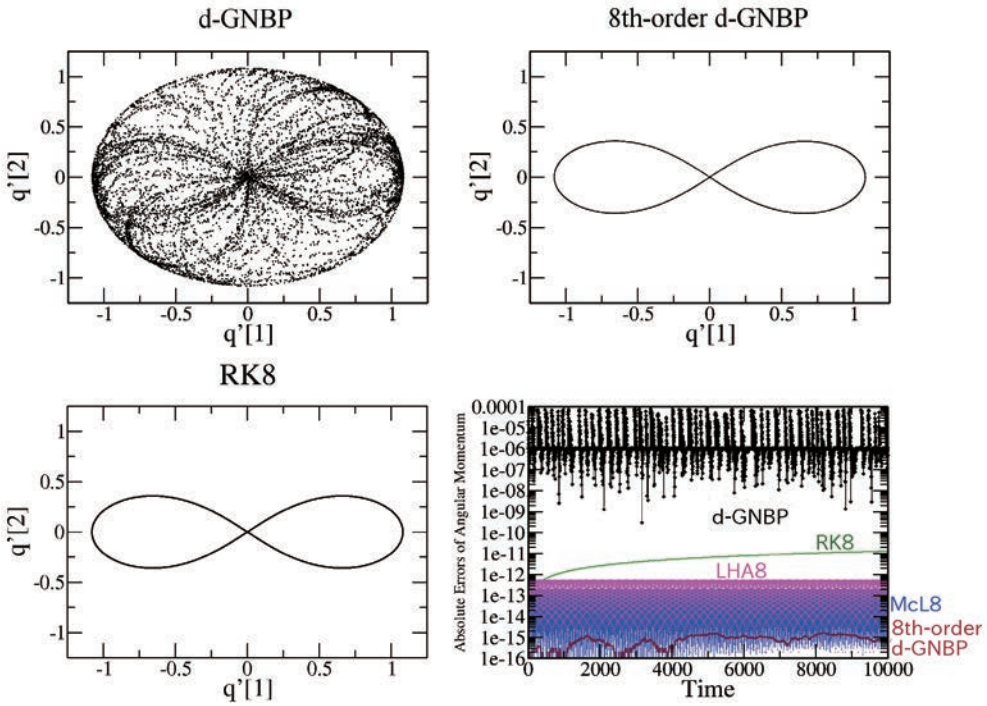

Figure 2: Figure-eight orbit in the G3BP of m_1 in the barycentric inertial reference frame, and absolute error growth of the angular momentum.

We show that d-GNBP can precisely compute some elliptic relative equilibrium orbits of G5BP in Figure 1, and eighth-order d-GNBP can trace a figure-eight orbit of G3BP [2, 8] in Figure 2. Although McL8, LHA8, and d-GNBP preserve the energy with high accuracy, only d-GNBP can reproduce elliptic relative equilibrium orbits. d-GNBP does not conserve the angular momentum, so that it cannot trace a figure-eight orbit. Contrastively, because eighth-order d-GNBP precisely conserves both of the energy and angular momentum, it can reproduce a figure-eight orbit.

Acknowledgment

This study was supported by a grant-in-aid for exploratory research (16K13781) from the Ministry of Education, Culture, Sports, Science and Technology of Japan.

References

[1] Betsch, P. 2005, Comput. Methods Appl. Mech. Engrg. 194, 5159

[2] Chenciner, A., & Montgomery, R. 2000, Ann. Math., 152, 881.

[3] Levi-Civita, T. 1920, AcMa, 42, 99

[4] McLachlan, R. I. 1995, SIAM J. Sci. Comp., 16, 151

[5] Minesaki, Y. 2015, AJ, 150, 102

[6] Minesaki, Y. & Nakamura, Y. 2002, PhLA, 306, 127

[7] Mikkola, S., & Tanikawa, K. 1999, CeMDA, 74, 287

[8] Simó C. 2001, in Proceedings of the European Congress of Mathematics, eds. Casacuberta C., Mirò-Roig R. M., Verdera J., Xambó S. (Basel: Birkhuser Verlag)

[9] Yoshida, H. 1990, Phys. Lett. A 150, 262

Gradient descent in a generalised Bregman distance framework

Martin Benning[1], Marta M. Betcke[2], Matthias J. Ehrhardt[1], and Carola-Bibiane Schönlieb[1]

University of Cambridge, Dept. of Applied Mathematics & Theoretical Physics, Wilberfore Road, Cambridge CB3 0WA, United Kingdom
{mb941, me404, cbs31}@cam.ac.uk

University College London, Dept. of Computer Science, Gower Street, London WC1E 6BT, United Kingdom
m.betcke@ucl.ac.uk

1 Introduction

In this work we study a generalisation of classical gradient descent that has become known in the literature as the so-called linearised Bregman iteration [8, 7], and – as the key novelty of this publication – apply it to minimise smooth but not necessarily convex objectives $E : \mathcal{U} \to \mathbb{R}$ over a Banach space $\mathcal{U}$. For this generalisation we want to consider proper, lower semi-continuous (l.s.c.), convex but not necessarily smooth functionals $J : \mathcal{U} \to \mathbb{R} \cup \{\infty\}$, and consider their generalised Bregman distances

$$D_J^p(u, v) = J(u) - J(v) - \langle p, u - v \rangle \,,$$

for $u, v \in \mathcal{U}$ and $p \in \partial J(v)$, where $\partial J(v)$ denotes the subdifferential of J. Note that in case J is smooth we omit p in the notation of the Bregman distance, as the subdifferential is single-valued in this case. We further assume that there exists a proper, l.s.c., convex and not necessary smooth functional $F : \mathcal{U} \to \mathbb{R} \cup \{\infty\}$ such that the functional $G := F - E$ is also convex. This will imply $D_G^{q-\nabla E(v)}(u, v) \geq 0$ for all $u, v \in \mathrm{dom}(G)$ and $q \in \partial F(v)$, since $q - \nabla E$ is the gradient of G. Hence, the convexity of G yields the descent estimate

$$E(u) \leq E(v) + \langle \nabla E(v), u - v \rangle + D_F^q(u, v) \,, \tag{1}$$

for all $u, v \in \mathrm{dom}(F)$ and $q \in \partial F(v)$. We want to emphasise that in case of $F(u) = \frac{L}{2}\|u\|_2^2$ (for some constant $L > 0$) (1) reduces to the classical Lipschitz estimate; this generalisation has also been discovered in [2] simultaneously to this work (without the generalisation of Bregman distances to non-smooth functionals, though).

2 Linearised Bregman iteration applied to non-convex problems

The linearised Bregman iteration that we are going to study in this work is defined as

$$u^{k+1} = \operatorname*{arg\,min}_{u \in \mathrm{dom}(J)} \left\{ \tau^k \langle u - u^k, \nabla E(u^k) \rangle + D_J^{p^k}(u, u^k) \right\}, \tag{2a}$$

$$p^{k+1} = p^k - \tau^k \nabla E(u^k), \tag{2b}$$

for $k \in \mathbb{N}$, some $u^0 \in \mathcal{U}$ and $p^0 \in \partial J(u^0)$. Here $J : \mathcal{U} \to \mathbb{R} \cup \{\infty\}$ is not only proper, l.s.c. and convex, but also chosen such that the overall functional in (2a) is coercive and strictly convex and thus, its minimiser well-defined and unique.

We want to highlight that this model has been studied for several scenarios in which E is the convex functional $E(u) = \frac{1}{2}\|Ku - f\|_2^2$, for data f and linear and bounded operators K (cf. [8, 7]), for more general convex functionals E and smooth J in [6, 3], as well as for the non-convex functional $E(u) = \frac{1}{2}\|K(u) - f\|_2^2$ for data f and a smooth but non-linear operator K in [1]. However, to our knowledge this is the first work that studies (2) for general smooth but not necessarily convex functionals E.

3 A sufficient decrease property

We want to show that together with the descent estimate (1) we can guarantee a sufficient decrease property of the iterates (2) in terms of the symmetric Bregman distance. The symmetric Bregman distance $D_J^{\mathrm{symm}}(u, v)$ (cf. [5]) is simply defined as $D_J^{\mathrm{symm}}(u, v) = D_J^q(u, v) + D_J^p(v, u) = \langle u - v, p - q \rangle$ for all $u, v \in \mathrm{dom}(J)$, $p \in \partial J(u)$ and $q \in \partial J(v)$.

Lemma 1 (Sufficient decrease property)**.** *Let $E : \mathcal{U} \to \mathbb{R}$ be a l.s.c. and smooth functional that is bounded from below and for which a proper, l.s.c. and convex functional $F : \mathcal{U} \to \mathbb{R} \cup \{\infty\}$ exists such that $G := F - E$ is also convex. Further, let $J : \mathcal{U} \to \mathbb{R} \cup \{\infty\}$ be a proper, l.s.c. and convex functional such that* (2a) *is well defined and unique. Further we choose τ^k such that the estimate*

$$\rho D_J^{symm}(u^{k+1}, u^k) \leq \frac{1}{\tau^k} D_J^{symm}(u^{k+1}, u^k) - D_F^{q^k}(u^{k+1}, u^k) \tag{3}$$

holds true, for all $k \in \mathbb{N}$, $q^k \in \partial F(u^k)$ and a fixed constant $0 < \rho < \infty$. Then the iterates of the linearised Bregman iteration (2) *satisfy the descent estimate*

$$E(u^{k+1}) + \rho D_J^{symm}(u^{k+1}, u^k) \leq E(u^k). \tag{4}$$

In addition, we observe

$$\lim_{k \to \infty} D_J^{symm}(u^{k+1}, u^k) = 0.$$

Proof. First of all, we easily see that update (2b), i.e.

$$\tau^k \nabla E(u^k) + (p^{k+1} - p^k) = 0,$$

is simply the optimality condition of (2a), for $p^{k+1} \in \partial J(u^{k+1})$. Taking a dual product of (2b) with $u^{k+1} - u^k$ yields

$$\langle \nabla E(u^k), u^{k+1} - u^k \rangle = -\frac{1}{\tau^k} D_J^{\mathrm{symm}}(u^{k+1}, u^k). \tag{5}$$

Due to (1) we can further estimate

$$E(u^{k+1}) \leq E(u^k) + \langle u^{k+1} - u^k, \nabla E(u^k) \rangle + D_F^{q^k}(u^{k+1}, u^k)\,,$$

for $q^k \in \partial F(u^k)$. Together with (5) we therefore obtain

$$E(u^{k+1}) + \frac{1}{\tau^k} D_J^{\mathrm{symm}}(u^{k+1}, u^k) - D_F^{q^k}(u^{k+1}, u^k) \leq E(u^k)\,.$$

Using (3) then allows us to conclude

$$0 \leq \rho D_J^{\mathrm{symm}}(u^{k+1}, u^k) \leq E(u^k) - E(u^{k+1})\,;$$

hence, summing up over all N iterates and telescoping yields

$$\begin{aligned}\sum_{k=0}^{N} \rho D_J^{\mathrm{symm}}(u^{k+1}, u^k) &\leq \sum_{k=0}^{N} E(u^k) - E(u^{k+1})\,,\\ &= E(u^0) - E(u^{N+1})\,,\\ &\leq E(u^0) - \overline{E} < \infty\,,\end{aligned}$$

where $\overline{E}$ denotes the lower bound of E. Taking the limit $N \to \infty$ then implies

$$\sum_{k=0}^{\infty} \rho D_J^{\mathrm{symm}}(u^{k+1}, u^k) < \infty\,,$$

and thus, we have $\lim_{k\to\infty} D_J^{\mathrm{symm}}(u^{k+1}, u^k) = 0$ due to $\rho > 0$. □

Remark 1. *We want to emphasise that Lemma 1 together with the duality $D_J^{symm}(u^{k+1}, u^k) = D_{J^*}^{symm}(p^{k+1}, p^k)$, for $p^{k+1} \in \partial J(u^{k+1})$ and $p^k \in \partial J(u^k)$, further implies*

$$\lim_{k\to\infty} D_{J^*}^{symm}(p^{k+1}, p^k) = 0\,,$$

and hence, a sufficient decrease property holds also for the dual iterates. Here $J^* : \mathcal{U}^* \to \mathbb{R} \cup \{\infty\}$ denotes the Fenchel conjugate of J, and $\mathcal{U}^*$ is the dual space of $\mathcal{U}$.

4 A global convergence statement

For the following part we assume that both J and J^* are strongly convex w.r.t. the $\mathcal{U}$- respectively the $\mathcal{U}^*$-norm, i.e. there exist constants $\gamma > 0$ and $\delta > 0$ such that

$$\gamma \|u - v\|_{\mathcal{U}}^2 \leq D_J^{\mathrm{symm}}(u, v) \qquad \text{and} \qquad \delta \|p - q\|_{\mathcal{U}^*}^2 \leq D_{J^*}^{\mathrm{symm}}(p, q) \tag{6}$$

hold true for all $u, v \in \mathcal{U}$ and $p, q \in \mathcal{U}^*$. From Lemma 1 and (6) we readily obtain

$$\rho_1 \|u^{k+1} - u^k\|_{\mathcal{U}}^2 \leq E(u^k) - E(u^{k+1})\,, \tag{7}$$

for $\rho_1 := \gamma/\rho$, which implies $\lim_{k\to\infty} \|u^{k+1} - u^k\|_{\mathcal{U}} = 0$.

We follow [4] and establish a global convergence result by proving that the dual norm of the gradient is bounded by the iterates gap in addition to the already proven descent result (7). Together with a generalised Kurdyka-Łojasiewicz property we will be able to prove a global convergence statement for (2).

Given (6), we obtain the necessary iterates gap in the corresponding Banach space norm as an upper bound for the gradient in the dual Banach space norm, as follows.

Lemma 2 (Gradient bound)**.** *Let the same assumptions hold true as in Lemma 1, and let* (6) *be fulfilled. Then the iterates* (2) *satisfy*

$$\|\nabla E(u^k)\|_{\mathcal{U}^*} \leq \rho_2 \|u^{k+1} - u^k\|_{\mathcal{U}}\,, \tag{8}$$

for $\rho_2 := 1/(\delta\overline{\tau})$ *and* $\overline{\tau} := \inf_k \tau^k$.

Proof. As pointed out in Remark 1, we have the duality $D^{\mathrm{symm}}_{J^*}(p^{k+1}, p^k) = D^{\mathrm{symm}}_{J}(u^{k+1}, u^k)$ for the symmetric Bregman distances. Together with the duality estimate $\langle u, p\rangle \leq \|u\|_{\mathcal{U}}\|p\|_{\mathcal{U}^*}$ we therefore obtain

$$D^{\mathrm{symm}}_{J^*}(p^{k+1}, p^k) = \langle p^{k+1} - p^k, u^{k+1} - u^k\rangle \leq \|u^{k+1} - u^k\|_{\mathcal{U}}\|p^{k+1} - p^k\|_{\mathcal{U}^*}\,.$$

Hence, using (2b) yields

$$\frac{D^{\mathrm{symm}}_{J^*}(p^k - \tau^k\nabla E(u^k), p^k)}{\tau^k\|\nabla E(u^k)\|_{\mathcal{U}^*}} \leq \|u^{k+1} - u^k\|_{\mathcal{U}}\,.$$

Together with the δ-strong convexity (6) and $\rho_2 := 1/(\delta\overline{\tau})$ we get (8). □

Remark 2. *Note that we have to ensure* $\overline{\tau} > 0$ *in order to ensure* $\rho_2 < \infty$. *Due to* (3) *we can ensure this as long as* $D^{q^k}_F(u^{k+1}, u^k)$ *is bounded from above for all* $k \in \mathbb{N}$.

Before we can establish a global convergence result, we have to restrict the functionals E to the following class of functionals satisfying a generalised Kurdyka-Łojasiewicz property.

Definition 1 (Generalised Kurdyka-Łojasiewicz (KL) property)**.** *We assume for* $\eta > 0$ *that* $\varphi : [0, \eta[\to \mathbb{R}_{>0}$ *is a function that is continuous at zero and satisfies* $\varphi(0) = 0$, $\varphi \in C^1(]0, \eta[)$. *Let further* $E : \mathcal{U} \to \mathbb{R}$ *be a proper, l.s.c. and smooth functional.*

1. *The functional* E *fulfils the (generalised) KL property at a point* $\overline{u} \in \mathcal{U}$ *if there exists* $\eta \in]0, \infty]$, *a neighbourhood* U *of* $\overline{u}$ *and a function* φ *satisfying the conditions above, such that for all*

$$u \in U \cap \{u \mid E(\overline{u}) < E(u) < E(\overline{u}) + \eta\}$$

we observe

$$\varphi'(E(u) - E(\overline{u}))\|\nabla E(u)\|_{\mathcal{U}^*} \geq 1\,. \tag{9}$$

2. *If* E *satisfies the (generalised) KL property for all arguments in* $\mathcal{U}$, E *is called a (generalised) KL functional.*

Together with the previous results the generalised KL condition (9) allows to establish the following global convergence result.

Theorem 1 (Global convergence)**.** *Let the Banach space* $\mathcal{U}$ *be the dual of a separable normed space. Suppose that* E *is coercive, sequentially weak*-continuous and a KL function in the sense of Definition 1. Then the sequences* $\{u^k\}_{k\in\mathbb{N}}$ *and* $\{p^k\}_{k\in\mathbb{N}}$ *generated by* (2) *each have a strongly convergent subsequence with limits* $\hat{u}$ *and* $\hat{p}$, *with* $\nabla E(\hat{u}) = 0$ *and* $\hat{p} \in \partial J(\hat{u})$. *If* $\dim(\mathcal{U}) < \infty$, *then the convergence holds true for the entire sequences.*

Proof. The proof utilises (4), (8) and (9) to derive the statement. Due to page restrictions, the full length proof will be published separately in an extended version of this manuscript. □

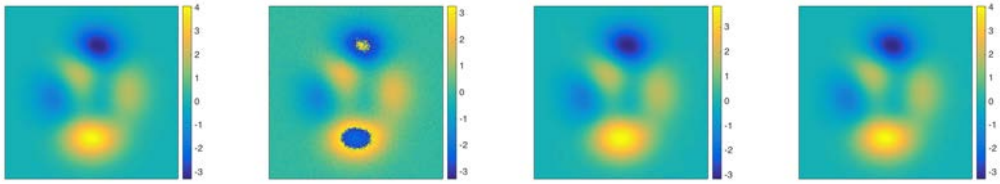

(a) Ground truth (b) Gradient descent (c) $R(u) = \frac{1}{2}\|\nabla u\|_{L^2}^2$ (d) $R(u) = \|Cu\|_{\ell^1}$

Figure 1: A phase unwrapping example. Figure 1(a) shows the unknown, noise-free, ground truth signal. Figure 1(b) shows the result of classical gradient descent computation. Figure 1(c) visualises the solution of model 2.) with $\alpha = 1000$. Figure 1(d) shows the solution of model 3.) with $\alpha = 50$. All reconstructions have been computed from zero initialisations and were stopped according to the same discrepancy principle.

5 Phase unwrapping as a toy example

We want to conclude this paper with a numerical toy example for which we consider to minimise $E(u) := \frac{1}{2}\|K(u) - f\|_{L^2(\Omega;\mathbb{R}^2)}^2$ for $K(u) = (\cos(u), \sin(u))^T$, and choose $F(u) = \frac{L}{2}\|u\|_{L^2(\Omega)}^2$ with $L = 1$. We will minimise E via (2) with $J(u) := \frac{1}{2}\|u\|_{L^2(\Omega)}^2 + \alpha R(u)$, for a positive scalar $\alpha > 0$ and three different choices of R: 1.) $R(u) = 0$, 2.) $R(u) = \frac{1}{2}\|\nabla u\|_{L^2(\Omega;\mathbb{R}^2)}^2$, and 3.) $R(u) = \|Cu\|_{\ell^1}$, where C denotes the two-dimensional discrete Cosine transform. The first case simply corresponds to classical gradient descent, case 2.) is gradient descent in a Hilbert space metric and 3.) corresponds to gradient descent in a non-smooth Bregman distance setting that does not correspond to a metric. Note that the question, whether E and J satisfy all conditions that are necessary for global convergence, will be omitted due to the page limit, but addressed in an extended version of this manuscript in the future. We do want to mention, though, that it is easy to see that J in 3.) does not meet the requirement (7); this, however, can be corrected via a smoothing of the ℓ^1-norm, for instance via a Huberised ℓ^1-norm.

In order to consider numerical examples, we discretise the above scenarios in a straight forward fashion. Input data f is created by applying the non-linear operator K to a multiple of the built-in MATLAB© signal 'peaks' (see Figure 1(a)) and additive normal distributed noise with mean zero and standard deviation $\sigma = 0.15$. Due to noise in the data, the iteration (2) is stopped as soon as $E(u^k) \leq \sigma^2 m/2$ is satisfied. Here m denotes the number of discrete samples. Reconstruction results for zero initialisations and the choice $\tau^k = 1.5$ for all $k \in \mathbb{N}$ can be found in Figure 1(b), 1(c) and 1(d). We want to emphasise that this example is just a toy example to demonstrate the impact of different choices of J; there are certainly much better unwrapping strategies, particularly for the unwrapping of smooth signals.

Code statement: The corresponding MATLAB© code can be downloaded at `https://doi.org/10.17863/CAM.6714`.

6 Conclusions & Outlook

We have presented a short convergence analysis of the linearised Bregman iteration for the minimisation of general smooth but non-convex functionals. We have proven a sufficient decrease property, and confirmed that the dual norm of the gradient is bounded by the

primal iterates under additional strong convexity assumptions of the convex functional that builds the basis for the Bregman iteration. Under a generalised KL condition, we have stated a global convergence result that we are going to refine in detail in a future release. We have concluded with a numerical toy example of phase unwrapping for three different Bregman distances. In a future work we are going to analyse the linearised Bregman iteration and its convergence behaviour in more detail and in a more generalised setting, and are going to investigate different Bregman distance choices as well as different numerical applications.

Acknowledgment

MB acknowledges support from the Leverhulme Trust Early Career project 'Learning from mistakes: a supervised feedback-loop for imaging applications' and the Isaac Newton Trust. MMB acknowledges support from the Engineering and Physical Sciences Research Council (EPSRC) 'EP/K009745/1'. MJE and CBS acknowledge support from the Leverhulme Trust project 'Breaking the non-convexity barrier'. CBS further acknowledges support from EPSRC grant 'EP/M00483X/1', EPSRC centre 'EP/N014588/1' and the Cantab Capital Institute for the Mathematics of Information. All authors acknowledge support from CHiPS (Horizon 2020 RISE project grant) that made this contribution possible.

References

[1] Markus Bachmayr and Martin Burger. Iterative total variation methods for nonlinear inverse problems. *Inverse Problems*, 25(10):26, 2009.

[2] Heinz Bauschke, Jérôme Bolte, and Marc Teboulle. A descent lemma beyond Lipschitz gradient continuity: first-order methods revisited and applications. *Mathematics of Operations Research (to appear.)*.

[3] Amir Beck and Marc Teboulle. Mirror descent and nonlinear projected subgradient methods for convex optimization. *Operations Research Letters*, 31(3):167–175, 2003.

[4] Jérôme Bolte, Shoham Sabach, and Marc Teboulle. Proximal alternating linearized minimization for nonconvex and nonsmooth problems. *Mathematical Programming*, 146(1-2):459–494, 2014.

[5] Martin Burger, Elena Resmerita, and Lin He. Error estimation for Bregman iterations and inverse scale space methods in image restoration. *Computing*, 81(2-3):109–135, 2007.

[6] Arkadi Nemirovski and David Borisovich Yudin. Problem complexity and method efficiency in optimization. 1982.

[7] Wotao Yin. Analysis and generalizations of the linearized Bregman method. *SIAM Journal on Imaging Sciences*, 3(4):856–877, 2010.

[8] Wotao Yin, Stanley Osher, Donald Goldfarb, and Jerome Darbon. Bregman iterative algorithms for ℓ_1-minimization with applications to compressed sensing. *SIAM Journal on Imaging Sciences*, 1(1):143–168, 2008.

A computationally inexpensive coordinate map for Lie group integrators

CURRY, C.[1], OWREN, B.[1]

1 Norwegian University of Science and Technology (NTNU), N-7491 Trondheim, NORWAY
{curry, bryn}@ntnu.no

1 INTRODUCTION

Lie group integrators have been studied systematically for more than two decades, and there exists several survey articles, such as [3, 1]. Some of these integrators can be derived via a change of variables. There is a finite dimensional Lie group G acting transitively on a manifold M. The Lie algebra of G is denoted $\mathfrak{g}$. A usual assumption is that there is a coordinate map $\Psi : \mathfrak{g} \to G$ such that the solution of the differential equation can be expressed as

$$y(t) = \Psi(u(t)) \cdot y_0$$

in some neighborhood of the point $y_0 \in M$. Vector fields on M are represented by means of a map $f : M \to \mathfrak{g}$ [4] and the corresponding differential equation can be pulled back to $\mathfrak{g}$ locally such that $u(t)$ obeys the differential equation

$$\dot{u} = \mathrm{d}\Psi_u^{-1}(f(\Psi(u(t))))$$

In this note we shall focus on a choice of Ψ which is computationally inexpensive and we shall show how the derivative map $\mathrm{d}\Psi_u$ can be inverted efficiently as well. The definition of this map is

$$\mathrm{d}\Psi_u(v) = \left.\frac{\mathrm{d}}{\mathrm{d}t}\right|_{t=0} \Psi(u + tv) \cdot \Psi(u)^{-1} \tag{1}$$

so that $\mathrm{d}\Psi_u : \mathfrak{g} \to \mathfrak{g}$. The coordinate map we shall consider is called *canonical coordinates of the second kind* and is defined relative to a basis $\mathbf{e}_1, \ldots, \mathbf{e}_d$ for $\mathfrak{g}$, More

precisely, for any

$$u = \sum_{i=1}^{d} u_i \mathbf{e}_i, \quad \Psi(u) = \mathrm{e}^{u_1 \mathbf{e}_1} \cdot \mathrm{e}^{u_2 \mathbf{e}_2} \cdots \mathrm{e}^{u_d \mathbf{e}_d} \tag{2}$$

In parts of this exposition we shall follow relatively closely the paper [5]. It might seem counter intuitive to use such a large number of exponentials in a coordinate map. Comparing the standard Runge–Kutta–Munthe–Kaas integrators [3], the coordinate map is simply $\Psi = \exp$. Standard general software for computing matrix exponential to machine accuracy typically require Cn^3 floating point operation per exponential, where C is in typically in the range 20–30.

Example For illustration, we now consider the example $G = \mathrm{SL}(n)$ of unit determinant $n \times n$ matrices. Its Lie algebra is $\mathfrak{g} = \mathfrak{sl}(n)$ consisting of $n \times n$-matrices with zero trace. A very simple and intuitive basis for the Lie algebra $\mathfrak{sl}(n)$ is obtained by taking matrices of the form

$$\mathbf{e}_{i,j} = \mathrm{e}_i \mathrm{e}_j^\top, \ i \neq j, \text{ and } \mathbf{e}_{ii} = \mathrm{e}_{i+1} \mathrm{e}_{i+1}^\top - e_i e_i^\top, \ 1 \leq i \leq n-1$$

where e_i is the ith canonical unit vector. The computation of $\Psi(u) = \sum_{i,j=1}^{n^2-1} u_{i,j} \mathbf{e}_{i,j}$ can now be obtained through a simple iteration. Start by defining the diagonal matrix D with diagonal elements $d_{ii} = \mathrm{e}^{u_{i,i} - u_{i-1,i-1}}$, $1 \leq i \leq n$ where $u_{0,0} = u_{n,n} = 0$ and then

$M := D$
for $i, j = 1$ to n $(i \neq j)$ in some preferred order **do**
    $M = \mathbf{e}^{u_{ij} \mathbf{e}_{ij}} M = (I + u_{ij} \mathbf{e}_{ij}) M = M + u_{ij} \mathrm{e}_i^\top (\mathrm{e}_j^\top M)$
end

Note that the update in the for-loop just amounts to incrementing the ith row of m by a multiple $u_{i,j}$ of row j. □

2 THE DIFFERENTIAL OF THE COORDINATE MAP AND ITS FACTORIZATION

Substituting (2) into (1) we get after some calculations

$$\mathrm{d}\Psi_u(v) = v_1 \mathbf{e}_1 + A_1(v_2 \mathbf{e}_2) + A_1 A_2 (v_3 \mathbf{e}_3) + \cdots + A_1 A_2 \cdots A_{d-1}(v_d \mathbf{e}_d) \tag{3}$$

where

$$v = \sum_{i=1}^{d} v_i \mathbf{e}_i \text{ and } A_i := \mathrm{Ad}_{\mathrm{e}^{u_i \mathbf{e}_i}}$$

By first sight it might not be straightforward to see how this map can be inverted in an inexpensive way. Our approach to the problem is to search for modified operators $\hat{A}_i$ depending only on the coordinate u_i such that the expression can be turned into the form

$$\mathrm{d}\Psi_u = \hat{A}_1 \hat{A}_2 \cdots \hat{A}_{d-1} \tag{4}$$

A candidate for such a modified operator $\hat{A}_i$ might be

$$\hat{A}_i = Q_i + A_i(I - Q_i) \tag{5}$$

where Q_i is the linear projector defined on the basis as

$$Q_i \mathbf{e}_j = \begin{cases} \mathbf{e}_j, & j \leq i \\ 0 & j > i \end{cases}$$

This allows us trivially to write

$$\mathrm{d}\Psi_u(v) = \sum_{i=1}^{d-1} A_1 \cdots A_{i-1} \hat{A}_i \cdots \hat{A}_{d-1}(v_i \mathbf{e}_i)$$

since by (5) $\hat{A}_i(\mathbf{e}_j) = \mathbf{e}_j$ when $j \leq i$. If it would hold that

$$\hat{A}_1 \cdots \hat{A}_{i-1}(I - Q_i) = A_1 \cdots A_{i-1}(I - Q_i), \ i = 1, \ldots d, \tag{6}$$

then our desired factorization (4) would result. A criterion for (6) to hold was given and proved in [5, Theorem 3]. For any two integers i, j such that $0 \leq i < j \leq d$, we define the space

$$W_{i,j} = \mathrm{span}(\mathbf{e}_{i+1}, \ldots \mathbf{e}_j)$$

Theorem 2.1. *Suppose that for each operator A_i one lets r be the smallest integer such that*

$$A_i w \in W_{i-r,d-1}, \qquad w \in W_{i,d-1},$$

If whenever $r \geq 1$, the space $W_{i-r,i}$ is an abelian subalgebra of $\mathfrak{g}$ the condition (6) *holds, and we have the desired factorization* (4)*.*

Remark Theorem 2.1 gives sufficient conditions for an ordered basis for a Lie algebra $\mathfrak{g}$ to yield a coordinate map whose trivialized tangent map factors into elementary operators each depending on a single coordinate u_i.

3 COMPUTING THE INVERSE DIFFERENTIAL

Each individual $\hat{A}_i$ in (4) must be invertible so that

$$\mathrm{d}\Psi_u^{-1} = \hat{A}_{d-1}^{-1}\hat{A}_{d-2}^{-1}\cdots\hat{A}_1^{-1} \tag{7}$$

We may take advantage of the well known identity

$$A_i = \mathrm{Ad}_{\mathrm{e}^{u_i\mathbf{e}_i}} = \exp(\mathrm{ad}_{u_i\mathbf{e}_i}) = I + u_i\mathrm{ad}_{\mathbf{e}_i} + \frac{1}{2}u_i^2\mathrm{ad}_{\mathbf{e}_i}^2 + \cdots,$$

so that

$$A_i^{-1} = \exp(-\mathrm{ad}_{u_i\mathbf{e}_i}) = I - u_i\mathrm{ad}_{\mathbf{e}_i} + \frac{1}{2}u_i^2\mathrm{ad}_{\mathbf{e}_i}^2 + \cdots,$$

On the other hand, under the conditions of Theorem 2.1 it also holds that A_i commutes with $I - Q_i$, this allows us to write a similar expression for the inverse of $\hat{A}_i$,

$$\hat{A}_i^{-1} = Q_i + A_i^{-1}(I - Q_i) = I + (-u_i\mathrm{ad}_{\mathbf{e}_i} + \frac{1}{2}u_i^2\mathrm{ad}_{\mathbf{e}_i}^2 + \cdots)(I - Q_i)$$

Not surprisingly, we shall consider basis vectors $\mathbf{e}_i$ which are ad-nilpotent thus the infinite expansions become finite.

Remark Suppose that among the basis vectors there is a mutually commutative subset spanning an abelian subalgebra of $\mathfrak{g}$. If these are ordered at the end, i.e. as $(\mathbf{e}_{d^*+1}, \ldots, \mathbf{e}_d)$, then the corresponding $\hat{A}_{d^*+i}$ each reduce to the identity operator and therefore can be ignored in the expression (7).

4 CHOOSING AND ORDERING THE BASIS – SEMISIMPLE CASE

For semisimple Lie algebras, there is a natural intrinsic decomposition of $\mathfrak{g}$ called the Cartan decomposition which gives rise to a particular basis called the Chevalley basis. This comes from the structure theory of Lie algebras related to root systems, for details, see [2]. A particular property of the Chevalley basis is that all structure constants are integers. One can identify a *maximal toral subalgebra* $\mathfrak{h}$ of dimension ℓ, this is an abelian subalgebra of $\mathfrak{g}$ often given as the diagonal matrices in representations of $\mathfrak{g}$. Its dual $\mathfrak{h}^*$ contains the *roots*, each of which corresponds to a one-dimensional subspace. For a root $\alpha \in \mathfrak{h}^*$, we have for any $h \in \mathfrak{h}$ that $\mathrm{ad}_h\mathbf{e}_\alpha = \alpha(h)\mathbf{e}_\alpha$, and we set $\mathfrak{g}_\alpha = \mathrm{span}(\mathbf{e}_\alpha)$. We can pick a basis for $\mathfrak{h}$ and let $\mathfrak{h} = \mathrm{span}(\mathbf{h}_1, \ldots, \mathbf{h}_\ell)$, and

as indicated order them last. The ordering if the roots $\alpha_1, \ldots, \alpha_{d^*}$ must be done carefully in order to satisfy the conditions of Theorem 2.1. Thanks to the properties of root systems, the basis obtained in this way has several favourable properties. For instance, for any root α, $\mathrm{ad}_{\mathbf{e}_\alpha}$ is nilpotent. Also it holds that if α, β are roots then $[\mathfrak{g}_\alpha, \mathfrak{g}_\beta] \subset \mathfrak{g}_{\alpha+\beta}$ where by convention $\mathfrak{g}_0 = \mathfrak{h}$ (though 0 is not itself a root). It turns out that if α is a root then so is $-\alpha$, this makes it natural to split the sett of roots into the positive and negative roots. A complete description of how such a Chevalley basis can be ordered was given in [5]. In this short note we just give one example, we shall revisit the example from the introduction where $\mathfrak{g} = A_\ell = \mathfrak{sl}(\ell+1, \mathbb{C})$. It turns out that the basis we listed is precisely the Chevalley basis for this Lie algebra. Representing A_ℓ by means of $(\ell+1) \times (\ell+1)$-matrices of vanishing trace, we find that the elements

$$\mathbf{h}_i = \mathbf{e}_{ii} = \mathrm{e}_i \mathrm{e}_i^\top - \mathrm{e}_{i+1} \mathrm{e}_{i+1}^\top, \quad i = 1, \ldots, \ell$$

spans a maximal toral subalgebra. There are a total of $\ell(\ell+1)$ roots, the positive ones are denoted $\alpha_{i,j},\ 1 \leq i \leq j \leq \ell$ and are associated to the root spaces

$$\mathfrak{g}_{\alpha_{i,j}} = \mathrm{span}(\mathrm{e}_i \mathrm{e}_{j+1}^\top)$$

The negative roots, $-\alpha_{i,j},\ 1 \leq i \leq j \leq \ell$ define the rootspaces

$$\mathfrak{g}_{-\alpha_{i,j}} = \mathrm{span}(\mathrm{e}_{j+1} \mathrm{e}_i^\top)$$

There are several possible orderings which all lead to the condition (6) being satisfied. We begin by the positive roots, then the negative roots, and finally the basis for $\mathfrak{h}$, more precisely, we order as follows

$$(\mathbf{e}_{\alpha_{i_1,j_1}}, \ldots, \mathbf{e}_{\alpha_{i_m,j_m}}, \mathrm{e}_{-\alpha_{i_1,j_1}}, \ldots, \mathbf{e}_{-\alpha_{i_m,j_m}}, \mathbf{h}_1, \ldots, \mathbf{h}_\ell)$$

where $i_1 \leq i_2 \leq \cdots \leq i_m$ and $m = \frac{1}{2}\ell(\ell+1)$.

A similar study was performed for all the remaining classical semisimple Lie algebras in [5] and even for the exceptional Lie algebra G_2.

References

[1] E. Celledoni, H. Marthinsen, and B. Owren. An introduction to Lie group integrators—basics, new developments and applications. *J. Comput. Phys.*, 257(part B):1040–1061, 2014.

[2] J. E. Humphreys. *Introduction to Lie Algebras and Representation Theory*. Graduate Texts in Mathematics. Springer–Verlag, 1972.

[3] A. Iserles, H. Z. Munthe-Kaas, S. P. Nørsett, and A. Zanna. Lie-group methods. *Acta Numerica*, 9:215–365, 2000.

[4] H. Munthe-Kaas. High order Runge–Kutta methods on manifolds. *Appl. Numer. Math.*, 29:115–127, 1999.

[5] B. Owren and A. Marthinsen. Integration methods based on canonical coordinates of the second kind. *Numer. Math.*, 87(4):763–790, 2001.

Størmer-Cowell methods revisited

MITSUI, Taketomo[1]

1 Nagoya University, Furo-cho, Chikusa-ku, Nagoya, 464-8601 JAPAN
tom.mitsui@nagoya-u.jp

Abstract

Størmer-Cowell method is known to numerically integrate a second-order ordinary differential equation not including the first derivative explicitly. We show a non-conventional way to derive the methods systematically. Numerical experiments suggest that the methods have a potential to solve the special type of ODEs directly, even though they have many constraints in stability and symplecticness.

1 What is Størmer-Cowell method

To integrate second-order ordinary differential equation (ODE) given in the special form

$$\frac{\mathrm{d}^2 y}{\mathrm{d}x^2} = f(x, y) \quad (a < x < b), \tag{1.1}$$

a method, not including $\mathrm{d}y/\mathrm{d}x$, is desired. Here y and f denote functions of $[a, b] \to \mathbb{R}^d$ and $[a, b] \times \mathbb{R}^d \to \mathbb{R}^d$, respectively. Series of discrete variable method written in the form

$$y_{n+1} - 2y_n + y_{n-1} = h^2 \sum_{j=0}^{k} \beta_j f_{n+1-j} = h^2(\beta_0 f_{n+1} + \beta_1 f_n + \beta_2 f_{n-1} + \cdots + \beta_k f_{n+1-k}) \tag{1.2}$$

is often called the Størmer[1]-Cowell method (p.255 of [3]). Hereafter we refer them by SC methods. Of course we assume an equi-distant step-points $x_n = a + nh$ $(h = (b - a)/N)$ and the approximate value y_j stands for $y(x_j)$ and f_j means $f(x_j, y_j)$ $(j = 0, 1, 2, \ldots, N)$. If $\beta_0 = 0$, the method is explicit, otherwise it is implicit.

Two well-known examples of explicit and implicit are:

$$y_{n+1} - 2y_n + y_{n-1} = h^2 f_n, \tag{1.3}$$

which is referred to Størmer's or Encke's method, and

$$y_{n+1} - 2y_n + y_{n-1} = \frac{h^2}{12}(f_{n+1} + 10f_n + f_{n-1}), \tag{1.4}$$

[1]The name Størmer is often spelled as Störmer. However, since he was a Norwegian mathematician, Fredrik Carl Mulertz Størmer (3 September 1874 – 13 August 1957). it should be correctly spelled as this.

which is called Numerov's method (III.10 of [2]) or 'the royal road formula' (p. 255 of [3]). The derivation process of SC method, *e.g.,* in p. 463 of [2] starts with twice integrations of the ODE (1.1) by Cauchy's lemma to give

$$y(x_n + h) = y(x_n) + hy'(x_n) + h^2 \int_0^1 (1 - s) f(x_n + sh, y(x_n + sh))\, \mathrm{d}s.$$

Similarly we obtain

$$y(x_n - h) = y(x_n) - hy'(x_n) + h^2 \int_0^1 (1 - s) f(x_n - sh, y(x_n - sh))\, \mathrm{d}s.$$

Thus we can attain

$$\begin{aligned} &y(x_n + h) - 2y(x_n) + y(x_n - h) = \\ &\quad h^2 \int_0^1 (1 - s) \left(f(x_n + sh, y(x_n + sh)) + f(x_n - sh, y(x_n - sh)) \right) \mathrm{d}s. \end{aligned}$$

Employing the interpolating polynomial in terms of backward differences, we have the approximation

$$f(x_n + sh, y(x_n + sh)) \approx p(x_n + sh) = \sum_{j=0}^{k-1} (-1)^j \binom{-s}{j} \nabla^j f_n,$$

where the symbol $\binom{-s}{j}$ denotes the generalized binomial coefficient. Then, substitution gives the explicit formula $y_{n+1} - 2y_n + y_{n-1} = h^2 \sum_{j=0}^{k-1} \sigma_j \nabla^j f_n$, where

$$\sigma_j = (-1)^j \int_0^1 (1 - s) \left\{ \binom{-s}{j} + \binom{s}{j} \right\} \mathrm{d}s.$$

Similarly, the implicit formula can be derived as $y_{n+1} - 2y_n + y_{n-1} = h^2 \sum_{j=0}^{k} \sigma_j^* \nabla^j f_{n+1}$, where

$$\sigma_j^* = (-1)^j \int_0^1 (1 - s) \left\{ \binom{-s+1}{j} + \binom{s+1}{j} \right\} \mathrm{d}s$$

Descriptions about (1.2) from the view point of geometric numerical integration can be found in Chapter XIV of [1].

2 New way of derivation

We start by integrating *three times* both sides of the ODE (1.1). For the left-hand side we obtain

$$\begin{aligned} \int_{x_{n-1}}^{x_n} \int_{x_n}^{x_{n+1}} \int_s^t \frac{\mathrm{d}^2 y}{\mathrm{d}x^2}(x)\, \mathrm{d}x\, \mathrm{d}t\, \mathrm{d}s &= \int_{x_{n-1}}^{x_n} \int_{x_n}^{x_{n+1}} \left\{ \frac{\mathrm{d}\, y}{\mathrm{d}\, x}(t) - \frac{\mathrm{d}\, y}{\mathrm{d}\, x}(s) \right\} \mathrm{d}s\, \mathrm{d}t \\ &= h \left(y(x_{n+1}) - 2y(x_n) + y(x_{n-1}) \right), \end{aligned}$$

while the right-hand side becomes

$$\int_{x_{n-1}}^{x_n}\int_{x_n}^{x_{n+1}}\int_s^t f(x,y(x))\,\mathrm{d}x\,\mathrm{d}t\,\mathrm{d}s.$$

This means analytically we obtain

$$y(x_{n+1})-2y(x_n)+y(x_{n-1})=\frac{1}{h}\int_{x_{n-1}}^{x_n}\int_{x_n}^{x_{n+1}}\int_s^t f(x,y(x))\,\mathrm{d}x\,\mathrm{d}t\,\mathrm{d}s. \tag{2.1}$$

Then, we replace the integrand $f(x,y(x))$ with the interpolating polynomial $p(x)$. For instance, suppose we employ the formula

$$p(x)=p(x_n+\theta h)=\sum_{j=0}^{k}(-1)^j\binom{-\theta+1}{j}\nabla^j f_{n+1}. \tag{2.2}$$

By putting $\psi(\theta)\equiv p(x_n+\theta h)$ together with the variable transformation $\tau=(t-x_n)/h, \sigma=(s-x_n)/h$, we obtain

$$\int_{x_{n-1}}^{x_n}\int_{x_n}^{x_{n+1}}\int_s^t p(x)\,\mathrm{d}x\,\mathrm{d}t\,\mathrm{d}s=h^3\int_{-1}^{0}\int_0^1\int_\sigma^\tau \psi(\theta)\,\mathrm{d}\theta\,\mathrm{d}\tau\,\mathrm{d}\sigma.$$

Consequently, defining the coefficients

$$S_j^*=(-1)^j\left\{\int_{-1}^{0}\int_0^1\int_\sigma^\tau\binom{-\theta+1}{j}\,\mathrm{d}\theta\,\mathrm{d}\tau\,\mathrm{d}\sigma\right\}\quad(j=0,1,2,\ldots), \tag{2.3}$$

we arrive at the k-step implicit SC method as $y_{n+1}-2y_n+y_{n-1}=h^2\sum_{j=0}^{k}S_j^*\nabla^j f_{n+1}$ $(k=0,1,2,\ldots)$. By carrying out the integration in (2.3), we can obtain

$$\begin{aligned} y_{n+1}-2y_n+y_{n-1} &= h^2\left(f_{n+1}-\nabla f_{n+1}+\frac{1}{12}\nabla^2 f_{n+1}-0\cdot\nabla^3 f_{n+1}-\frac{1}{240}\nabla^4 f_{n+1}\right.\\ &\quad -\frac{1}{240}\nabla^5 f_{n+1}-\frac{221}{60480}\nabla^6 f_{n+1}-\frac{19}{6048}\nabla^7 f_{n+1}-\frac{9829}{3628800}\nabla^8 f_{n+1}\\ &\quad \left.-\frac{407}{172800}\nabla^9 f_{n+1}-\frac{330157}{159667200}\nabla^{10} f_{n+1}+\cdots\right). \end{aligned} \tag{2.4}$$

Similarly, when the interpolating polynomial (2.2) is replaced with the explicit one

$$p(x)=p(x_n+\theta h)=\sum_{j=0}^{k-1}(-1)^j\binom{-\theta}{j}\nabla^j f_n\quad(k=1,2,\ldots),$$

introduction of $\varphi(\theta)\equiv p(x_n+\theta h)$ with $\tau=(t-x_n)/h$ and $\sigma=(s-x_n)/h$ derives

$$\int_{x_{n-1}}^{x_n}\int_{x_n}^{x_{n+1}}\int_s^t p(x)\,\mathrm{d}x\,\mathrm{d}t\,\mathrm{d}s=h^3\int_{-1}^{0}\int_0^1\int_\sigma^\tau \varphi(\theta)\,\mathrm{d}\theta\,\mathrm{d}\tau\,\mathrm{d}\sigma.$$

Thus, we arrive at

$$h^2\sum_{j=0}^{k-1}(-1)^j\nabla^j f_n\left\{\int_{-1}^{0}\int_0^1\int_\sigma^\tau\binom{-\theta}{j}\,\mathrm{d}\theta\,\mathrm{d}\tau\,\mathrm{d}\sigma\right\}$$

for the right-hand side of (2.1) instead. Defining the coefficients

$$S_j = (-1)^j \left\{ \int_{-1}^{0} \int_{0}^{1} \int_{\sigma}^{\tau} \binom{-\theta}{j} \,\mathrm{d}\theta \,\mathrm{d}\tau \,\mathrm{d}\sigma \right\} \quad (j = 0, 1, 2, \ldots), \tag{2.5}$$

we can obtain the k-step explicit SC method as $y_{n+1} - 2y_n + y_{n-1} = h^2 \sum_{j=0}^{k-1} S_j \nabla^j f_n$. In fact we attain

$$\begin{aligned} y_{n+1} - 2y_n + y_{n-1} &= h^2 \left(f_n + 0 \cdot \nabla f_n + \frac{1}{12}\nabla^2 f_n + \frac{1}{12}\nabla^3 f_n + \frac{19}{240}\nabla^4 f_n \right. \\ &\quad + \frac{3}{40}\nabla^5 f_n + \frac{863}{12096}\nabla^6 f_n + \frac{275}{4032}\nabla^7 f_n + \frac{33953}{518400}\nabla^8 f_n \\ &\quad \left. + \frac{8183}{129600}\nabla^9 f_n + \frac{3250433}{53222400}\nabla^{10} f_n + \cdots \right). \end{aligned}$$

The above process of course means the identities $\sigma_j = S_j$ and $\sigma_j^* = S_j^*$, that is, we establish two integral identities w.r.t. the binomial coefficients:

$$\int_{-1}^{0} \int_{0}^{1} \int_{\sigma}^{\tau} \binom{-\theta + 1}{j} \,\mathrm{d}\theta \,\mathrm{d}\tau \,\mathrm{d}\sigma = \int_{0}^{1} (1 - s) \left\{ \binom{-s + 1}{j} + \binom{s + 1}{j} \right\} \mathrm{d}s$$

and

$$\int_{-1}^{0} \int_{0}^{1} \int_{\sigma}^{\tau} \binom{-\theta}{j} \,\mathrm{d}\theta \,\mathrm{d}\tau \,\mathrm{d}\sigma = \int_{0}^{1} (1 - s) \left\{ \binom{-s}{j} + \binom{s}{j} \right\} \mathrm{d}s.$$

Also the expressions can lead that the k-step implicit and explicit SC methods at least attain $(k + 1)$-st and k-th order of convergence, respectively. It happens, however, the actual order exceeds it by calculating the backward differences explicitly. Numerov's method, which has the fourth-order convergence, is the case.

3 Stability and symplecticness

Significant issues of numerical solution of Eq. (1.1) are stability and symplecticness, for the equation of autonomous case is naturally regarded as a Hamiltonian system by considering x, y and $\mathrm{d}y/\mathrm{d}x$ as t, q and p, respectively. That is, we solve the problem

$$\frac{\mathrm{d}\, q}{\mathrm{d}\, t} = p, \quad \frac{\mathrm{d}\, p}{\mathrm{d}\, t} = f(q),$$

which has the Hamiltonian $H(p, q) = (p^{\mathsf{T}} p)/2 + U(q)$. One of the major problems is to analyse the stability of the SC methods. Our standpoint is the linear stability analysis to examine the solution behaviour when the method is applied to the scalar test equation

$$y'' + \lambda^2 y = 0 \quad (\lambda > 0). \tag{3.1}$$

Let H denote λh. The method (1.2) reduces to

$$\begin{aligned} &\sum_{j=0}^{k} R_j(H^2) y_{n+1-j} \equiv \\ &\qquad (1 + \beta_0 H^2) y_{n+1} - (2 - \beta_1 H^2) y_n + (1 + \beta_2 H^2) y_{n-1} + H^2 \sum_{j=3}^{k} \beta_j y_{n+1-j} = 0 \end{aligned} \tag{3.2}$$

when applied to (3.1), where $R_j(Z)$ is a polynomial of first degree in Z. Since two fundamental solutions of (3.1) at $x_n = nh$ are expressed by $e^{\mathrm{i}n\lambda h}$ and $e^{-\mathrm{i}n\lambda h}$, the question is how large we can take the magnitude of the step-size h so that the numerical solution follows the periodic behaviour of the analytical solution when the number of steps n is getting large. The biggest interval $(0, H_0^2)$ of H which keeps the property is called the interval of periodicity and, furthermore, the method is called P-stable if it has the interval of periodicity $(0, \infty)$.

However, Lambert and Watson [4] proved that a P-stable linear multistep method is necessarily implicit and its order of accuracy cannot exceed two. Furthermore, they showed the interval of periodicity of Numerov's method is $[0, 6]$ by applying the boundary locus technique. On the other hand, [4] asserted the interval of periodicity of Encke's method is $[0, 4]$. Unfortunately the method which is proved to be P-stable in [4] does not fall in the SC family.

Since the SC methods are within the class of linear multistep methods, much restriction is imposed on them with respect to the symplecticness. In fact, **Theorem 3.1** of Chapter XIV of [1] says:

> *The underlying one-step method of an irreducible linear multistep method cannot be symplectic.*

This can be interpreted that a linear multistep method cannot be symplectic generally. The problem is how far it is from 'symplecticness'. In particular, since SC methods do not evaluate $\mathrm{d}y/\mathrm{d}x$ explicitly in the integration process, they may have an advantage in computation process.

Here we will give a short remark about the Størmer-Verlet method, which is known to be symplectic and of the second order of convergence for general Hamiltonian systems, when applied to (1.1). By introducing an auxiliary discrete variable $z_{n+1/2}$ which approximates $\dfrac{\mathrm{d}\,y}{\mathrm{d}\,x}\left(x_n + \dfrac{h}{2}\right)$, the method is expressed as

$$z_{n+1/2} = z_{n-1/2} + hf(x_n, y_n), \quad y_{n+1} = y_n + hz_{n+1/2}.$$

Note at the start ($n = 0$) it requires y_0 and $z_{-1/2}$. Instead, an alternate formulation can be given by

$$\begin{cases} y_{n+1} = y_n + hz_n + \dfrac{h^2}{2} f(x_n, y_n), \\ z_{n+1} = z_n + \dfrac{h}{2}\left(f(x_n, y_n) + f(x_{n+1}, y_{n+1})\right), \end{cases} \tag{3.3}$$

which requires (y_0, z_0) at the start. The function value $f(x_{n+1}, y_{n+1})$ should be stored and substituted for the next computation of y_{n+2}.

In the autonomous case ($f(x, y) \equiv f(y)$), it is still a symplectic transformation. Let F denote the mapping by the method from $\begin{bmatrix} y_n \\ z_n \end{bmatrix}$ to $\begin{bmatrix} y_{n+1} \\ z_{n+1} \end{bmatrix}$. Then, it is possible to write it as

$$F\left(\begin{bmatrix} y_n \\ z_n \end{bmatrix}\right) = \begin{pmatrix} y_n + hz_n + \dfrac{h^2}{2} f(y_n) \\ z_n + \dfrac{h}{2} f(y_n) + \dfrac{h}{2} f\left(y_n + hz_n + \dfrac{h^2}{2} f(y_n)\right) \end{pmatrix}.$$

Its Jacobian matrix $\mathcal{D}$ is given by

$$\mathcal{D} = \begin{pmatrix} 1 + \dfrac{h^2}{2} f'(y_n) & h \\ \dfrac{h}{2} f'(y_n) + \dfrac{h}{2} f'\left(y_n + h z_n + \dfrac{h^2}{2} f(y_n) \right) \left(1 + \dfrac{h^2}{2} f'(y_n) \right) & 1 + \dfrac{h^2}{2} f'\left(y_n + h z_n + \dfrac{h^2}{2} f(y_n) \right) \end{pmatrix}.$$

Hence we can confirm the identity $\mathcal{D}^{\mathsf{T}} \begin{pmatrix} O & I \\ -I & O \end{pmatrix} \mathcal{D} = \begin{pmatrix} O & I \\ -I & O \end{pmatrix}$ holds.

4 Numerical results

We carried out numerical computations to show the feature of the SC methods through the simple pendulum problem, that is,

$$\frac{\mathrm{d}^2 q}{\mathrm{d}\, t^2} = -\sin\, q \quad (0 < t < T), \quad q(0) = q_0, \quad \frac{\mathrm{d}\, q}{\mathrm{d}\, t}(0) = p_0 \tag{4.1}$$

whose Hamiltonian is $H(p, q) = p^2/2 - \cos(q)$ as described in §3. We compared the results by Numerov's, Encke's, the Størmer-Verlet and the classical Runge-Kutta methods. Here we only show the results by Numerov's method.

There are several issues in implementing the SC methods. First, starting values are required for SC methods, even though Encke's and Numerov's require only p_1. Our numerical computations adopted the classical Runge-Kutta solution for this purpose. To carry through the numerical procedure not evaluating the first derivative, Runge-Kutta-Nyström methods must be employed. Second, a nonlinear equation solver is called for Numerov's method. We simply applied the fixed point iteration with a pre-assigned tolerance. This has another advantage that it is efficient for small h. Third, since SC methods never calculate $p_1, p_2, \ldots$ in the numerical process, the problem is how to evaluate the Hamiltonian and the phase plane plot of $\{(q_n, p_n)\}$. We employed an approximation by the simple difference quotient $p_n \approx (q_n - q_{n-1})/h$, which is, however, to be studied more carefully.

Variation of the Hamiltonian by Numerov's method starting with $(q_0, p_0) = (2.2, 0)$ and $(q_0, p_0) = (0, 1.2)$ for $0 \leq t \leq 10$ is depicted in Figs. 4.1 and 4.2, respectively. Phase plane plots by Numerov's method on (q, p)-plane over the intervals $0 \leq t \leq 10$, $50 \leq t \leq 60$ and $90 \leq t \leq 100$ with $(q_0, p_0) = (2.2, 0)$ and $(q_0, p_0) = (0, 1.2)$ are in Figs. 4.3 and 4.4, respectively. For comparison's sake, the exact curves of the closed loop are shown on the phase plane in each right-hand side. Colours distinguish the difference of computation intervals ($[0, 10]$ by red, $[50, 60]$ by blue, $[90, 100]$ by green), but almost no difference is observed on the figures.

Our temporal conclusions are:

- Even though SC methods cannot attain excellent stability and genuine symplecticness, they might have a potential to apply to the real problems.
- Close numerical results to the symplectic integrators can be attained in our initial trials.
- Computational costs can be reduced by SC methods.
- The future problem is to estimate how close (or far) they are theoretically and numerically.

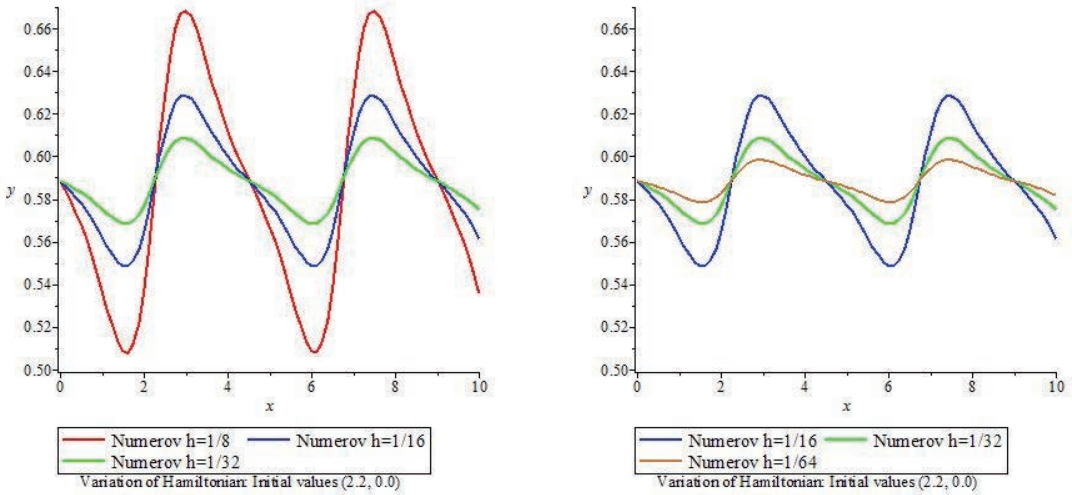

Figure 4.1: Variation of Hamiltonian by Numerov's method $(q_0, p_0) = (2.2, 0)$ ($h = 1/8$ (red), 1/16 (blue), 1/32 (green), 1/64 (gold))

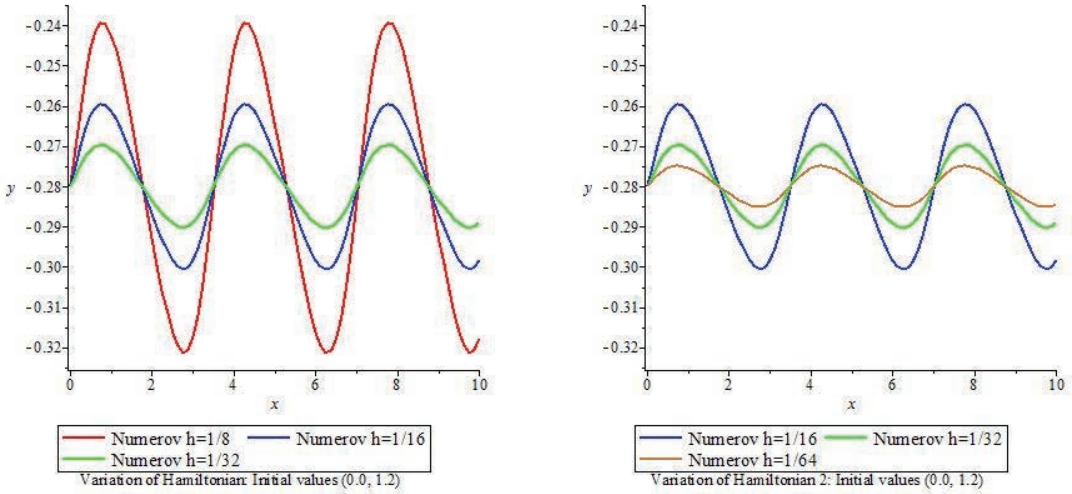

Figure 4.2: Variation of Hamiltonian by Numerov's method $(q_0, p_0) = (0, 1.2)$ ($h = 1/8$ (red), 1/16 (blue), 1/32 (green), 1/64 (gold))

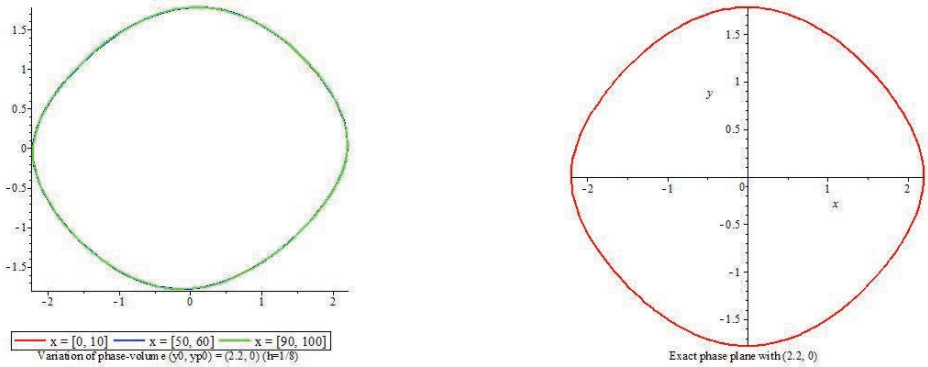

Figure 4.3: Phase plane plot of Numerov's method $(q_0, p_0) = (2.2, 0)$ with the exact one ($[0, 10]$ red, $[50, 60]$ blue, $[90, 100]$ green)

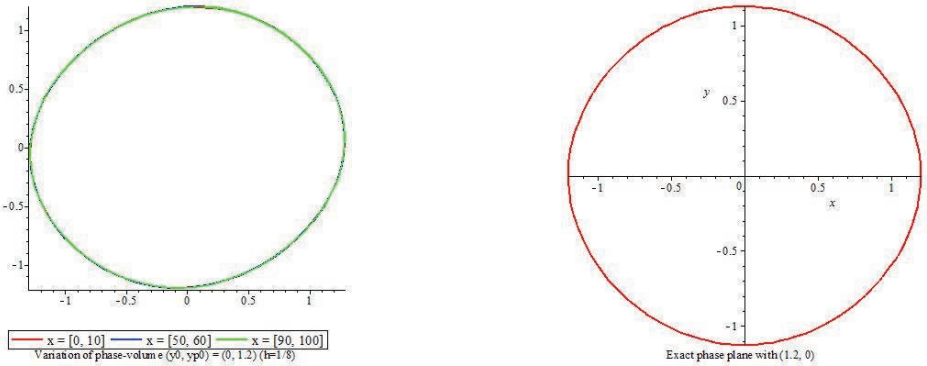

Figure 4.4: Phase plane plot of Numerov's method $(q_0, p_0) = (0, 1.2)$ with the exact one ($[0, 10]$ red, $[50, 60]$ blue, $[90, 100]$ green)

References

[1] Hairer, E., Lubich, Ch. and Wanner, G., *Geometric Numerical Integration — Structure-Preserving Algorithms for Ordinary Differential Equations*, Springer-V., 2002.

[2] Hairer, E., Nørsett, S.P. and Wanner, G., *Solving Ordinary Differential Equations I, Nonstiff Problems*, 2nd revised ed., Springer-V., 1993.

[3] Lambert, J. D., *Computational Methods in Ordinary Differential Equations* (esp. Chapt. 9), John Wiley and Sons, 1973.

[4] Lambert, J. D. and Watson, I. A., *Symmetric multistep methods for periodic initial value problems,* J. Inst. Math. Appl., **18** (1976), pp.189-202.

Two classes of quadratic vector fields for which the Kahan discretization is integrable

Elena Celledoni[1], Robert I. McLachlan [2], David I. McLaren[3],
Brynjulf Owren[1], G.R.W. Quispel[3],

1 Norwegian University of Science and Technology, 7491, Trondheim, Norway
2 Massey University, Palmerston North, New Zealand
3 La Trobe University, Victoria 3086, Australia

1 INTRODUCTION

Kahan's method for discretizing quadratic differential equations was introduced in [1]. It was rediscovered in the context of integrable systems by Hirota and Kimura [2]. Suris and collaborators extended the applications to integrable systems significantly in a series of papers [3], [4], [5], [6], [7]. Applications to non-integrable Hamiltonian systems and the use of polarisation to discretise arbitrary degree Hamiltonian systems were studied in [8], [9] and [10].

The present paper contains an extract of the talk one of the authors (GRWQ) gave on 6th July 2016 at the 12th International Conference on Symmetries and Integrability of Difference Equations (SIDE12) in Sainte Adele, Quebec, Canada. We present two classes of 2-dimensional ODE systems of quadratic vector fields where the Kahan discretization is integrable. Both classes of systems can be cast in the form

$$\frac{dX}{dt} = \varphi(X) K \nabla H(X), \tag{1}$$

where

$$X^t = (x, y), \qquad K = \begin{pmatrix} 0 & 1 \\ -1 & 0 \end{pmatrix},$$

and $\varphi(X)$ is a scalar function of the components of X. In the first class the Hamiltonian function is quartic and in the second class it is sextic. These systems can be seen as generalisations of the examples of the reduced Nahm equations presented in [6]. Some of the results in this paper were found independently by Petrera and Zander [11].

2 Quartic Hamiltonians in 2D

Consider the 2-dimensional ODE system (1) where $\varphi(X) = \frac{1}{ax+by}$, and the homogeneous Hamiltonian has the form $H = (ax + by)^2(cx^2 + 2dxy + ey^2)$. Then the Kahan map for this system preserves the modified Hamiltonian:

$$\widetilde{H}(X) = \frac{H}{(1 + h^2 D(ax + by)^2 + h^2 E(cx^2 + 2dxy + ey^2))(1 + h^2 9D(ax + by)^2 + h^2 E(cx^2 + 2dxy + ey^2)},$$

and the measure:

$$m(x,y) = \frac{dxdy}{(ax+by)(cx^2+2dxy+ey^2)}.$$

Here, $D := ce - d^2$ and $E := 2abd - a^2e - b^2c$. It follows that the Kahan map is integrable.

3 Sextic Hamiltonians in 2D

Consider the 2-dimensional ODE system (1) with $\varphi(X) = \frac{1}{(cx+dy)(ex+fy)^2}$ and with the *homogeneous* sextic Hamiltonian $H = (ax+by)(cx+dy)^2(ex+fy)^3$. Then the Kahan map for this system preserves the modified Hamiltonian:

$$\widetilde{H}(X) = \frac{H}{(1+a_5l_2^2)(1+a_3l_1^2+a_4l_3^2+a_7l_1l_3)(1+a_5l_2^2+a_6l_3^2))}$$

where

$$l_1 := ax+by, \quad l_2 := cx+dy, \quad l_3 := ex+fy,$$

and $d_{1,2} := h(ad-bc)$, $d_{2,3} := h(cf-ed)$, $d_{3,1} := h(eb-fa)$ and $a_3 := \frac{-9d_{2,3}^2}{4}$, $a_4 := \frac{-d_{1,2}^2}{4}$, $a_5 := \frac{-9d_{3,1}^2}{4}$; $a_6 := -4d_{1,2}^2$, $a_7 := \frac{3d_{1,2}d_{2,3}}{2}$. In this case the Kahan map also preserves the modified measure

$$m(x,y) = \frac{dxdy}{(ax+by)(cx+dy)(ex+fy)}.$$

Again, the Kahan map is integrable.

Acknowledgment

This work was supported by the Australian Research Council, by the Research Council of Norway, by the Marsden Fund of the Royal Society of New Zealand, and by the European Union's Horizon 2020 research and innovation programme under the Marie Sklodowska-Curie grant agreement No. 691070.

References

[1] W Kahan, *Unconventional numerical methods for trajectory calculations*, Unpublished lecture notes, 1993.

[2] K Kimura and R Hirota, *Discretization of the Lagrange top*, J. Phys. Soc. Jap. **69** (2000), 3193–3199.

[3] M Petrera and Y B Suris, *On the Hamiltonian structure of Hirota-Kimura discretization of the Euler top*, Mathematische Nachrichten **283** (11) (2010), 1654–1663.

[4] M Petrera and Y B Suris, *SV Kovalevskaya system, its generalization and discretization*, Frontiers of Mathematics in China **8** (2012), 1047–1065.

[5] M Petrera and Y B Suris, *Spherical geometry and integrable systems*, Geometriae Dedicata **169** (2014), 83–98.

[6] M Petrera, A Pfadler and Y B Suris, *On integrability of Hirota-Kimura type discretizations,* Regular and Chaotic Dynamics **16** (2011), 245–289.

[7] A Hone and M Petrera, *Three-dimensional discrete systems of Hirota-Kimura type and deformed Lie-Poisson algebras*, Journal of Geometric Mechanics **1** (2009), 55-85.

[8] E Celledoni, R I McLachlan, B Owren and G R W Quispel, *Geometric properties of Kahan's method* J Phys. A **46** (2013), 025001.

[9] E Celledoni, R I McLachlan, B Owren and G R W Quispel, *Integrability properties of Kahan's method,* J. Phys. A **47** (2014), 365202.

[10] E Celledoni, R I McLachlan, B Owren and G R W Quispel, *Discretization of polynomial vector fields by polarisation*, Proc. Roy. Soc. **A471** (2015) 20150390, 10pp.

[11] M Petrera and R. Zander, *New classes of quadratic vector fields admitting integral-preserving Kahan-Hirota-Kimura discretizations*, arXiv:1610.03664 [nlin.SI].

Energy-Preserving Discrete Gradient Schemes for the Hamilton Equation Based on the Variational Principle

ISHIKAWA, A.[1] and YAGUCHI, T.[2]

1 Kobe University, 1-1 Rokkodai-cho, Nada-ku, Kobe, 657-8501 JAPAN

a-ishikawa@stu.kobe-u.ac.jp

2 Kobe University, 1-1 Rokkodai-cho, Nada-ku, Kobe, 657-8501 JAPAN

JST PRESTO, 4-1-8 Honcho, Kawaguchi, Saitama, 332-0012, JAPAN

yaguchi@pearl.kobe-u.ac.jp

1 INTRODUCTION

Recently, as a technique to design numerical schemes that preserve a structure and a property of a given differential equation, methods so-called the structure-preserving numerical method are studied widely. The discrete gradient method [1, 2] and the method of the symmetry [3] are known in particular as methods aiming at the law of the conservation of energy. The discrete gradient method is a method for the Hamilton mechanics. In this method numerical schemes are obtained by replacing the gradient with the discrete gradient, which is defined so that it has a similar property to the usual gradient. Although schemes that are obtained in this way usually show superior stability in practice, from the theoretical perspective, the natural relations to the variational principle, which is a foundation of analytical mechanics, are not apparent. In contrast, a method to derive the energy-preserving numerical schemes based on a combination of the variational principle and the discrete gradient was suggested recently [4]. Because this method has the variational principle as the base of the method, the wide applications including those to dissipative systems are possible. Besides, the scheme is shown to be explicit under a certain mild condition. Moreover, this method shares the idea with the method based on the symmetry, which is a method for the Lagrange mechanics, and actually the relation between these two methods was revealed in some specific examples.

On the other hand, we cannot use it for the general Hamilton equation, which includes the advection equation and the KdV equation, because the Hamilton equations only on cotangent bundles

$$\dot{q} = \frac{\partial \mathcal{H}}{\partial p}, \quad \dot{p} = -\frac{\partial \mathcal{H}}{\partial q} \tag{1}$$

are considered in [4]. Indeed the action integral considered in [4] is defined only on the cotangent bundles, and in order to apply the method to the Hamilton equations on general symplectic manifolds, an action integral that derives the Hamilton equation on those manifolds is necessary. In this paper, we extend this method to the general

Hamilton equations defined on symplectic affine spaces by using a variational principle which is defined by using the almost complex structure equipped on those spaces.

2 ALMOST COMPLEX STRUCTURE

The almost complex structure is defined as follows.

Definition 1 *Let $\mathcal{TM}$ be the tangent bundle of a differential manifold $\mathcal{M}$ whose dimension is even. A self-isomorphism $J : \mathcal{TM} \to \mathcal{TM}$, $(x, v) \mapsto (x, J_x v)$ that satisfies*

$$J_x^2 = -Id$$

is called an almost complex structure, where for each $x \in \mathcal{M}$, J_x is the self-isomorphism on $\mathcal{T}_x\mathcal{M}$.

It is known that every symplectic manifold $(\mathcal{M}, \omega)$ has an almost complex structure that is compatible of the symplectic form ω in the following sense.

Definition 2 *Let $(\mathcal{M}, \omega)$ be a symplectic manifold and J an almost complex structure on $(\mathcal{M}, \omega)$. J is compatible with ω if for all $u, v \in \mathcal{T}_x\mathcal{M}$,*

- *$\omega_x(J_x u, J_x v) = \omega_x(u, v)$ and*
- *$u \neq 0$ implies $\omega_x(u, J_x u) > 0$.*

Theorem 1 *The following two are equivalent.*

- *For all $u, v \in T_x\mathcal{M}$, $\omega_x(J_x u, J_x v) = \omega_x(u, v)$ and $u \neq 0$ implies $\omega_x(u, J_x u) > 0$.*
- *$g_x(u, v) \coloneqq \omega_x(u, J_x v)$ is a Riemannian metric on $\mathcal{M}$.*

In the following, we denote the compatible almost complex structure by the triplet (J, ω, g) for a fixed manifold $\mathcal{M}$.

Theorem 2 *There exists an compatible almost complex structure for any symplectic manifolds $(\mathcal{M}, \omega)$.*

The compatible almost complex structure is obtained in the following way.
For any Riemannian metric $\langle \cdot, \cdot \rangle_x$, define a linear operator A on $\mathcal{TM}$ by requiring

$$\omega_x(u, v) = \langle A_x u, v \rangle_x.$$

Let A_x^* be the adjoint operator with respect to the Riemannian metric $\langle \cdot, \cdot \rangle_x$. Then

$$\langle A_x u, v \rangle_x = \omega_x(u, v) = -\omega_x(v, u) = -\langle A_x v, u \rangle_x = -\langle A_x^* u, v \rangle_x$$

and hence $A_x^* = -A_x$. Since for all $u \in \mathcal{T}_x\mathcal{M}$, $\langle A_x u, A_x u \rangle_x = \langle A_x^* A_x u, u \rangle_x > 0$, $A_x^* A_x = -A_x^2 = A_x A_x^*$ is positive definite. Thus $A_x A_x^*$ admits a non-singular square root $(A_x A_x^*)^{\frac{1}{2}}$. J is defined by

$$J_x \coloneqq A_x (A_x A_x^*)^{-\frac{1}{2}}.$$

This J_x is actually a compatible almost complex structure. Firstly, because A_x and $(A_xA_x^*)^{-\frac{1}{2}}$ commute, it is shown that

$$J_x^2 = A_x(A_xA_x^*)^{-\frac{1}{2}}A_x(A_xA_x^*)^{-\frac{1}{2}} = A_xA_x(A_xA_x^*)^{-\frac{1}{2}}(A_xA_x^*)^{-\frac{1}{2}} = -A_xA_x^*(A_xA_x^*)^{-1} = -\mathrm{Id},$$

and hence J_x is an almost complex structure. This also shows that $J_x = -J_x^{-1}$. In addition, the fact that A_x and $(A_xA_x^*)^{-\frac{1}{2}}$ commute shows that

$$\begin{aligned} J_x &= A_x(A_xA_x^*)^{-\frac{1}{2}} = -(A_xA_x^*)^{-\frac{1}{2}}A_x^* = -J_x^*, \\ J_xA_x &= A_x(A_xA_x^*)^{-\frac{1}{2}}A_x = A_xA_x(A_xA_x^*)^{-\frac{1}{2}} = A_xJ_x. \end{aligned}$$

Secondly, it is shown that

$$\begin{aligned} \omega_x(J_xu, J_xv) &= \langle A_xJ_xu, J_xv\rangle_x \\ &= \langle J_xA_xu, J_xv\rangle_x \\ &= \langle A_xu, J_x^*J_xv\rangle_x \\ &= \langle A_xu, -J_x^2v\rangle_x \\ &= \langle A_xu, v\rangle_x \\ &= \omega_x(u, v) \end{aligned}$$

and

$$\begin{aligned} \omega_x(u, J_xu) &= \langle A_xu, J_xu\rangle_x \\ &= \langle J_x^*A_xu, u\rangle_x \\ &= \langle J_x^{-1}A_xu, u\rangle_x \\ &= \langle (A_xA_x^*)^{\frac{1}{2}}u, u\rangle_x \\ &> 0 \end{aligned}$$

since $(A_xA_x^*)^{\frac{1}{2}}$ is positive. Thus J is compatible with ω.

Because the above calculation also shows that $\omega_x(u, J_xu) = \langle (A_xA_x^*)^{\frac{1}{2}}u, u\rangle_x$, $g_x(u, v) = \langle (A_xA_x^*)^{\frac{1}{2}}u, v\rangle_x$ can be used as the Riemannian metric in the triplet (J, ω, g).

3 THE ENERGY-PRESERVING SCHEME

Let $\mathcal{M}$ be a symplectic affine space. The Hamilton equation on $\mathcal{M}$ is defined by

$$X \lrcorner \omega = \mathrm{d}\mathcal{H}, \quad \dot{u} = X \tag{2}$$

where $\mathcal{H}$ is the Hamiltonian, X the Hamiltonian vector field and $\lrcorner$ the contraction. We also assume that the triplet (J, ω, g) is independent of the position on $\mathcal{M}$, and write them not as J_x, ω_x, g_x but as J, ω, g for all $x \in \mathcal{M}$. Also we denote by $\mathcal{TM}$ the tangent space at any $x \in \mathcal{M}$. As explained below, by using (J, ω, g), (2) can be written as

$$\dot{u} = -J\nabla\mathcal{H}. \tag{3}$$

Since $\nabla\mathcal{H}$ is the gradient of $\mathcal{H}$, it holds that

$$\mathrm{d}\mathcal{H}(\delta u) = g(\nabla\mathcal{H}, \delta u).$$

Then, because the left-hand side of the first equation of (2) can be written as

$$X \lrcorner \omega(\delta u) = \omega(\dot{u}, \delta u) = -\omega(\dot{u}, J^2 \delta u) = -g(\dot{u}, J\delta u) = g(J\dot{u}, \delta u),$$

we get

$$\dot{u} = J^{-1}\nabla\mathcal{H} = -J\nabla\mathcal{H}. \tag{4}$$

This equation is obtained by the principle of least action with the action integral

$$S(u) = \int_0^T \left(\frac{1}{2} g(J\dot{u}(t), u(t)) - \mathcal{H}(u(t))\right) \mathrm{d}t.$$

Since $\mathcal{M}$ is an affine space, $\mathcal{M}$ and $\mathcal{TM}$ is isomorphic with the isomorphism Id, and hence $g(J\dot{u}(t), u(t))$ makes sense. A straightforward calculation shows that the variation of $S(u)$ is

$$\begin{aligned}\delta S(u) &= \int_0^T \left\{\frac{1}{2}(g(J\delta\dot{u}, u) + g(J\dot{u}, \delta u)) - g(\nabla\mathcal{H}, \delta u)\right\} \mathrm{d}t \\ &= \int_0^T g(J\dot{u} - \nabla\mathcal{H}, \delta u)\mathrm{d}t,\end{aligned}$$

which yields (4).

The combination of this variational principle and the method in [4] gives the following energy-preserving scheme.

Theorem 3 *Let $\mathcal{M}$ be a symplectic affine space and (J, ω, g) the compatible almost complex structure. Suppose that a given Hamiltonian $\mathcal{H}$ is not dependent on the time variable explicitly, and also suppose that the initial conditions are given so that $\delta^+ u^0, \delta^+ u^1 \in \mathcal{M} \simeq \mathcal{TM}$. Then, for a given discrete gradient $\overline{\nabla}\mathcal{H}$ of the Hamiltonian $\mathcal{H}$ with respect to the Riemannian structure g, the scheme*

$$\frac{u^{n+2} + u^{n+1} - u^n - u^{n-1}}{4\Delta t} = -J\overline{\nabla}\mathcal{H}(u^{n+1}, u^n) \tag{5}$$

has the following energy-conservation law:

$$\mathcal{H}(u^n) - \frac{\Delta t}{4} g(J\delta^+ u^n, \delta^- u^n) = \textit{const.} \tag{6}$$

where δ^+ and δ^- are the forward and the backward difference operators respectively.

4 EXAMPLE

As an illustration, we show an energy-preserving scheme for the wave equation

$$\begin{pmatrix} u_t \\ v_t \end{pmatrix} = \begin{pmatrix} 0 & 1 \\ -1 & 0 \end{pmatrix} \begin{pmatrix} -u_{xx} \\ v \end{pmatrix}, \tag{7}$$

$$\mathcal{H}_{\mathrm{W}}(u, v) = \int_0^L \left(\frac{1}{2}v^2 + \frac{1}{2}u_x^2\right) \mathrm{d}x \tag{8}$$

under the periodic boundary condition. We applied the method in the previous section to a semi-discretized wave equation:

$$\frac{\mathrm{d}}{\mathrm{d}t}\begin{pmatrix}\vec{u}\\ \vec{v}\end{pmatrix} = \begin{pmatrix}O_N & I_N\\ -I_N & O_N\end{pmatrix}\begin{pmatrix}-\delta_x^-\delta_x^+\vec{u}\\ \vec{v}\end{pmatrix}$$

which is a Hamilton equation with the Hamiltonian

$$\mathcal{H}_{\mathrm{W,d}}(\vec{u},\vec{v}) \coloneqq \frac{1}{2}\|\vec{v}\|_2^2 + \frac{1}{4}(\|\delta_x^+\vec{u}\|_2^2 + \|\delta_x^-\vec{u}\|_2^2)$$

and the standard symplectic 2-form $\omega_{\mathrm{W,d}}$. δ_x^+ and δ_x^- are the forward and the backward difference operators in the x direction. $\|\cdot\|_2$ is the L^2 norm:

$$\langle\vec{u},\vec{v}\rangle = \sum_{j=1}^{N} u_j v_j \Delta x, \quad \|\vec{u}\|_2 = \sqrt{\langle\vec{u},\vec{u}\rangle}.$$

We derive a compatible almost complex structure by using the L^2 inner product. The symplectic 2-form $\omega_{\mathrm{W,d}}$ is written as

$$\omega_{\mathrm{W,d}}(\begin{pmatrix}\vec{u}\\ \vec{v}\end{pmatrix},\begin{pmatrix}\vec{u}'\\ \vec{v}'\end{pmatrix}) = \sum_{j=1}^{N}(u_j v_j' - v_j u_j')\Delta x = \langle\begin{pmatrix}-\vec{v}\\ \vec{u}\end{pmatrix},\begin{pmatrix}\vec{u}'\\ \vec{v}'\end{pmatrix}\rangle = \langle\begin{pmatrix}O_N & -I_N\\ I_N & O_N\end{pmatrix}\begin{pmatrix}\vec{u}\\ \vec{v}\end{pmatrix},\begin{pmatrix}\vec{u}'\\ \vec{v}'\end{pmatrix}\rangle.$$

Hence we can define the operator A by

$$A = \begin{pmatrix}O_N & -I_N\\ I_N & O_N\end{pmatrix}. \tag{9}$$

This operator A gives the almost complex structure J and the Riemannian metric g as

$$J = A(AA^*)^{-\frac{1}{2}} = A(AA^{-1})^{-\frac{1}{2}} = AI^{-\frac{1}{2}} = A, \tag{10}$$

$$g(\vec{u},\vec{v}) = \langle(AA^*)^{\frac{1}{2}}\vec{u},\vec{v}\rangle = \langle\vec{u},\vec{v}\rangle. \tag{11}$$

It is straightforward to check that

$$\overline{\nabla}\mathcal{H}_{\mathrm{W,d}}(\begin{pmatrix}\vec{u}^{n+1}\\ \vec{v}^{n+1}\end{pmatrix},\begin{pmatrix}\vec{u}^{n}\\ \vec{v}^{n}\end{pmatrix}) = \begin{pmatrix}-\dfrac{\delta_x^-\delta_x^+(\vec{u}^{n+1}+\vec{u}^{n})}{2}\\ \dfrac{\vec{v}^{n+1}+\vec{v}^{n}}{2}\end{pmatrix}$$

is a discrete gradient. Hence Theorem 3 shows that the scheme

$$\frac{\vec{u}^{n+2}+\vec{u}^{n+1}-\vec{u}^{n}-\vec{u}^{n-1}}{4\Delta t} = \begin{pmatrix}O_N & I_N\\ -I_N & O_N\end{pmatrix}\begin{pmatrix}-\dfrac{\delta_x^-\delta_x^+(\vec{u}^{n+1}+\vec{u}^{n})}{2}\\ \dfrac{\vec{v}^{n+1}+\vec{v}^{n}}{2}\end{pmatrix} \tag{12}$$

is energy-preserving.

We show the numerical results in Figure 1. In this numerical test, we set the initial condition by $u(t,x) = \exp(-100(0.5-x)^2)$. The step sizes are $\Delta t = 1/50, \Delta x = 1/24$. We used the explicit Euler method as the starting method. The figures show the numerical solution at $t = 10000$ and the energy behavior. These show that the scheme is quite stable. Actually we have shown the following theorem.

Theorem 4 *If we rewrite the scheme to the form $U^{n+1} = SU^n$ $(\in \mathbb{R}^{6N})$ and $j = 1,\ldots,N$, then S is diagonalizable and all the absolute values of the eigenvalues are 1.*

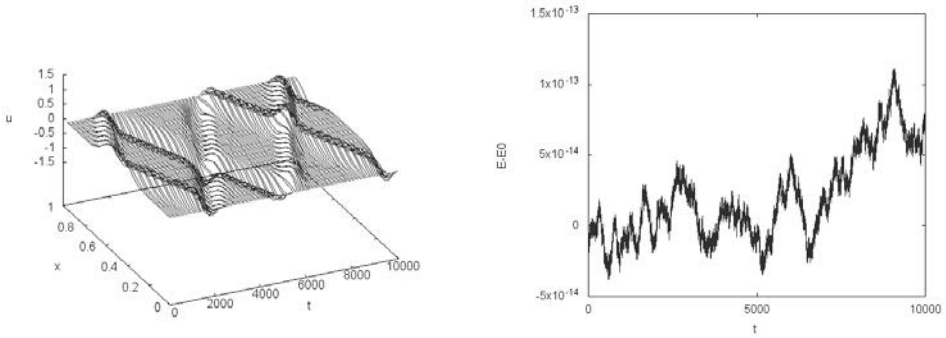

Figure 1: These figures show the numerical solution (left) and the energy behavior (right) from $t = 0$ to $t = 10000$. The step sizes are set to $\Delta x = 1/24$ and $\Delta t = 1/50$. The periodic boundary condition is imposed. The numerical solution under these conditions seems to be stable.

Acknowledgment

This work was supported by JSPS KAKENHI Grant Number 26400200 and JST PRESTO.

References

[1] Gonzalez, O., *Time Integration and Discrete Hamiltonian Systems*, J. Nonlinear Sci., 6 (1996), pp. 449–467.

[2] Furihata D. and Matsuo T., *Discrete Variational Derivative Method: A Structure-Preserving Method for Partial Differential Equations*, CRC Press, Boca Raton, 2011.

[3] Yaguchi T., *Lagrangian Approach to Derive Energy-Preserving Numerical Schemes for the Euler–Lagrange Partial Differential Equation*, M2AN, 47 (2013), 1493–1513.

[4] Ishikawa A. and Yaguchi T., *Application of the Variational Principle to Deriving Energy-Preserving Schemes for the Hamilton Equation*, JSIAM Lett., 8 (2016), pp. 53–56.

Implementation of discrete gradient methods for dissipative PDEs in image processing on GPUs

GRIMM, V.[1]

Karlsruhe Institute of Technology (KIT), D-76128 Karlsruhe, Germany
volker.grimm@kit.edu

1 INTRODUCTION

In many applications in image processing, dissipative partial differential equations (PDEs) appear. Let $\mathcal{H}$ be a Hilbert space with inner product $\langle\cdot,\cdot\rangle$ and let $V : \mathcal{H} \to \mathbb{R}$ be a differentiable functional. The gradient of V at $x \in \mathcal{H}$ is the unique element $\nabla V(x)$ satisfying

$$\langle \nabla V(x), v\rangle = \frac{d}{dt} V(x+tv)\Big|_{t=0} \qquad \text{for all} \quad v \in \mathcal{H}\,.$$

A gradient flow is the solution of the initial value problem

$$\dot{x} = -\nabla V(x), \qquad x(0) = x_0, \tag{1}$$

where the dot represents differentiation with respect to time. The dissipative character is seen by the decay

$$\frac{d}{dt} V(x(t)) = \langle \nabla V(x(t)), \dot{x}\rangle = -\|\nabla V(x(t))\|^2 \le 0\,. \tag{2}$$

In many applications in image processing, e.g. scale-space theory or time marching schemes for minimisation of the functional V, the preservation of the dissipativity of the PDE is more important than accuracy of the solution of the differential equation. With the help of discrete gradients, which are functions $\overline{\nabla} V : \mathcal{H} \times \mathcal{H} \to \mathcal{H}$, that are continuous and satisfy

$$\left\{ \begin{array}{rcl} \langle \overline{\nabla} V(x,x'), (x'-x)\rangle &=& V(x') - V(x), \\ \overline{\nabla} V(x,x) &=& \nabla V(x) \end{array} \right. \qquad \text{for all} \quad x, x' \in \mathcal{H} \tag{3}$$

one obtains discrete gradient methods with step sizes τ_n

$$x_{n+1} - x_n = -\tau_n \overline{\nabla} V(x_n, x_{n+1}) \tag{4}$$

that naturally preserve the decay

$$\begin{aligned} V(x_{n+1}) - V(x_n) &= \langle \overline{\nabla} V(x_n, x_{n+1}), (x_{n+1} - x_n)\rangle \\ &= -\tau_n \|\overline{\nabla} V(x_n, x_{n+1})\|^2 \\ &\le 0\,. \end{aligned} \tag{5}$$

2 DISCRETISATION AND COMPUTATION

With respect to simplicity, finite differences are the most widely used discretisation of PDEs in image processing. In [1], a general procedure is described to derive a discrete functional $V : \mathbb{R}^n \to \mathbb{R}$ based on finite differences. The discretised PDE is represented by the gradient flow (1) which is now an ordinary differential equation. In order to apply the discrete gradient method, an implicit equation needs to be solved. If Newton's method is used, one has to solve a huge linear system, $Ax = b$, $A \in \mathbb{R}^{N\times N}$, $b \in \mathbb{R}^N$, in every iteration. N represents the number of pixels in a grayscale picture or three times the number of pixels of a RGB picture. A common method to solve these systems is the method of conjugated gradients (CG method), cf. [3], that requires the multiple computation of A times a vector. Since the computation of A times a vector includes the Hessian of the discretised functional V in every step of Newton's method, it is often believed that an efficient implementation of this method were not possible. This changes if an implementation on a graphics processing unit (GPU) is considered. GPUs are custom-built for computer graphics and image processing and their highly parallel structure allows for the efficient implementation of the Hessian of V for large images. This can be illustrated by a total variation denoising experiment as discussed in [2]. The timings for the evaluation of the gradient of V and the Hessian matrix of V do not show significant differences in Table 1 for different sizes of grayscale pictures. Using the Gonzalez discrete gradient,

$$\begin{aligned}\overline{\nabla} V(x,x') &= \nabla V\left(\tfrac{x'+x}{2}\right) \\ &\quad + \frac{V(x')-V(x)-\left\langle \nabla V\left(\frac{x'+x}{2}\right), x'-x\right\rangle}{\|x-x'\|^2}(x'-x)\,, \qquad (x \neq x'),\end{aligned}$$

the evaluation of the discrete gradient takes longer than the application of the Hessian matrix to a vector due to non-local operations. For a large time step, the number of iterations in Newton's method (outer iterations) and the number of CG iterations (inner iterations) for this experiment stay reasonably small as shown in Table 2.

Table 1: GPU/CPU time comparison

GPU/CPU time	512×512	1024×1024	2048×2048	4096×4096
∇V	$< 50\,[\mu s]$	$< 50\,[\mu s]$	$< 50\,[\mu s]$	$< 50\,[\mu s]$
Hessian	$< 50\,[\mu s]$	$< 50\,[\mu s]$	$< 50\,[\mu s]$	$< 50\,[\mu s]$
DG eval	$< 15\,[ms]$	$< 38\,[ms]$	$< 140\,[ms]$	$< 550\,[ms]$

Table 2: Number of inner and outer iterations

Number of iterations	512×512	1024×1024	2048×2048	4096×4096
outer iterations	6	6	6	6
CG iterations	9	9	10	11

Altogether, the rise of specialized computing hardware alters the requirements for algorithms to run efficiently and reliably. This works in favour of discrete gradient methods,

whose implementation is more involved. To explore the possibilities and advantages of the rich class of discrete gradient methods applied to the numerous dissipative flows in image processing seems worthwhile.

References

[1] Celledoni, E., Grimm, V., McLachlan, R. I., McLaren, D. I., O'Neale, D., Owren, B. and Quispel, G. R. W., *Preserving energy resp. dissipation in numerical PDEs using the "average vector field" method*, J. Comput. Phys., 231:20 (2012), pp.6770–6789.

[2] Grimm, V., McLachlan, R. I., McLaren, D. I., Quispel, G. R. W., and Schönlieb, C.-B., *The use of discrete gradient methods for total variation type regularization problems in image processing*, arXiv preprint arXiv:1603.07515, (2016).

[3] Hestenes, M. R. and Stiefel, E. *Methods of conjugate gradients for solving linear systems*, J. Research Nat. Bur. Standards, 49 (1952), pp.409–436.

MI レクチャーノートシリーズ刊行にあたり

本レクチャーノートシリーズは、文部科学省 21 世紀 COE プログラム「機能数理学の構築と展開」(H.15-19 年度) において作成した COE Lecture Notes の続刊であり、文部科学省大学院教育改革支援プログラム「産業界が求める数学博士と新修士養成」(H19-21 年度) および、同グローバル COE プログラム「マス・フォア・インダストリ教育研究拠点」(H.20-24 年度) において行われた講義の講義録として出版されてきた。平成 23 年 4 月のマス・フォア・インダストリ研究所 (IMI) 設立と平成 25 年 4 月の IMI の文部科学省共同利用・共同研究拠点として「産業数学の先進的・基礎的共同研究拠点」の認定を受け、今後、レクチャーノートは、マス・フォア・インダストリに関わる国内外の研究者による講義の講義録、会議録等として出版し、マス・フォア・インダストリの本格的な展開に資するものとする。

平成 26 年 10 月
マス・フォア・インダストリ研究所
所長　福本康秀

IMI-La Trobe Joint Conference

Geometric Numerical Integration and its Applications

発　行　2017年３月31日
編　集　QUISPEL, G. Reinout W. / BADER, Philipp / MCLAREN, David I. / TAGAMI, Daisuke
発　行　九州大学マス・フォア・インダストリ研究所
九州大学大学院数理学府
〒819-0395 福岡市西区元岡744
九州大学数理・IMI 事務室
TEL 092-802-4402　FAX 092-802-4405
URL http://www.imi.kyushu-u.ac.jp/

印　刷　城島印刷株式会社
〒810-0012 福岡市中央区白金２丁目９番６号
TEL 092-531-7102　FAX 092-524-4411

シリーズ既刊

Issue	Author／Editor	Title	Published
COE Lecture Note	Mitsuhiro T. NAKAO Kazuhiro YOKOYAMA	Computer Assisted Proofs - Numeric and Symbolic Approaches - 199pages	August 22, 2006
COE Lecture Note	M.J.Shai HARAN	Arithmetical Investigations - Representation theory, Orthogonal polynomials and Quantum interpolations- 174pages	August 22, 2006
COE Lecture Note Vol.3	Michal BENES Masato KIMURA Tatsuyuki NAKAKI	Proceedings of Czech-Japanese Seminar in Applied Mathematics 2005 155pages	October 13, 2006
COE Lecture Note Vol.4	宮田　健治	辺要素有限要素法による磁界解析 - 機能数理学特別講義 21pages	May 15, 2007
COE Lecture Note Vol.5	Francois APERY	Univariate Elimination Subresultants - Bezout formula, Laurent series and vanishing conditions - 89pages	September 25, 2007
COE Lecture Note Vol.6	Michal BENES Masato KIMURA Tatsuyuki NAKAKI	Proceedings of Czech-Japanese Seminar in Applied Mathematics 2006 209pages	October 12, 2007
COE Lecture Note Vol.7	若山　正人 中尾　充宏	九州大学産業技術数理研究センター キックオフミーティング 138pages	October 15, 2007
COE Lecture Note Vol.8	Alberto PARMEGGIANI	Introduction to the Spectral Theory of Non-Commutative Harmonic Oscillators 233pages	January 31, 2008
COE Lecture Note Vol.9	Michael I.TRIBELSKY	Introduction to Mathematical modeling 23pages	February 15, 2008
COE Lecture Note Vol.10	Jacques FARAUT	Infinite Dimensional Spherical Analysis 74pages	March 14, 2008
COE Lecture Note Vol.11	Gerrit van DIJK	Gelfand Pairs And Beyond 60pages	August 25, 2008
COE Lecture Note Vol.12	Faculty of Mathematics, Kyushu University	Consortium “MATH for INDUSTRY” First Forum 87pages	September 16, 2008
COE Lecture Note Vol.13	九州大学大学院 数理学研究院	プロシーディング「損保数理に現れる確率モデル」 ― 日新火災・九州大学 共同研究 2008 年 11 月 研究会 ― 82pages	February 6, 2009

シリーズ既刊

Issue	Author／Editor	Title	Published
COE Lecture Note Vol.14	Michal Beneš, Tohru Tsujikawa Shigetoshi Yazaki	Proceedings of Czech-Japanese Seminar in Applied Mathematics 2008 77pages	February 12, 2009
COE Lecture Note Vol.15	Faculty of Mathematics, Kyushu University	International Workshop on Verified Computations and Related Topics 129pages	February 23, 2009
COE Lecture Note Vol.16	Alexander Samokhin	Volume Integral Equation Method in Problems of Mathematical Physics 50pages	February 24, 2009
COE Lecture Note Vol.17	矢嶋　　徹 及川　正行 梶原　健司 辻　　英一 福本　康秀	非線形波動の数理と物理 66pages	February 27, 2009
COE Lecture Note Vol.18	Tim Hoffmann	Discrete Differential Geometry of Curves and Surfaces 75pages	April 21, 2009
COE Lecture Note Vol.19	Ichiro Suzuki	The Pattern Formation Problem for Autonomous Mobile Robots —Special Lecture in Functional Mathematics— 23pages	April 30, 2009
COE Lecture Note Vol.20	Yasuhide Fukumoto Yasunori Maekawa	Math-for-Industry Tutorial: Spectral theories of non-Hermitian operators and their application 184pages	June 19, 2009
COE Lecture Note Vol.21	Faculty of Mathematics, Kyushu University	Forum “Math-for-Industry” Casimir Force, Casimir Operators and the Riemann Hypothesis 95pages	November 9, 2009
COE Lecture Note Vol.22	Masakazu Suzuki Hoon Hong Hirokazu Anai Chee Yap Yousuke Sato Hiroshi Yoshida	The Joint Conference of ASCM 2009 and MACIS 2009: Asian Symposium on Computer Mathematics Mathematical Aspects of Computer and Information Sciences 436pages	December 14, 2009
COE Lecture Note Vol.23	荒川　恒男 金子　昌信	多重ゼータ値入門 111pages	February 15, 2010
COE Lecture Note Vol.24	Fulton B.Gonzalez	Notes on Integral Geometry and Harmonic Analysis 125pages	March 12, 2010
COE Lecture Note Vol.25	Wayne Rossman	Discrete Constant Mean Curvature Surfaces via Conserved Quantities 130pages	May 31, 2010
COE Lecture Note Vol.26	Mihai Ciucu	Perfect Matchings and Applications 66pages	July 2, 2010

シリーズ既刊

Issue	Author／Editor	Title	Published
COE Lecture Note Vol.27	九州大学大学院 数理学研究院	Forum “Math-for-Industry” and Study Group Workshop Information security, visualization, and inverse problems, on the basis of optimization techniques 100pages	October 21, 2010
COE Lecture Note Vol.28	ANDREAS LANGER	MODULAR FORMS, ELLIPTIC AND MODULAR CURVES LECTURES AT KYUSHU UNIVERSITY 2010 62pages	November 26, 2010
COE Lecture Note Vol.29	木田　雅成 原田　昌晃 横山　俊一	Magma で広がる数学の世界 157pages	December 27, 2010
COE Lecture Note Vol.30	原　　隆 松井　　卓 廣島　文生	Mathematical Quantum Field Theory and Renormalization Theory 201pages	January 31, 2011
COE Lecture Note Vol.31	若山　正人 福本　康秀 高木　　剛 山本　昌宏	Study Group Workshop 2010 Lecture & Report 128pages	February 8, 2011
COE Lecture Note Vol.32	Institute of Mathematics for Industry, Kyushu University	Forum “Math-for-Industry” 2011 “TSUNAMI-Mathematical Modelling” Using Mathematics for Natural Disaster Prediction, Recovery and Provision for the Future 90pages	September 30, 2011
COE Lecture Note Vol.33	若山　正人 福本　康秀 高木　　剛 山本　昌宏	Study Group Workshop 2011 Lecture & Report 140pages	October 27, 2011
COE Lecture Note Vol.34	Adrian Muntean Vladimír Chalupecký	Homogenization Method and Multiscale Modeling 72pages	October 28, 2011
COE Lecture Note Vol.35	横山　俊一 夫　　紀恵 林　　卓也	計算機代数システムの進展 210pages	November 30, 2011
COE Lecture Note Vol.36	Michal Beneš Masato Kimura Shigetoshi Yazaki	Proceedings of Czech-Japanese Seminar in Applied Mathematics 2010 107pages	January 27, 2012
COE Lecture Note Vol.37	若山　正人 高木　　剛 Kirill Morozov 平岡　裕章 木村　正人 白井　朋之 西井　龍映 栄　伸一郎 穴井　宏和 福本　康秀	平成 23 年度 数学・数理科学と諸科学・産業との連携研究ワークショップ　拡がっていく数学　～期待される “見えない力” ～ 154pages	February 20, 2012

シリーズ既刊

Issue	Author／Editor	Title	Published
COE Lecture Note Vol.38	Fumio Hiroshima Itaru Sasaki Herbert Spohn Akito Suzuki	Enhanced Binding in Quantum Field Theory 204pages	March 12, 2012
COE Lecture Note Vol.39	Institute of Mathematics for Industry, Kyushu University	Multiscale Mathematics: Hierarchy of collective phenomena and interrelations between hierarchical structures 180pages	March 13, 2012
COE Lecture Note Vol.40	井ノ口順一 太田　泰広 筧　　三郎 梶原　健司 松浦　　望	離散可積分系・離散微分幾何チュートリアル 2012 152pages	March 15, 2012
COE Lecture Note Vol.41	Institute of Mathematics for Industry, Kyushu University	Forum “Math-for-Industry” 2012 “Information Recovery and Discovery” 91pages	October 22, 2012
COE Lecture Note Vol.42	佐伯　　修 若山　正人 山本　昌宏	Study Group Workshop 2012 Abstract, Lecture & Report 178pages	November 19, 2012
COE Lecture Note Vol.43	Institute of Mathematics for Industry, Kyushu University	Combinatorics and Numerical Analysis Joint Workshop 103pages	December 27, 2012
COE Lecture Note Vol.44	萩原　　学	モダン符号理論からポストモダン符号理論への展望 107pages	January 30, 2013
COE Lecture Note Vol.45	金山　　寛	Joint Research Workshop of Institute of Mathematics for Industry (IMI), Kyushu University “Propagation of Ultra-large-scale Computation by the Domain-decomposition-method for Industrial Problems (PUCDIP 2012)” 121pages	February 19, 2013
COE Lecture Note Vol.46	西井　龍映 栄　伸一郎 岡田　勘三 落合　啓之 小磯　深幸 斎藤　新悟 白井　朋之	科学・技術の研究課題への数学アプローチ ―数学モデリングの基礎と展開― 325pages	February 28, 2013
COE Lecture Note Vol.47	SOO TECK LEE	BRANCHING RULES AND BRANCHING ALGEBRAS FOR THE COMPLEX CLASSICAL GROUPS 40pages	March 8, 2013
COE Lecture Note Vol.48	溝口　佳寛 脇　　隼人 平坂　　貢 谷口　哲至 島袋　　修	博多ワークショップ「組み合わせとその応用」 124pages	March 28, 2013

シリーズ既刊

Issue	Author／Editor	Title	Published
COE Lecture Note Vol.49	照井　章 小原　功任 濱田　龍義 横山　俊一 穴井　宏和 横田　博史	マス・フォア・インダストリ研究所　共同利用研究集会 II 数式処理研究と産学連携の新たな発展　137pages	August 9, 2013
MI Lecture Note Vol.50	Ken Anjyo Hiroyuki Ochiai Yoshinori Dobashi Yoshihiro Mizoguchi Shizuo Kaji	Symposium MEIS2013: Mathematical Progress in Expressive Image Synthesis　154pages	October 21, 2013
MI Lecture Note Vol.51	Institute of Mathematics for Industry, Kyushu University	Forum “Math-for-Industry” 2013 “The Impact of Applications on Mathematics”　97pages	October 30, 2013
MI Lecture Note Vol.52	佐伯　修 岡田　勘三 髙木　剛 若山　正人 山本　昌宏	Study Group Workshop 2013 Abstract, Lecture & Report 142pages	November 15, 2013
MI Lecture Note Vol.53	四方　義啓 櫻井　幸一 安田　貴徳 Xavier Dahan	平成25年度　九州大学マス・フォア・インダストリ研究所 共同利用研究集会　安全・安心社会基盤構築のための代数構造 ～サイバー社会の信頼性確保のための数理学～　158pages	December 26, 2013
MI Lecture Note Vol.54	Takashi Takiguchi Hiroshi Fujiwara	Inverse problems for practice, the present and the future　93pages	January 30, 2014
MI Lecture Note Vol.55	栄　伸一郎 溝口　佳寛 脇　隼人 渋田　敬史	Study Group Workshop 2013 数学協働プログラム Lecture & Report 98pages	February 10, 2014
MI Lecture Note Vol.56	Yoshihiro Mizoguchi Hayato Waki Takafumi Shibuta Tetsuji Taniguchi Osamu Shimabukuro Makoto Tagami Hirotake Kurihara Shuya Chiba	Hakata Workshop 2014 ~ Discrete Mathematics and its Applications ~　141pages	March 28, 2014
MI Lecture Note Vol.57	Institute of Mathematics for Industry, Kyushu University	Forum “Math-for-Industry” 2014: “Applications + Practical Conceptualization + Mathematics = fruitful Innovation”　93pages	October 23, 2014
MI Lecture Note Vol.58	安生健一 落合啓之	Symposium MEIS2014: Mathematical Progress in Expressive Image Synthesis　135pages	November 12, 2014

シリーズ既刊

Issue	Author／Editor	Title	Published
MI Lecture Note Vol.59	西井　龍映 岡田　勘三 梶原　健司 髙木　　剛 若山　正人 脇　　隼人 山本　昌宏	Study Group Workshop 2014 数学協働プログラム Abstract, Lecture & Report　196pages	November 14, 2014
MI Lecture Note Vol.60	西浦　　博	平成 26 年度九州大学 IMI 共同利用研究・研究集会（I） 感染症数理モデルの実用化と産業及び政策での活用のための新たな展開　120pages	November 28, 2014
MI Lecture Note Vol.61	溝口　佳寛 Jacques Garrigue 萩原　　学 Reynald Affeldt	研究集会 高信頼な理論と実装のための定理証明および定理証明器 Theorem proving and provers for reliable theory and implementations (TPP2014)　138pages	February 26, 2015
MI Lecture Note Vol.62	白井　朋之	Workshop on “β-transformation and related topics”　59pages	March 10, 2015
MI Lecture Note Vol.63	白井　朋之	Workshop on “Probabilistic models with determinantal structure” 107pages	August 20, 2015
MI Lecture Note Vol.64	落合　啓之 土橋　宜典	Symposium MEIS2015: Mathematical Progress in Expressive Image Synthesis　124pages	September 18, 2015
MI Lecture Note Vol.65	Institute of Mathematics for Industry, Kyushu University	Forum “Math-for-Industry” 2015 “The Role and Importance of Mathematics in Innovation”　74pages	October 23, 2015
MI Lecture Note Vol.66	岡田　勘三 藤澤　克己 白井　朋之 若山　正人 脇　　隼人 Philip Broadbridge 山本　昌宏	Study Group Workshop 2015 Abstract, Lecture & Report 156pages	November 5, 2015
MI Lecture Note Vol.67	Institute of Mathematics for Industry, Kyushu University	IMI-La Trobe Joint Conference “Mathematics for Materials Science and Processing” 66pages	February 5, 2016
MI Lecture Note Vol.68	古庄　英和 小谷　久寿 新甫　洋史	結び目と Grothendieck-Teichmüller 群 116pages	February 22, 2016
MI Lecture Note Vol.69	土橋　宜典 鍛治　静雄	Symposium MEIS2016: Mathematical Progress in Expressive Image Synthesis　82pages	October 24, 2016
MI Lecture Note Vol.70	Institute of Mathematics for Industry, Kyushu University	Forum “Math-for-Industry” 2016 “Agriculture as a metaphor for creativity in all human endeavors” 98pages	November 2, 2016
MI Lecture Note Vol.71	小磯　深幸 二宮　嘉行 山本　昌宏	Study Group Workshop 2016 Abstract, Lecture & Report　143pages	November 21, 2016

シリーズ既刊

Issue	Author／Editor	Title	Published
MI Lecture Note Vol.72	新井　朝雄 小嶋　　泉 廣島　文生	Mathematical quantum field theory and related topics　133pages	January 27, 2017
MI Lecture Note Vol.73	穴田　啓晃 Kirill Morozov 須賀　祐治 奥村　伸也 櫻井　幸一	Secret Sharing for Dependability, Usability and Security of Network Storage and Its Mathematical Modeling　211pages	March 15, 2017

九州大学マス・フォア・インダストリ研究所
九州大学大学院 数理学府
〒819-0395 福岡市西区元岡744　TEL 092-802-4402　FAX 092-802-4405
URL http://www.imi.kyushu-u.ac.jp/